



REMOTE SENSING
LABORATORY

*Operated by Bechtel Nevada for the
U.S. Department of Energy*

DOE/NV/11718--324

DECEMBER 1999

AN AERIAL RADIOLOGICAL SURVEY OF THE NEVADA TEST SITE

NEVADA TEST SITE, NEVADA

Thane J. Hendricks
Steven R. Riedhauser
Bechtel Nevada
Las Vegas, Nevada

SURVEY DATES — AUGUST TO SEPTEMBER 1994

Approved for Public Release; Further Dissemination Unlimited.

DISCLAIMER

This report was prepared as an account of work sponsored by an agency of the United States Government. Neither the United States Government nor an agency thereof, nor any of their employees, nor any of their contractors and subcontractors, or their employees, makes a warranty, express or implied, or assumes legal liability or responsibility for the accuracy, completeness, or any third party's use or the results of such use of any disclosed information, apparatus, product, or process or represents that its use would not infringe privately owned rights. Reference herein to any specific commercial product, process, or service by trade name, trademark, manufacturer, or otherwise, does not necessarily constitute or imply an endorsement, recommendation, or favoring by the United States government or an agency thereof or its contractors or subcontractors. The views and opinions of the authors expressed herein do not necessarily state or reflect those of the United States Government or an agency thereof.

Available electronically at <http://www.doe.gov/bridge>.

Available for a processing fee to the U.S. Department of Energy and its contractors, in paper, from:

U.S. Department of Energy
Office of Scientific and Technical Information
P.O. Box 62
Oak Ridge, TN 37831-0062
Phone: 423.576.8401
Fax: 423.576.5728
E-mail: reports@adonis.osti.gov

Available to the public, in paper, from:

U.S. Department of Commerce
National Technical Information Service
5285 Port Royal Road
Springfield, VA 22161
Phone: 800.553.6847 or 703-605-6000
Fax: 703.605.6900
E-mail: orders@ntis.fedworld.gov
Online ordering: <http://www.ntis.gov/ordering.htm>

AN AERIAL RADIOLOGICAL SURVEY OF THE NEVADA TEST SITE

NEVADA TEST SITE, NEVADA

SURVEY DATES — AUGUST TO SEPTEMBER 1994

Thane J. Hendricks
Steven R. Riedhauser
Project Scientists

REVIEWED BY

Alan J. Will, Manager
Remote Sensing and Applied Technology Department

Michael F. Mohar, Manager
Aerial Measuring System Project

Clifton M. Bluit, Manager
Radiation Sciences Section

ABSTRACT

A team from the Remote Sensing Laboratory conducted an aerial radiological survey of the U.S. Department of Energy's Nevada Test Site including three neighboring areas during August and September 1994. The survey team measured the terrestrial gamma radiation at the Nevada Test Site to determine the levels of natural and man-made radiation. This survey included the areas covered by previous surveys conducted from 1962 through 1993.

The results of the aerial survey showed a terrestrial background exposure rate that varied from less than 6 microentgens per hour ($\mu\text{R/h}$) to 50 $\mu\text{R/h}$ plus a cosmic-ray contribution that varied from 4.5 $\mu\text{R/h}$ at an elevation of 900 meters (3000 feet) to 8.5 $\mu\text{R/h}$ at 2400 meters (8000 feet). In addition to the principal gamma-emitting, naturally occurring isotopes (potassium-40, thallium-208, bismuth-214, and actinium-228), the man-made radioactive isotopes found in this survey were cobalt-60, cesium-137, europium-152, protactinium-234m (an indicator of depleted uranium), and americium-241, which are due to human actions in the survey area. Individual, site-wide plots of gross terrestrial exposure rate, man-made exposure rate, and americium-241 activity (approximating the distribution of all transuranic material) are presented. In addition, expanded plots of individual areas exhibiting these man-made contaminations are given.

A comparison is made between the data from this survey and previous aerial radiological surveys of the Nevada Test Site. Some previous ground-based measurements are discussed and related to the aerial data. In regions away from man-made activity, the exposure rates inferred from the gamma-ray measurements collected during this survey agreed very well with the exposure rates inferred from previous aerial surveys.

CONTENTS

Abstract	ii
List of Figures	v
List of Tables	v
List of Acronyms	vi
List of Physical Units	vi

SECTIONS

1.0 Introduction	1
2.0 Site Description and Survey History	1
2.1 Previous Aerial Radiological Surveys	1
2.2 Other Radiological Surveys	3
3.0 Measured Radiation Fields	4
3.1 Natural Background Radiation	4
Naturally Occurring Radioisotopes	4
Radon and its Daughters	5
Cosmic Radiation	5
Worldwide Cesium	5
3.2 Changes in the Radiation Fields	5
4.0 Survey Equipment and Procedures	6
4.1 Aerial Measuring System	6
4.2 Survey Procedures	8
5.0 Data Reduction Procedures	9
5.1 Flight-Path Recovery	9
5.2 Gross Count Algorithm	9
Altitude Profile	10
5.3 Conversion of Gross Count Rate to Exposure Rate	11
5.4 MMGC Algorithm	11
5.5 Isotopic Extraction Algorithms	12
2-window	12
3-window	13
5.6 Gamma Spectral Analysis	14
Time Normalization	15
High-Energy Count Normalization	15
Spectral Distortions	16
6.0 Discussion of Results	16
6.1 Gamma-Ray Exposure Rate	17
6.2 MMGC Rate and Individual Isotopic Contours	17
6.3 Discussion of Anomalies in Each Area	18
Area 1	20
Area 2	20
Area 3	21
Area 4	23
Area 5 and the NAFR	24
Area 6	25
Area 7	26
Area 8	27
Area 9	28
Area 10	29
Area 11	29
Area 12	30
Area 14	31
Area 15 and the NAFR	31
Area 16	32
Area 17	32
Area 18	33
Area 19	34
Area 20 and the NAFR	34
Area 22	35

CONTENTS

Area 23	35
Area 25	35
Area 26	35
Area 27	36
Area 29	36
Area 30	36
7.0 Summary	37
8.0 References	61

APPENDIXES

A Survey Parameters and Results	63
B List of the Elements	66

LIST OF FIGURES

1	MBB BO-105 Helicopter with Detector Pods	7
2	2-window and 3-window Algorithms Applied to a Typical Spectrum	8
3	Definition of Peak and Background Areas around a Radiation Anomaly	15
4	Site-Wide Terrestrial Exposure-Rate Contour Plot	38
5	Site-Wide MMGC-Rate Contour Plot	39
6	Net Gamma Spectra for ROIs Identified in Figure 7	40
7	Man-Made Activity in Area 20	41
8	Net Gamma Spectra for ROIs Identified in Figure 9	42
9	Man-Made Activity in Areas 18 and 30	43
10	Net Gamma Spectra for ROIs Identified in Figure 11	44
11	Man-Made Activity in Area 25	45
12	Net Gamma Spectra for ROIs Identified in Figure 13	46
13	Man-Made Activity in Areas 6 and 16	47
14	Net Gamma Spectra for ROIs Identified in Figure 15	48
15	Man-Made Activity in Areas 5 and 11	49
16a	Net Gamma Spectra for ROIs Identified in Figure 17	50
16b	Net Gamma Spectra for ROIs Identified in Figure 17	51
16c	Net Gamma Spectra for ROIs Identified in Figure 17	52
17	Man-Made Activity in Yucca Flat	53
18	Site-Wide Isotopic ²⁴¹ Am Contour Plot	54
19	²⁴¹ Am Activity in Area 20	55
20	²⁴¹ Am Activity in Areas 18 and 30	56
21	Net Gamma Spectra for ROIs Identified in Figure 22	57
22	²⁴¹ Am Activity in Areas 5 and 11	58
23	Net Gamma Spectra for ROIs Identified in Figure 24	59
24	²⁴¹ Am Activity in Yucca Flat	60

LIST OF TABLES

6-1	Radioisotopes and Half-Lives	19
6-2	Summary of Detected Man-Made Sources in Area 1	20
6-3	Summary of Detected Man-Made Sources in Area 2	21
6-4	Summary of Detected Man-Made Sources in Area 3	22
6-5	Summary of Detected Man-Made Sources in Area 4	23
6-6	Summary of Detected Man-Made Sources in Area 5	24
6-7	Summary of Detected Man-Made Sources in Area 6	26
6-8	Summary of Detected Man-Made Sources in Area 7	26
6-9	Summary of Detected Man-Made Sources in Area 8	27
6-10	Summary of Detected Man-Made Sources in Area 9	28
6-11	Summary of Detected Man-Made Sources in Area 10	29
6-12	Summary of Detected Man-Made Sources in Area 11	30
6-13	Summary of Detected Man-Made Sources in Area 12	31
6-14	Summary of Detected Man-Made Sources in Area 15	31
6-15	Summary of Detected Man-Made Sources in Area 16	32
6-16	Summary of Detected Man-Made Sources in Area 18	33
6-17	Summary of Detected Man-Made Sources in Area 20	34
6-18	Summary of Detected Man-Made Sources in Area 25	36
6-19	Summary of Detected Man-Made Sources in Area 30	36
A-1	Summary of Average Exposure Rate by Area	74

LIST OF ACRONYMS

The following list of acronyms occur in this document. Chemical symbols are listed with their names and other nomenclature in Appendix B.

ADC	analog-to-digital converter
AGL	above ground level
AMS	Aerial Measuring System
CP	control point
DOE	U.S. Department of Energy
EMAD	Engine Maintenance, Assembly, and Disassembly
FS	full scale
GC	gross count
GPS	Global Positioning System
GZ	ground zero
LT	live time
MBB	Messerschmitt-Bolkow-Blohm
MM	man-made
MMGC	man-made gross count
NAFR	Nellis Air Force Range
NRDS	Nuclear Rocket Development Station
NTS	Nevada Test Site
RDGPS	Real-time Differential Global Positioning System
REDAR IV	Radiation and Environmental Data Acquisition and Recorder, Model IV
RMAD	Reactor Maintenance, Assembly, and Disassembly
ROI	region of interest
RSL	Remote Sensing Laboratory
RWMS	Radioactive Waste Management Site
USGS	U.S. Geological Survey

LIST OF PHYSICAL UNITS

Bq	becquerel (a unit of activity; disintegrations per second)
Ci	curie (a unit of activity)
cm	centimeter
ft	foot
g	gram
h	hour
in	inch
keV	kiloelectronvolt (a unit of energy)
kg	kilogram
km	kilometer
kt	kiloton
m	meter
mi	mile
min	minute
μ R	microroentgen (a unit of exposure)
mR	milliroentgen (a unit of exposure)
mrem	millirem (a unit of dose)
nCi	nanocurie (a unit of activity)
pCi	picocurie (a unit of activity)
rem	roentgen equivalent man (a unit of dose)
s	second
yr	year

1.0 INTRODUCTION

The U.S. Department of Energy's (DOE) Remote Sensing Laboratory (RSL) maintains the Aerial Measuring System (AMS), which is an aerial radiological surveillance system. The RSL has offices at Nellis Air Force Base in Las Vegas, Nevada, and at Andrews Air Force Base near Washington, D.C. During this survey, the AMS was operated under contract to the DOE by EG&G Energy Measurements, Inc. Since 1996, the RSL has been operated by Bechtel Nevada. Aerial surveys provide data that assist in effective environmental management at nuclear facilities. The surveys, if performed at the appropriate times, can also provide information on the radiation environment before, during, and after a facility is operating with radioactive materials.

The Atomic Energy Commission (a predecessor of the DOE) began a program in 1958 to map the terrestrial gamma radiation environment in and around facilities that produce, use, or store radioactive materials. As part of this ongoing program, the RSL routinely conducts aerial surveys for the DOE, the Nuclear Regulatory Commission, and other government agencies.

During August and September 1994, a team from the RSL conducted an aerial radiological survey (which will be referred to as "*the 1994 survey*") of the Nevada Test Site (NTS) and three adjacent areas on the Nellis Air Force Range (NAFR). The purpose of the survey was to provide a more detailed measurement of the NTS gamma radiation natural background and, in particular, some areas of man-made activity identified during a 1992 survey of the NTS.¹ During that survey, two Beechcraft B-200 airplanes were flown at an altitude of 150 meters (500 feet) above ground level (AGL) and a 1600-meter (1-mile) flight-line spacing so that the whole site plus a large fraction of the land around the NTS could be surveyed in a few weekends. The present survey used a Messerschmitt-Bolkow-Blohm (MBB) BO-105 helicopter at an altitude of 60 meters (200 feet) with a 150-meter (500-foot) flight-line spacing. The spatial resolution was correspondingly better, and the sensitivity was much better for the present survey. On a helicopter at an altitude of 60 meters, the detectors interrogate an area of the ground about 15 percent the size interrogated by the detectors on the airplane at an altitude of 150 meters. The increase in sensitivity arises from the nearly 100 percent coverage of the ground surface by the helicopter system versus the approximately 20 percent coverage conducted by the airplane system.

2.0 SITE DESCRIPTION AND SURVEY HISTORY

The NTS covers roughly 3500 square kilometers (1350 square miles) of federally owned land located northwest of Las Vegas, Nevada. The base camp of Mercury (situated at the southeast corner of the NTS) is approximately 100 kilometers (62 miles) from Las Vegas. The test site is surrounded on the east, north, and west by the NAFR. Highway US 95 is the nominal southern boundary. The survey area includes all of the NTS as well as three parcels of land on the NAFR. These three parcels were added to the survey to allow measurement of the complete fallout plumes from several nuclear tests performed near the NTS borders. The elevation of the survey area ranges from 850 meters (2800 feet) in the south to 2250 meters (7400 feet) in the northwest.

The NTS served as the main testing area for aboveground and underground nuclear weapons tests from its establishment in 1951 through 1992.² Most of the descriptions and information of the various nuclear tests in this report derive from this reference. Almost all high-yield weapons tests were conducted in the Pacific. In total, 100 aboveground tests were conducted on the NTS. Also, a number of other tests on the NTS were conducted underground but were not designed to contain the radioactive products of the explosion. Several tests designed to be contained resulted in the release of radioactive material. In addition, several other projects at the NTS produced radioactive material that was dispersed at a number of sites. All of these actions should produce regions that are easily observable through their gamma radiation.

2.1 Previous Aerial Radiological Surveys

The desire to map the fallout from nuclear tests at the NTS was the principal impetus behind the development of aerial radiological surveys in the 1950s. The history of these early efforts

is described in detail in another publication.³ The NTS has been the subject of numerous aerial surveys conducted by the RSL since 1962. Most of the aerial support for the nuclear testing program has been routine, and only some of the very early measurements have been published. Since 1963, nuclear tests have been conducted exclusively underground, so the aerial support has been used principally in a standby mode. Many different aircraft and detector systems have been used. Detailed comparisons of the data from one survey to another are not easily made since the spatial resolutions and detection sensitivities vary greatly.

In 1962, aircraft from the U.S. Geological Survey (USGS) and EG&G mapped the fallout pattern from the Sedan⁴ and Small Boy⁵ tests. During these surveys, fixed-wing aircraft (a DC-3 operated by the USGS and a Beechcraft Model 50 Twin Bonanza operated by EG&G) were flown winding paths over the terrain at 150 meters (500 feet) AGL. The pre-test survey work included recording the natural background radiation levels along four arcs in the expected downwind direction from the ground zero (GZ). The Small Boy fallout pattern was mapped from about 20 kilometers (12 miles) east of the GZ to almost 200 kilometers (120 kilometers) northeast of the GZ. The Sedan fallout pattern was measured from the NTS border (about 8 kilometers [5 miles] from the GZ) to more than 300 kilometers (190 miles) from the GZ.

In June 1967, the EG&G fixed-wing aircraft was used in a search for missing cobalt-60 (⁶⁰Co) sources near the Sedan crater. The survey⁶ was principally an exercise to determine how well the detection system could find point sources rather than mapping large-area distributions. Areas of anomalous activity were located during the aerial search, but a ground-based search team could not locate any sources.

In December 1968, two fixed-wing aircraft (the Twin Bonanza and another small airplane) were used to map the ground deposition⁷ of the radioactive plume from the Schooner test. One aircraft was used to follow the radioactive plume from the NTS to the East Coast of the United States. The second aircraft was used to map the radioactive ground deposition north of the test location on three different occasions, from roughly one to three weeks after the test. Each aircraft carried an array of fourteen 10-centimeter-diameter by 10-centimeter-thick (4-inch-diameter by 4-inch-thick) sodium iodide (NaI) detectors.

A survey⁸ conducted during 1970 to 1971 ("*the 1970 survey*") covered fourteen regions (mostly the flat and easily flown areas) in and around the NTS. In this survey, a fixed-wing aircraft was flown at a 90-meter (300-foot) altitude and an 800-meter (one-half-mile) flight-line spacing. The survey covered portions of most NTS Operational Areas. The aircraft was equipped with fourteen 10-centimeter-diameter by 10-centimeter-thick (4-inch-diameter by 4-inch-thick) NaI detectors. Since the survey was restricted to areas where the aircraft could easily fly at an altitude of 90 meters AGL, the survey consisted of many geographically separated sections.

In the next several years, the RSL used the radiation fields on the NTS to test new equipment and procedures. The data from these mini-surveys in Area 11 (August 1975) and Area 5 (April 1976 and April 1977) were not reported.

Three small regions within Areas 25 and 26 were surveyed⁹ in September 1976 using a U.S. Air Force UH-1N helicopter at a 45-meter (150-foot) altitude and 60-meter (200-foot) flight-line spacing. The detector array consisted of 40 NaI detectors, each 12.5 centimeters (5 inches) in diameter and 5 centimeters (2 inches) thick. The three regions were situated over a portion of Forty-Mile Canyon, the location of the former Nuclear Rocket Development Station (NRDS) in Area 25 and over the southwest corner of Area 26.

In August and September 1978, a helicopter system with improved sensitivity and spatial resolution as compared to the previously-used, fixed-wing aircraft was employed to survey the NTS¹⁰ ("*the 1978 survey*"). This survey covered portions of many NTS Operational Areas but mainly covered all of Yucca Flat. The Hughes H-500 helicopter was flown at an altitude of 30 meters (100 feet) with a flight-line spacing of 60 meters (200 feet) using an array of twenty 12.5-centimeter-diameter by 5-centimeter-thick (5-inch-diameter by 2-inch-thick) NaI detectors. Both the aerial gamma-ray spectra and the analyses of soil samples led to the identification of isotopes.

In October and November 1980, two surveys¹¹ were conducted in Areas 18 and 20. These surveys were also designed to compare the operation of the MBB BO-105 helicopters with the previously-used Hughes H-500. Twenty 12.5-centimeter-diameter by 5-centimeter-thick (5-inch-diameter by 2-inch-thick) NaI detectors collected a gamma-ray spectrum each second

as the helicopters traversed the survey area at an altitude of 45 meters (150 feet) AGL and a flight-line spacing of 75 meters (250 feet).

Plutonium Valley, which lies in Areas 11 and 3 of the NTS, was surveyed¹² in January 1982 using an MBB BO-105 helicopter operating at an altitude of 30 meters (100 feet) AGL and a flight-line spacing of 45 meters (150 feet) and flying at a speed of 30 meters per second (60 knots). This survey also employed an array of twenty 12.5-centimeter-diameter by 5-centimeter-thick (5-inch-diameter by 2-inch-thick) NaI detectors. During February to May 1982, a survey¹³ of Frenchman Flat, most of Area 5 and the southeastern portions of Areas 6 and 11, was conducted using essentially the same equipment as was used for the Plutonium Valley survey.

All of Area 30 and most of Area 16 were surveyed¹⁴ in June 1983 using the MBB BO-105 helicopter. The survey was conducted at an altitude of 60 meters (200 feet) and a flight-line spacing of 100 meters (330 feet). This survey used the same 20-detector array of NaI detectors that were used in the previous four surveys.

A survey¹⁵ was conducted in October and November 1984 to map the radiation field in almost all of Area 19 and a small section of Area 12 at a 45-meter (150 feet) altitude and 75-meter (250 feet) flight-line spacing. As part of the survey, all of Area 17 and roughly one-half of Area 15 were surveyed at a 45-meter (150-foot) altitude and a 300-meter (1000-foot) flight-line spacing. The same detector array as used in the previous surveys was used. Since this survey was started so late in the year, snow in the higher elevations and hazardous weather in the mountainous regions prevented the completion of the survey. The wide-flight-line spacing used in Areas 15 and 17 caused the data to be under sampled.

Intermittently during the months of May to August 1992, the RSL conducted a site-wide survey¹ ("*the 1992 survey*") of the NTS using two Beechcraft B-200 airplanes. This was the first survey of the NTS that actually covered the entire site. These aircraft flew at a 150-meter (500-foot) altitude, a 1600-meter (1-mile) flight-line spacing, and a speed of 77 meters per second (150 knots). Each aircraft contained a detector array of eight 10- × 10- × 40-centimeter (4- × 4- × 16-inch) NaI detectors. The analysis of the data focused on the exposure rate and man-made gross count (MMGC) rate plots. No spectral analysis was conducted to determine which isotopes were present at any specific location.

The survey included much of the surrounding NAFR and, to avoid air-space conflicts with the U.S. Air Force, was restricted to work only on selected weekends during the summer. The high altitude and wide-flight-line spacing were necessary to complete the survey within time and money constraints. With these concessions, the survey was not meant to be a detailed measurement but more a preview to determine if anything unusual existed. The radius of the footprint that the detector array measured on the ground was about equal to the altitude of the aircraft. Since the flight-line spacing was approximately five times the aircraft's altitude, only about 20 percent of the ground surface was actually measured during this survey. Radioactively contaminated sites that were small in area could have been missed by this survey unless the flight path happened to be directly over the site or the activity of the site was sufficiently high to be detected from large distances. The survey did locate fallout plumes from three nuclear weapons tests that extended outside the boundaries of the NTS.

As a follow-up to the airplane survey, a helicopter survey¹⁶ of the Schooner, Sedan, and Small Boy fallout plumes was conducted in October 1992. This survey was concentrated on three small, off-site areas with the helicopter flying at an altitude of 30 meters (100 feet) to enhance the detection of americium-241 (²⁴¹Am). The helicopter carried a set of eight 5- × 10- × 40-centimeter (2- × 4- × 16-inch) NaI detectors.

2.2 Other Radiological Surveys

In May and June 1992, the RSL performed a series of high-purity germanium (Ge) *in situ* measurements to support environmental restoration work by another DOE contractor. The first Ge survey¹⁷ was performed in Plutonium Valley in Area 11. The survey measured the amounts of ²⁴¹Am and uranium-235 (²³⁵U) still present at three of the four test locations (Project 56, No. 1, 2, and 3 sites). These three locations were chosen because the nuclear weapons safety shots conducted there produced no measurable fission yields. The No. 4 site produced a small fission yield and was, therefore, not of interest for that particular survey.

A secondary RSL purpose for the survey was to test the procedures and instrumentation then being developed for ground-based, *in situ* surveys. The detector was suspended from a 7.5-meter (25-foot) mast mounted on the rear of a four-wheel-drive vehicle. The n-type germanium detector was shielded by a 30-millimeter-thick (1.2-inch-thick) lead and cadmium collimator that produced a roughly 35-meter-diameter (115-foot-diameter) field of view for the gamma rays of interest. This compares to a roughly 100-meter (330-foot) field of view for a helicopter system flying at an altitude of 45 meters (150 feet). Instead of the second-by-second recording of data by the helicopter systems, the Ge detectors recorded gamma radiation from a single location for 900 seconds of live time (LT).

From early 1996 through 1998, a series of small-area surveys were conducted to assist NTS crews in identifying and marking areas of past contamination. In January 1996, a survey of the T-1 site was performed by the Kiwi vehicle. The Kiwi was constructed the previous spring by placing the aerial detector system on a four-wheel-drive vehicle and incorporating new advances in commercially available, differential Global Positioning System (GPS) hardware that permitted positioning accuracies of about ±1 meter (3 feet). Additional surveys in Area 3 (April 1996) and Area 7 (June 1996) were conducted with the Kiwi.

Several regions in Area 3 (December 1996), Area 8 (July 1997), Area 9 (May 1998), and Area 18 (June 1998) were surveyed with a helicopter-based detector system flown slowly at an altitude of 15 meters (50 feet) AGL. These surveys were possible only because there were no obstructions in the areas that would pose a hazard to the aerial operation. Additional low-altitude surveys were conducted at selected locations in Areas 5, 11, 18, 20, 25, and 30 during June 1999. None of the data from the Kiwi or low-altitude aerial surveys have been published.

3.0 MEASURED RADIATION FIELDS

Many components—radiation from sources of interest to the particular investigation, radiation from sources not currently of interest, and electrical noise—contribute to forming the total measured gamma-ray energy spectrum. These components can be summarized as the five terms in the following equation:

$$\text{Measured Radiation Spectrum} = \begin{array}{l} \text{Natural Terrestrial Radionuclides} \\ + \text{Airborne Radon and Its Daughters} \\ + \text{Cosmic Rays} \\ + \text{Man-Made Terrestrial Radionuclides} \\ + \text{Equipment Contributions} \end{array} \quad (1)$$

The term "natural background radiation" is generally considered to comprise the first three terms in the equation: namely, natural terrestrial radionuclides, airborne radon gas and its daughter products, and cosmic rays. The man-made radionuclides (such as ⁶⁰Co and ¹³⁷Cs), produced through human actions, are generally the components of the radiation field of most interest. The final term in this equation represents radioisotopes present in the measuring equipment and all sources of "noise" in the final spectrum—including electrical noise in the electronics.

3.1 Natural Background Radiation

Naturally Occurring Radioisotopes. Long-lived radionuclides present in the earth's crust are usually the largest source of natural background radiation. Naturally occurring, gamma-ray-emitting isotopes found in the soil and bedrock consist mainly of radionuclides from the uranium-238 (²³⁸U) and thorium-232 (²³²Th) decay chains and from potassium-40 (⁴⁰K). The contributions from the ²³⁵U decay chain are a negligible contribution to the natural background (only a few percent as large as the ²³⁸U chain) and are usually ignored. The last of the four major decay chains (beginning with neptunium-237, ²³⁷Np) has a half-life that is too short compared to the earth's age to exist from primordial times and only exists¹⁸ as trace

amounts created by cosmic-ray interactions on ^{238}U . In urban areas, the distribution of these naturally occurring radioisotopes in the roadway and building materials may be different than the composition of the area's bedrock and soil.

The most prominent natural isotopes usually seen in aerial gamma-ray spectra are ^{40}K (0.12 percent of natural potassium), thallium-208 (^{208}Tl) and actinium-228 (^{228}Ac) (daughters in the ^{232}Th chain), and lead-214 (^{214}Pb) and bismuth-214 (^{214}Bi) (daughters in the ^{238}U chain). The naturally occurring isotopes typically contribute 1–15 $\mu\text{R}/\text{h}$ to the background radiation field.¹⁹

Radon and its Daughters. Radon is a noble gas and a member of both the uranium and thorium decay chains. After being created in the soil from its parent radium, radon can diffuse through the soil and become airborne. While the isotopes of radon have relatively short half-lives, their daughters may become attached to dust particles in the atmosphere and contribute to the airborne radiation field until the dust eventually settles to the ground. During a rain shower, much of the airborne particles are washed out of the air and deposited on the ground thus temporarily increasing the amount of terrestrial radiation that is detected.

The contribution of radon and its daughters to the background radiation field depends on several factors including the concentration of uranium and thorium isotopes in the soil, the permeability of the soil, and the meteorological conditions at the time of measurement.²⁰ Average soil releases radon at a rate of 0.02 becquerels per square meter per second ($[\text{Bq}/\text{m}^2]/\text{s}$) and leads to an average air concentration of 8 becquerels per cubic meter (Bq/m^3) (216 picocuries per cubic meter, pCi/m^3) over the northern hemisphere.²¹ Typically, the amount of airborne radiation from radon and its daughters contributes 1–10 percent of the natural background radiation level seen in RSL aerial surveys.

Cosmic Radiation. Cosmic rays entering the earth's atmosphere are the third source of natural background radiation. High-energy cosmic rays (principally protons, alpha particles, and some heavier nuclei) interact with atoms in the upper atmosphere to produce showers of secondary radiation. The secondary radiation consists mainly of electrons, gamma rays, neutrons, and mesons.²² The NaI detectors used in the aerial surveys are sensitive to these secondary gamma rays and x-rays and to gamma rays produced when the electrons and mesons decelerate (producing bremsstrahlung radiation) and annihilate at or near the earth's surface.

The contribution of cosmic rays to the background radiation field varies with elevation above mean sea level and, to a lesser extent, with geomagnetic latitude and the 11-year solar sunspot cycle. The earth's magnetic field traps some of the cosmic rays, so a larger fraction of them reach the poles than the equator. In the continental United States, values range from 3.3 $\mu\text{R}/\text{h}$ at sea level to 12 $\mu\text{R}/\text{h}$ at an elevation of 3000 meters (9800 feet).²³ For surveys in the continental United States, the dependence on geomagnetic latitude is relatively small (15–30 percent with the larger variation occurring at higher elevations). Calculations of the cosmic-ray contribution used in the data analysis discussed later in this report depend solely on the variation with elevation. These calculations are based on the data presented by Lowder and Beck.²⁴

It is important to recognize that the exposure rate attributed to cosmic radiation is a combination of the exposure rates from the electrons, neutrons, and other particles as well as the gamma rays and x-rays. Most of the cosmic-ray exposure rate derives from these particles, not from the gamma rays measured by the NaI detectors on the aircraft. The count rate measured in the NaI detectors and attributable to cosmic rays will change very little through changes in the aircraft's altitude or elevation. Thus, an exposure rate of 1 $\mu\text{R}/\text{h}$ from cosmic rays will produce a very small count rate as compared to an exposure rate of 1 $\mu\text{R}/\text{h}$ from terrestrial radiation.

Worldwide Cesium. Although it is considered a man-made radionuclide, a measurable amount of ^{137}Cs is found throughout the world (initially as a surface deposition and then, over time, migrating several centimeters into the soil) as a result of the atmospheric testing of nuclear weapons. The exposure rate attributed to the ^{137}Cs worldwide fallout varies from 0.1–1 $\mu\text{R}/\text{h}$ ^{25,26} throughout the continental United States.

3.2 Changes in the Radiation Fields

The radiation environment at a survey site may change for any number of reasons. A brief

summary of the reasons follows.

- First, the radionuclides will decay over time. For the time periods between surveys, this is not a factor for the naturally occurring radioisotopes but may be important for the man-made isotopes. The decay chains of the naturally occurring radioisotopes are governed by the extremely long half-lives of the parent isotope that continually replenishes the levels of the daughter isotopes thus keeping the overall activity nearly constant over time. However, a pile of uranium mill tailings (where the uranium has been extracted) will contain all of the daughter decay products but very little of the long-lived parent isotope, and therefore, its activity will decay at the rate of the daughter products.
- Second, new sources of man-made radiation may be created and introduced to the environment. The detection and mapping of this additional radiation is the main impetus behind the aerial surveys.
- Third, old sources of man-made or natural radiation may be removed from the environment (through clean-up programs, mining, etc.). Clean-up operations around radiation laboratories or ore-processing plants will remove some or all of the man-made radiation introduced earlier.
- Fourth, natural or man-made sources of radiation may be transported to new areas (through human activities, rivers, winds, migration of surface-deposited isotopes into the soil, etc.). Through uranium mining operations, natural radioactive materials are removed from one location, transferred to another location, and deposited as unwanted refuse (depleted uranium and the members of both the ^{235}U and ^{238}U decay chains) at another site.
- Fifth, changes in land use can affect the radiation environment. Tilling the soil distributes surface contamination to deeper levels and makes less of the contamination visible to aerial detection. Excavation processes for uranium ore, coal, etc., expose more radioactivity to aerial detection. Construction of buildings on top of the soil changes the activity seen by an aerial detection system. Wood structures attenuate the gamma rays from the soil and produce a lower-measured activity. Brick and concrete buildings may increase or decrease the measured activity levels as compared to the virgin soil depending on whether the brick, sand, and gravel of the construction materials have more or less natural activity than the soil they cover. Similarly, roads may exhibit different radioactivity levels if they were constructed of materials significantly different than the surrounding landscape.
- Sixth, changes in soil moisture (principally from rain) will affect the amount of gamma radiation that is detected by an aerial detector.

4.0 SURVEY EQUIPMENT AND PROCEDURES

Appendix A provides a summary of the survey parameters. The following paragraphs in this section present a brief overview of the data collection procedures used in the survey. They are intended to give the reader a general introduction to the survey process.

4.1 Aerial Measuring System

The survey was conducted using three MBB BO-105 helicopters equipped with similar detection and data-recording systems. One of the helicopters used in this survey is shown in Figure 1 outfitted with two detector pods. The helicopter was flown at a nominal 60 meters (200 feet) AGL over most of the survey area. The flight-line spacing of 150 meters (500 feet) provides some overlap of the detectors' fields of view from one flight line to the next.

The size of this survey and the presence of the mountains and canyons throughout the area made this a difficult survey to determine precise helicopter positions. A navigational system, called the Real-Time Differential Global Positioning System (RDGPS), on board the helicopter determined the helicopter's position each second by receiving signals from the constellation of GPS satellites. Every four seconds, a GPS differential base station (programmed with the precise coordinates for its true position) also determined its position



FIGURE 1. MBB BO-105 HELICOPTER WITH DETECTOR PODS.

Each of the helicopters used during this survey operated the same types of equipment. The detector pods are the rectangular boxes attached to the skid struts on each side, just under the helicopter body. The pods contain a total of eight NaI detectors used during the survey.

from the available satellites and broadcasted a positional correction to the helicopter. The correction term adjusted the helicopter's calculated position, minimizing the errors caused by using only the satellites to determine the helicopter's position. The main GPS antenna sat atop the helicopter's tail fin, and the differential GPS antenna was mounted on the top front of the helicopter's body.

In addition to the GPS base station, two radio repeater systems were installed on sites within the NTS to rebroadcast the GPS base station signal on a different frequency. This arrangement worked well for most of the NTS. However, for surveying the Pahute Mesa area, a second GPS base station was installed in Area 20 since no other radio repeaters were available. The use of two base stations resulted in an offset in the position of the Pahute Mesa data. This positional offset was later corrected in the data analysis process. During the flights, the technician in the helicopter switched the helicopter's GPS receiver to monitor whichever frequency was best for the area. Even with all of these precautions, the differential signal was occasionally lost, and the pilot would then maintain the helicopter along a straight line using a distant landmark sighted during the time when the differential signal was providing accurate positional information.

The uncorrected position of the helicopter was limited by the errors intentionally introduced by the GPS system and could be as large as ± 100 meters (330 feet). With the correction applied, the uncertainty in the helicopter's position was ± 5 meters (15 feet). The mountains and canyons often blocked the differential correction signal; the sudden shift in position of the helicopter caused by the lack of the differential signal could be corrected later in the data analysis process by using a simple calculational algorithm and an appreciable amount of labor by a data analyst.

A radar altimeter system continuously monitored and provided feedback to the pilot of the helicopter's altitude. In the mountainous portions of the survey area, the helicopter could not follow the rapid changes in the elevation of the terrain and instead followed more gentle rises and falls over obstacles in its path. In the far northern region (principally north of Area 15), the pilot maintained the helicopter at a higher altitude while trying to retain contact with the differential GPS signal. For this survey, the accuracy of the radar altimeter was ± 2 percent of the helicopter's altitude.

Two detector "pods" were mounted on the skid struts under the body of the helicopter. Each detector pod carried four 5- \times 10- \times 40-centimeter (2- \times 4- \times 16-inch) rectangular NaI gamma-ray detectors plus a single 5- \times 10- \times 10-centimeter (2- \times 4- \times 4-inch) rectangular NaI gamma-ray detector. The eight rectangular detectors were shielded on the top with sheets of lead and cadmium and viewed the terrestrial radiation field as well as some of the airborne radon, cosmic-ray, and equipment components. The smaller, single rectangular detector was not used.

The computer system that controlled the data collection process is called the Radiation and Environmental Data Acquisition and Recorder, Model IV (REDAR IV). The signals from each of the eight large detectors, matched in amplitude and combined with summing amplifiers, were fed into one of the REDAR IV analog-to-digital converters (ADC).

After conversion, the 1-second spectral data were stored in electronic memory until they were recorded on magnetic tape at the end of each 4-second period. Simultaneously, the output from one of the eight detectors was also fed into another ADC, and its spectrum was recorded to magnetic tape. Since this ADC saw only one-eighth the count rate of the full array, this spectrum was used in those instances where a high-count rate distorted the full-array spectrum.

4.2 Survey Procedures

The data set collected every second during the flight consists of positional and altitude data, atmospheric information, and two gamma-ray energy spectra. The first flight of the survey was a reconnaissance flight conducted above 150 meters (500 feet) to verify and update the existing flight-hazard maps of the NTS. The hazards map was updated with the locations of towers, power lines, or other high structures that would present a hazard to the helicopters flying at 60 meters (200 feet) AGL.

The next two flights were the “perimeter” flights that consisted of flying the helicopters over a series of roads and other structures at the survey altitude. The path traced by the helicopters during these flights would be used to overlay the survey data on a base map or photograph. Since this survey covered such a large area, two helicopters were used to fly roads around the edges of the survey region.

The test line is a short flight path flown at the beginning and end of each flight that is used to check the performance of the detector system and to monitor changes in the nonterrestrial natural background. The path is flown at the survey altitude and survey speed and in the same direction each time. If the detectors are working properly, then any change in the amount of recorded radiation is an indication of a change in the amount of radon in the air (a variation that occurs over several hours) or a change in the cosmic radiation flux (a variation that occurs slowly over several days but can change abruptly due to sun spots). If the detectors are not working properly, the spectral changes will be much larger than those typically encountered as background radiation changes.

Another flight that is flown early in the survey is the altitude profile flight. This flight consists of several traversals of a specific path (usually the test line) conducted at five or six different altitudes. For the NTS survey, these altitudes were 45, 90, 150, 300, and 910 meters (150, 300, 500, 1000, and 3000 feet) AGL. From these data, the air attenuation coefficient and an initial background count rate are determined. These values are used to adjust the measurements for minor fluctuations in altitude during subsequent flights.

The NTS survey consisted of parallel flight lines flown in a north–south direction. The average flight-line length in the central portion of the survey was 80 kilometers (50 miles). This distance limited each flight from the Desert Rock base camp to include the test line, one survey line flying north, one survey line flying south, and the test line again before landing and preparing for the next flight. Each day of the survey, two helicopters were scheduled to fly a total of eight flights. Four flight crews (one pilot and one equipment technician) were used each day.

The detector arrays onboard the helicopters were calibrated against a test range^{27,28} near Lake Mead. A correlation is made between the count rate measured by the detectors flown at the survey altitude and the exposure rate measured with pressurized ionization chambers at 1 meter (3 feet) AGL. Since the detectors measure the radiation field at the altitude of the helicopter, a correction for the attenuation of the gamma-ray intensities through the air must be applied to obtain an exposure rate at 1 meter (3 feet) AGL.

In addition to the air attenuation, another factor that strongly affects the measurements is the presence of liquid water between the radiation source and the detectors. Changes in the relative humidity of the air (water vapor) are not of concern since the gamma-ray absorption for even 100 percent relative humidity is not that much different than for dry air. However, the uncollided gamma rays that reach the detectors originate within the top several centimeters (inches) of the soil, and changes in the amount of water in this region can introduce major discrepancies. The presence of water in the soil also significantly affects the diffusion of radon into the atmosphere. The official amounts of rainfall measured at various locations around the NTS were recorded by the National Weather Service station at the Desert Rock airstrip. During the survey period, the rain showers were generally light and usually occurred during the night or predawn. The ground appeared to be dry as the helicopter was flown over the specific survey area that day.

5.0 DATA REDUCTION PROCEDURES

The goals of data analysis are to locate and resolve areas of natural or man-made radioactivity, to identify radioisotopes that are present, and to quantify the amount of material present in those areas. The first two tasks are relatively easy. Obtaining an accurate, defensible, quantitative value from an aerial survey is much more difficult. The analysis of the radiation data begins with the general routine for calculating the exposure rate and becomes more specific at each following step. The second step is usually calculating the MMGC, which identifies areas that deviate significantly from the typical background radiation of the region. After this step, the analysis may proceed to the extraction of individual isotopes.

There are several methods of processing that may be employed to view the data. The most obvious method is the gross count (GC) algorithm, which is a simple integration of all gamma rays detected at each location. These data may be presented as a plot of gross count rate versus position, or it may be converted into an exposure rate before making the plot. The plot presents the data as a series of exposure-rate contours on a map or photograph of the survey area. With this display, variations in the whole radiation field may be easily seen.

However, variations in the total radiation field are not always of most interest. Often what is important are changes in isotopic concentrations (variations in the energy composition of the radiation field) or the ability to track a single radioactive isotope throughout the survey area. The MMGC algorithm is another integral-based analysis method used to locate regions where the energy content of the gamma-ray spectrum deviates significantly from the energy content of the natural background spectrum.

A third data processing algorithm that is often applied to the data is used to look for a specific isotope throughout the survey area. This algorithm relies on mapping the observed count rate in a narrow-energy window minus a suitably chosen background window to show how that isotope is distributed throughout the survey area.

5.1 Flight-Path Recovery

As discussed earlier, this survey was conducted over a very large area filled with mountains and valleys. Even with employing two radio repeaters and two separate GPS base stations, the helicopter frequently lost communication with the broadcast correction signal from the base station. (At the time of this publication, this was not a problem since several commercial organizations broadcast GPS correction signals from satellites. However, in 1994 those services were not available.) The loss of the correction signal produced a sudden shift in the helicopter's calculated position, which was easily identifiable in the data. However, the number of such occurrences during this survey made the correction process extremely time consuming.

The correction process involved identifying the interval of time when the differential GPS correction signal was lost. Once the start and stop points of this interval were identified, the processing algorithm could use the observed offsets of these points to calculate the apparent drift and drift-rate parameters. Applying the parameters to the drifted data restored the data to its proper location. The algorithm was superior to a simple linear interpolation, especially for long dropout periods since all real flight-path deviations are retained.

5.2 Gross Count Algorithm

The gross count rate measured at the survey altitude is the sum of the counts in the energy range from 38–3026 kiloelectronvolts (keV) divided by the live time minus the count rate attributable to nonterrestrial sources.

$$C_{GC} = \left(\frac{1}{t_{Live}} \sum_{E=38}^{3026} c(E) - C_N \right) e^{\lambda(H-H_0)} \quad (2)$$

where

- C_{GC} = gross count rate at the survey altitude (counts per second, counts/s)
- t_{Live} = live time during collection of gamma-ray spectrum (s)
- $c(E)$ = counts in the gamma-ray energy spectrum at the energy E (counts)
- C_N = count rate attributable to nonterrestrial sources (counts/s)

$$\begin{aligned}\lambda &= \text{air attenuation coefficient (1/meter, m}^{-1}\text{)} \\ H &= \text{actual aircraft height during the measurement (m)} \\ H_0 &= \text{desired aircraft height (m)}\end{aligned}$$

The lower-energy limit is an effective lowest energy that the airborne detector system can reliably record. Although the detector system processes and records all detected gamma rays up to 4000 keV, there are almost no gamma rays of interest having energies above 3000 keV, and the higher energies are generally ignored.

The total number of counts attributable to nonterrestrial sources, C_N , includes gamma rays emitted by airborne radon and its daughters, cosmic rays, and aircraft and equipment contributions. This term is measured by using an altitude profile (see following paragraphs). The radon contribution is generally constant over typical altitude variations during the flight, but can exhibit an appreciable variation from the beginning to the end of the flight due to the usual daily variations in the emission of radon from the ground. The cosmic-ray contribution is constant over typical altitude variations. The aircraft and equipment contribution is assumed to be constant.

The exponential factor corrects this net count rate for variations in altitude. (For example, if the aircraft is momentarily too high, this factor raises the net count rate to what it would have been if the aircraft had been at the desired survey altitude.) The attenuation coefficient λ in the exponential term represents the attenuation of the terrestrial background by the intervening air mass and was determined empirically for the aerial system by performing the altitude profile.

Altitude Profile. The altitude profile is conducted near the beginning of the survey to measure the count rate as a function of altitude. The count rate data from the different altitudes determine the air attenuation coefficient and the initial background count rate at the survey altitude. The count rate measured at each altitude is fit to an equation of the following form:

$$(C_i - C_N) = C_T e^{-\lambda h_i} \quad (3)$$

or alternatively, by taking the logarithm of each side of the equation:

$$\ln(C_i - C_N) = -\lambda h_i + \ln C_T \quad (4)$$

where

$$\begin{aligned}C_i &= \text{gamma-ray count rate measured at each altitude (counts/s)} \\ C_T &= \text{gamma-ray count rate from terrestrial sources (independent of the} \\ &\quad \text{aircraft's altitude) (counts/s)} \\ \lambda &= \text{air attenuation coefficient (m}^{-1}\text{)} \\ h_i &= \text{aircraft height during the measurement (m)}\end{aligned}$$

A background count rate is initially calculated from the lowest- and highest-altitude data using an assumed air attenuation coefficient. The background is assumed to be independent of altitude, even though the cosmic-ray contribution increases slightly over this change in altitude. Then, using this background value and the four lower-altitude data, a linear least-squares fit to $\ln(C_i - C_N)$ versus h_i yields the air attenuation coefficient. The cockpit display of the altitude is not very accurate at the highest altitude, which makes the uncertainty in the highest altitude quite large, so this altitude does not contribute a very useful data point to determine the air attenuation coefficient. If the air attenuation coefficient is much different from the initial (assumed) value, the procedure is iterated until the background count rate and air attenuation coefficient change little from one iteration to the next and are consistent with the measured data.

Using this technique, a value exists for the background count rate, which consists of contributions from airborne radon, cosmic rays, and equipment. The cosmic-ray and equipment contributions to the background count rate are assumed not to change during the

survey, but the amount of radon (and its decay daughters) in the atmosphere will change daily and even hourly. Therefore, the detectors are flown over the test line at the survey altitude at the beginning and end of each survey flight. Increases or decreases in the count rate as compared to the altitude profile count rate represent increases or decreases in the nonterrestrial background.

5.3 Conversion of Gross Count Rate to Exposure Rate

It is usually desired to express the measured radiation field as an exposure rate instead of a gross count rate. Strictly, this can only be performed by a detailed analysis of the gamma-ray spectrum and by using models that relate exposure rate to each gamma-ray energy in the spectrum. However, if the geology of the survey area is similar to the geology at the Bonelli Bay Calibration Range^{27,28} near Las Vegas, Nevada, then the gamma-ray spectra from the two areas will be similar. This calibration range has been calibrated to relate the count rate observed at different altitudes with different detector arrays to the exposure rate measured at 1 meter (3 feet) AGL using a pressurized ionization chamber. As a result of this calibration, an empirically determined factor converts the observed terrestrial count rate to an exposure rate.

$$X_{GC} = \frac{C_{GC}}{F} \quad (5)$$

where

$$\begin{aligned} X_{GC} &= \text{gamma-ray exposure rate at 1 meter AGL } (\mu\text{R/h}) \\ F &= \text{conversion factor } ([\text{counts/s}]/[\mu\text{R/h}]) \end{aligned}$$

The factor of F is the conversion from counts/s measured with the particular detector array at the flight altitude to $\mu\text{R/h}$ measured with a pressurized ionization chamber at 1 meter (3 feet) AGL. The conversion factor assumes a uniformly distributed radiation source over an area that is large compared to the detector's field of view and has a radioisotopic distribution similar to that of the natural background of the calibration range.

5.4 MMGC Algorithm

The GC algorithm maps the variations in the terrestrial radiation field. This is not always the most useful presentation of the data. Changes in the GC data may indicate the presence of man-made radionuclides or they may simply indicate changes in the quantity of natural radionuclides caused by changes in the types of rock or soil. Similar changes in the GC data may be caused by an abrupt change in the vegetation coverage. (A forest area will attenuate the gamma rays much more than a grassy meadow.) Generally, for purely background radiation, the shape of the gamma-ray energy spectrum is fairly constant, and variations in the GC data can be represented by scaling the energy spectrum measured at one location to fit the new location.

The MMGC algorithm is a means of identifying regions in the survey area where the shape of the energy spectrum deviates significantly from the shape of the background, or reference, spectrum. Through its definition, the MMGC algorithm is very sensitive to small changes in the abundance of man-made isotopes while being very insensitive to large changes in the abundance of natural isotopes.

The algorithm relies on two basic characteristics. First, the energies of naturally occurring isotopes occur throughout the measured energy range (0–4000 keV). Second, the man-made isotopes that have half-lives long enough to be dispersed from their creation site and then to be seen by an aerial survey generally have gamma-ray energies below about 1400 keV.

This situation can be exploited by measuring the gamma-ray spectrum in a reference (background) region known to contain only naturally occurring isotopes. This reference region provides a ratio of the low-energy to high-energy count rate, which will be applied to succeeding measurements to determine the gamma-ray spectrum attributable to activity by man-made isotopes in the area. This process is used effectively in locating regions of man-made isotopes, but "false-positives"—regions that deviate from the originally measured

background spectrum simply because they have different relative abundances of the naturally occurring radioactive isotopes embedded in their rock formations— can also be found. Usually, the number of regions identified by the MMGC algorithm is small enough that a detailed analysis of the gamma-ray spectrum for each region can be made to determine which isotopes are present.

Using an energy spectrum from an area known to contain only naturally occurring radioactive isotopes, the ratio of the number of counts in the spectrum below a cutoff energy to those above that energy is defined as K_{MM} . The following equation shows this ratio where the cutoff energy (1394 keV) is determined by details of how the spectrum is compressed and stored. Almost no gamma rays are observed beyond the ^{208}Tl peak at 2614 keV, so an arbitrary upper limit of 3026 keV is chosen as the end of the high-energy range.

$$K_{MM} = \frac{\sum_{E=38}^{1394} C_{ref}(E)}{\sum_{E=1394}^{3026} C_{ref}(E)} \quad (6)$$

where

$$\begin{aligned} K_{MM} &= \text{ratio of the low-energy counts to high-energy counts in the background spectrum} \\ C_{ref}(E) &= \text{count rate in the reference gamma-ray energy spectrum at the energy } E \text{ (counts/s)} \end{aligned}$$

Although this ratio is fairly constant over the survey area, the individual man-made ratio values were derived and used for each flight to optimize the data analysis procedures. The MMGC algorithm calculates the integrated counts **observed** below the cutoff energy minus the integrated counts **expected** below the cutoff energy. The MMGC rate is calculated as follows:

$$C_{MM} = \sum_{E=38}^{1394} C(E) - K_{MM} \sum_{E=1394}^{3026} C(E) \quad (7)$$

where

$$\begin{aligned} C_{MM} &= \text{MMGC rate at the survey altitude (counts/s)} \\ C(E) &= \text{count rate in the gamma-ray energy spectrum at the energy } E \text{ (counts/s)} \end{aligned}$$

In regions where there are no man-made isotopes, this equation reduces to statistical fluctuations about zero. In past studies, the MMGC algorithm described here has been shown to be sensitive to low levels of man-made radiation ($< 1 \mu\text{R/h}$) even in the presence of large variations in the natural background. In practice, this algorithm is a general search tool to locate regions of anomalous radioactivity.

5.5 Isotopic Extraction Algorithms

The algorithms employed in the search for particular isotopes are quite similar to the MMGC algorithm. The major difference is that instead of using the full gamma-ray energy spectrum, only a few small portions of it are used. Figure 2 illustrates the window algorithms discussed in the following paragraphs.

2-Window. The 2-window algorithm is the simplest of several window algorithms in use. It employs a narrow window centered on the energy of the specific photopeak. The algorithm assumes that the background counts in the photopeak window are proportional to the counts recorded in a background window located at higher energies. The background window may abut the photopeak window or may be separated from it in energy. Note that the form of the equation for $C_{2\text{-Window}}$ is identical in form to the equation for C_{MM} previously defined.

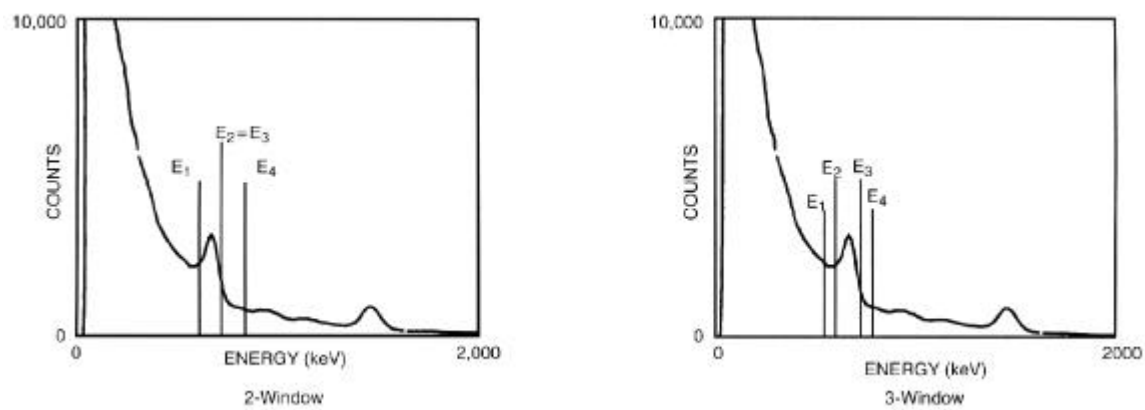


FIGURE 2. 2-WINDOW AND 3-WINDOW ALGORITHMS APPLIED TO A TYPICAL SPECTRUM

$$C_{2-Window} = \sum_{E=E_1}^{E_2} C(E) - K_2 \sum_{E=E_3}^{E_4} C(E) \quad (8)$$

with

$$K_2 = \frac{\sum_{E=E_1}^{E_2} C_{ref}(E)}{\sum_{E=E_3}^{E_4} C_{ref}(E)} \quad (9)$$

where

$$\begin{aligned} C_{2-Window} &= \text{count rate from the 2-window algorithm} \\ E_n &= \text{limiting energies of the windows } (E_1 < E_2 \leq E_3 < E_4) \\ K_2 &= \text{ratio of the counts in the photopeak window to the counts in the} \\ &\quad \text{background window in the reference region of the survey area} \end{aligned}$$

The proportionality factor is determined in a region of the survey that does not contain any of the specific isotope so that the photopeak window contains only its background counts and, therefore, can be simply related to the number of counts in the background window. If the principle source of background gamma rays in the photopeak window is from scattered gamma rays from photopeaks at higher energies, this is a good assumption. If there are other isotopes with photopeaks in or near the photopeak window, then this algorithm will likely fail.

3-Window. If a reference region, free of the specific isotope, cannot be found or if the composition of the other isotopes changes drastically between the reference region and the rest of the survey area, then a simple multiplicative factor will not relate the counts in the photopeak window to the counts in the background window. To solve this problem, the 3-window algorithm employs a background window on each side of the photopeak window. (The two background windows generally abut the photopeak window in energy.) This algorithm assumes that, for any spectrum, the number of background counts in the photopeak window is linearly related to the counts in the two background windows.

$$C_{3-Window} = \sum_{E=E_2}^{E_3} C(E) - K_3 \left(\sum_{E=E_1}^{E_2} C(E) + \sum_{E=E_3}^{E_4} C(E) \right) \quad (10)$$

with

$$K_3 = \frac{\sum_{E=E_2}^{E_3} C_{ref}(E)}{\sum_{E=E_1}^{E_2} C_{ref}(E) + \sum_{E=E_3}^{E_4} C_{ref}(E)} \quad (11)$$

where

- $C_{3-Window}$ = count rate from the 3-window algorithm
- E_n = limiting energies of the windows ($E_1 < E_2 < E_3 < E_4$)
- K_3 = ratio of the counts in the primary window to the counts in the two background windows in a reference region of the survey area

The 3-window algorithm is also very useful in extracting low-energy photopeak counts where the shape of the Compton-scatter contributions from other isotopes is changing significantly. This is the algorithm used for calculating the ^{241}Am contour plots.

5.6 Gamma Spectral Analysis

The MMGC algorithm is very general and is sensitive to any change in the low-energy portion of the spectrum. It does not identify the causes of the change. The changes can be caused by (a) a true man-made isotope present in the region, (b) the gamma rays from the naturally occurring isotopes having undergone more inelastic scatterings before reaching the detectors (for example, a change from a grassy meadow to a dense wooded area), or (c) the isotopic composition of the spectrum in this region of the survey being significantly different from where K_{MM} was determined (for example, granite versus limestone). Once a region appears in the man-made contours, the energy spectrum is searched for individual isotopes. An analysis of the gamma-ray spectrum will determine the isotopes that are present in the spectrum and caused the MMGC deviation.

Generally, the large background field (due to the naturally occurring isotopes) is not of interest—only the portion of the spectrum due to the man-made isotopes. Unfortunately, the number of counts at any given energy in a single 1-second measurement is so small as to make the identification of a particular isotope very difficult. To increase the number of counts in the spectrum (and thus produce better statistics), the spectra from neighboring locations are combined to produce a single spectrum showing the radiation measured over some larger area.

Figure 3 shows how the "net" spectra are determined for three closely spaced areas. Each area is divided into "peak" and "background" regions. The contour levels used to define the peak and background regions are usually MMGC levels. The peak and background boundaries may be defined by other means—GC contour levels or simple rectangular boxes may also be used. The peak region of the spectrum consists of the spectra contained in the area bounded by the chosen contour level. The background region consists of the spectra contained in the rectangular box but outside the chosen contour level (shaded area). This partitioning generally guarantees that the background spectrum is representative of the geology near the anomaly, but there will be some contribution of man-made radioactivity in the background region.

This technique produces a net spectrum that has very little contribution from the naturally occurring radionuclides in the region and makes the identification of the remaining isotopes fairly easy. The technique has one major drawback as it does not necessarily produce a true indication of the strength of the isotopes seen in the net spectrum. That is, comparing the intensity of an isotope in one net spectrum with the intensity of that same isotope in another spectrum may not be very meaningful.

There are two principal methods used to scale the background spectra when creating the net gamma-ray spectra. The first of these methods uses the live times of the peak and back

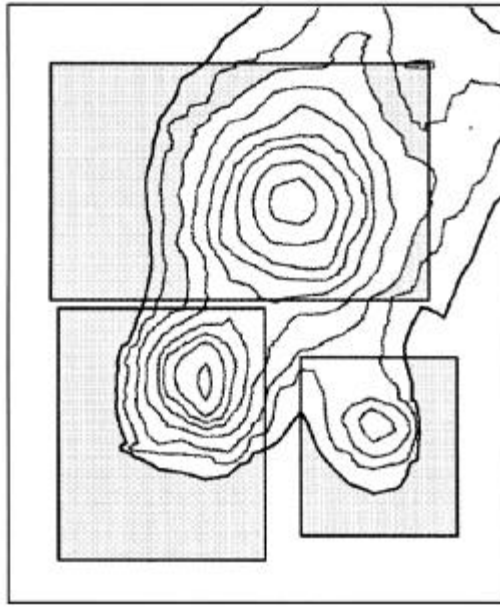


FIGURE 3. DEFINITION OF PEAK AND BACKGROUND AREAS AROUND A RADIATION ANOMALY. This figure illustrates the boundaries used for three spectra from closely-spaced anomalies. The net spectra presented in this report are created by subtracting the background spectrum from the peak spectrum. The peak spectrum is formed from all 1-second spectra collected within the boundaries of a specified contour level. The back-ground spectrum is formed from all 1-second spectra collected outside the boundaries of a specified contour level (but within a specific rectangular area).

ground regions to normalize the results while the second method normalizes the two spectra based on the total counts in a specific portion of the spectra. These two methods generally create spectra that are very similar, but there are subtle differences between the approaches.

Time Normalization. In this method, the net spectrum results from subtracting the background spectrum, normalized by the ratio of the peak live time to the background live time, from the peak spectrum.

$$c_{Net}(E) = c_{Peak}(E) - \frac{T_{Peak}}{T_{Bkg}} c_{Bkg}(E) \quad (12)$$

where

$$\begin{aligned} c_{Net}(E) &= \text{counts in the net energy spectrum at the energy } E \\ c_{Peak}(E) &= \text{counts in the peak energy spectrum at the energy } E \\ T_{Peak} &= \text{total live time for the spectrum comprised of all peak-region spectra (s)} \\ T_{Bkg} &= \text{total live time for the spectrum comprised of all background-region spectra (s)} \\ c_{Bkg}(E) &= \text{counts in the background energy spectrum at the energy } E \end{aligned}$$

This method of normalization is usually the first employed since it is relatively straightforward to calculate. If there is an excess of naturally occurring radioisotopes, the net spectrum will preserve the high-energy photopeaks of these isotopes. However, cleaner spectra are generally produced with the next normalization method.

High-Energy Count Normalization. The second method of normalizing the energy spectra assumes that the concentrations of the natural radioisotopes are the same in the peak and background spectra. If this is the case, then the background spectrum can be scaled by the ratio of the counts in the high-energy portion of the peak-region spectrum to the counts in the background-region spectrum before it is subtracted from the peak spectrum.

$$c_{Net}(E) = c_{Peak}(E) - \left(\frac{\sum_{E_1}^{E_2} c_{Peak}(E)}{\sum_{E_1}^{E_2} c_{Bkg}(E)} \right) c_{Bkg}(E) \quad (13)$$

where

$$\begin{aligned} E_1 &= \text{low-energy limit for the normalization range} \\ E_2 &= \text{high-energy limit for the normalization range} \end{aligned}$$

The two energies can be chosen in several ways. They can be chosen to cover the whole MMGC upper-energy range (1394–3026 keV), or they can be chosen to cover just a small range of energies (1700–2200 keV was chosen for some of the spectra shown in this report).

This method has the advantage of suppressing most, if not all, of the natural radioisotopes occurring in the upper-energy range of the net spectrum. This method generally produces the cleanest subtraction when trying to separate low-energy contributors. The major drawback of this method is also its main advantage. If naturally occurring radioisotopes contribute to the regions of man-made activity, this method will suppress the high-energy photopeaks and, since not all of the photopeaks necessary to identify an isotope will be present, the isotopic identification process will then be uncertain.

Spectral Distortions. When the survey has been performed over an area exhibiting large, rapid variations in the elevation of the terrain, the net spectra can suffer from another type of error. In the case where the aircraft is flown at a constant elevation over a canyon or begins to climb early to pass over a mountain, the added air mass distorts the gamma-ray spectrum by removing more of the low-energy gamma rays than the higher-energy gamma rays. If this increased altitude occurs in spectra that will be used to assemble the background spectrum, then the background will be slightly deficient in low-energy gamma rays. Subtracting the background from the peak spectrum will produce a net spectrum that has no discernable photopeaks but only a gently varying low-energy excess of gamma rays.

If the survey contains areas of very high activity, the count rate in the detectors may become high enough to distort the spectra. This distortion results from having insufficient time between the electrical pulses generated by the detector amplifiers. When these pulses reach the ADC, one pulse is superimposed on the tail of another pulse, and the ADC determines a voltage for this combined pulse that is no longer characteristic of the individual pulses. At moderate count rates, this distortion may appear as a broadening of the photopeak widths and possibly as a shift in the photopeak's apparent energy. At very high-count rates, these effects become more severe, and it may be nearly impossible to recognize any pattern to the photopeaks present in the spectrum.

6.0 DISCUSSION OF RESULTS

Since many of the regions of enhanced man-made radioactivity had already been located in the previous surveys of the NTS, the main data-reduction interest for this survey was the MMGC method. The GC method was used principally as a check to ensure that the data from adjacent flights matched each other and to provide a picture of the overall radiation field in the survey area.

The different results of this aerial radiological survey are presented as a series of colored regions superimposed on USGS maps. The aerial platforms collect data from a large area on the ground, and the count rates (or exposure rates) stated in the figures may not accurately reflect the situation at 1-meter above the ground. If a hot spot is 30 meters (100 feet) off to the side of the flight line, the count rate at the aircraft's position will be elevated above the

background count rate. The count rate directly below the aircraft at 1-meter above the ground may be much less since the hot spot is not visible at this altitude. For this reason, the figures contain a statement that the measurements are made at the aircraft's flight altitude and are extrapolated to 1-meter above ground.

If a measurement made at the one-meter height could detect the radiation emitted from the whole area seen by the aerial platform, then the plots could be compared directly with ground-based field measurements. In areas where the radiation field is fairly constant, this is a very good approximation. When a hot spot occurs that can be detected by the aerial platform but is shielded from a detector on the ground, there may be significant differences between the two measurement techniques. There will also be large differences between the two techniques for very hot spots that are located several flight lines away from the aircraft. Even though the source is quite far away, some of the gamma rays can reach the aerial detector and produce an elevated count rate at a location where increased activity would not be detected at ground level.

Since there are large variations in the elevation of the survey area, different cosmic-ray contributions occur at the different elevations. In these cases, the cosmic-ray contribution is left out of the figure (and a note describing the range of values is included in the legend).

6.1 Gamma-Ray Exposure Rate

The gross count-rate data have been converted into units of exposure rate ($\mu\text{R}/\text{h}$). As discussed in Section 5.3, a multiplicative factor was applied to the gross count rate after the nonterrestrial background count rate was subtracted. Over most of the NTS, the naturally occurring radioisotopes are the only contributors to the terrestrial exposure rate. In regions where there are man-made radionuclides present or where the composition of the natural radionuclides changes significantly from the calibration region (for example, the Black Mountain caldera in the northwest corner of the survey region), this calculation will not produce an accurate exposure-rate value, but it is a reasonable estimate useful for general comparisons.

Figure 4 presents the exposure rates inferred from the 1994 aerial data superimposed on a map of the NTS. The contour levels indicate the exposure rate at 1-meter AGL excluding the cosmic-ray exposure contribution. The cosmic contribution varies from 4.5–8.5 $\mu\text{R}/\text{h}$ at elevations ranging from 900–2400 meters (3000–8000 feet). Because such large changes in elevation occurred within the survey area and the cosmic contribution varied by almost a factor of two over the survey area, the cosmic-ray contribution was not included in the plot.

Note that the natural background exposure rates in the southeast corner of the site are in the 0–6 and 6–12 $\mu\text{R}/\text{h}$ ranges. The exposure rates increased toward the north, with the Pahute Mesa area (in the northwest corner of the NTS) mostly in the 12–24- $\mu\text{R}/\text{h}$ exposure-rate range but having numerous areas as high as the 24–30- $\mu\text{R}/\text{h}$ range. Also in this northwest corner of the survey region is a circular arc of activity predominantly at the “green and yellow” levels. This is part of the Black Mountain caldera, a natural geologic formation having an exposure-rate range of 24–50 $\mu\text{R}/\text{h}$.

Appendix A contains a table that summarizes the exposure rates reported from the different surveys conducted over the NTS from 1970 through 1994. In general, there is very good agreement between the different reported values. The exposure rates reported from the helicopter surveys in the 1983–1984 time period tend to be somewhat higher than the exposure rates from other surveys over the same areas. There are several exposure rates from the 1970 survey that are anomalously high. In some cases, these higher readings can be attributed to an error in the published 1970 report that presents hand-drawn contours at the 11–20- $\mu\text{R}/\text{h}$ and 31–50- $\mu\text{R}/\text{h}$ levels in the Yucca Flat area but does not show the 21–30- $\mu\text{R}/\text{h}$ contour level.

6.2 MMGC Rate and Individual Isotopic Contours

As discussed in Section 5.4, the GC-based exposure rate is not always the most informative presentation of the data. The MMGC analysis method emphasizes the portion of the energy spectrum that is most sensitive to radioactive isotopes produced through human actions. The MMGC determines the number of counts which should be present in the low-energy region of the spectrum based on the number of counts that are recorded in the high-energy region. The difference between the number of low-energy counts recorded and the number of counts

expected is a measure of the radioactivity caused by man-made nuclides.

Figure 5 displays the MMGC contour levels superimposed on a map of the survey area. The contour levels identify many locations of enhanced radiation that might be caused by human actions in the area. Since the elevated activities seen in this figure are caused by a variety of isotopes, the use of exposure-rate units is used simply as a relative reference. For the MMGC data, the conversion from count rate to exposure rate assumes the same conversion factor that is applied to the natural background. Depending upon whether the average energy of the radiation emitted by the man-made isotope is more or less than the average energy of the radiation emitted by the naturally occurring radioisotopes at the calibration range, this process will either underestimate or overestimate the exposure rate due to the man-made isotopes.

The areas of man-made contamination at the NTS are divided into six subsets for further detailed presentations. Figures 6–17 show the MMGC contour levels in these expanded regions plus the gamma-ray spectra associated with the locations of elevated activity. Each spectrum is labeled with a region of interest (ROI) number that also appears on the contour plot. The gamma-ray spectrum for each location must be studied to determine which isotopes are present.

A typical background spectrum is shown for each of the six subsets of man-made activity. The ^{238}U and ^{232}Th decay chains and ^{40}K produce the majority of the gamma activity in the background areas of the survey. In general, these background spectra are the same shape, but the amplitude of the peaks in the spectra vary directly with the change in exposure rate for the area they represent.

Very few gamma rays having energies between 3000 and 4000 keV were recorded by the detector system. To make the displayed spectra more readable, the few gamma rays observed above 3000 keV are not included. The spectra plotted in these figures are the result of subtracting the background spectrum from the peak spectrum. This technique is good for identifying the radionuclides that are present, but it is not necessarily the best way to determine the quantity of the particular radionuclide that is present.

Figure 18 displays the locations where the 3-window algorithm exhibits a net positive count rate for the ^{241}Am photopeak. Locations with high ^{241}Am count rates definitely are contaminated with ^{241}Am . Those locations having low ^{241}Am count rates require further investigation since there are other man-made isotopes that can interfere with the algorithm used to produce this plot. Locations having ^{241}Am contamination also contain significant quantities of the plutonium isotopes and thus are locations that can be considered areas posing inhalation or ingestion health risks. These isotopes are generally deposited near locations of safety shots or other tests where the weapons material was not significantly dispersed.

The value at each 1-second sample location along a flight line is averaged with its two closest neighbors (three-point averaging). This smooths the variations in the data set and slightly increases the detectability of the system compared to the original, unsmoothed data set. To further increase the detectability of the system for ^{241}Am , the lowest-count-rate contour in the ^{241}Am plots is calculated by averaging over 15 points.

The areas of ^{241}Am contamination at the NTS are divided into four regions for further detailed presentations. Figures 19–24 show the ^{241}Am contour levels in these expanded regions plus the gamma-ray spectra associated with the ROIs not identified in the man-made contour plots.

6.3 Discussion of Anomalies in Each Area

The major man-made isotopes identified in the various NTS surveys are listed with their respective half lives in Table 6-1. Many of the sites identified in previous surveys were contaminated with short-lived isotopes that decayed away by the next survey. Other sites, for example, the NRDS in Area 25, were handling large quantities of radioactive materials in the 1960s and 1970s. When the aerial surveys in the 1990s were conducted over Area 25, these operations had been halted for many years, and a significant amount of cleanup work had been conducted. Thus, the absence of short-lived, and even sometimes long-lived, isotopes in recent surveys should not be surprising.

Table 6.1 also lists the gamma-ray energies of the isotopes identified in this survey. Gamma-ray photopeak intensities at the energies listed in *italics* are sufficiently weaker than the intensities of the other energies for that isotope. Therefore, photopeaks listed in italics do not need to be visible in the spectra to confirm the presence of the isotope. In addition, interference from other isotopes may mask some of the photopeaks at other energies.

DISCUSSION OF RESULTS

Several surveys covered the whole site, or most of it, and will be mentioned in the discussion of each NTS area. These surveys will be identified solely by their generic name (“*the 1970 survey*,” “*the 1992 survey*,” and “*the 1994 survey*”) and were cited in Sections 1.0 and 2.1.

As described earlier, the 1970 and 1992 fixed-wing surveys used very wide flight-line spacings and were intended to locate and map large general features. It was recognized at the time that most small contaminated areas would be missed. Also, unless the aircraft flew directly over the contamination, the measured intensity would be low and the centroid of the activity would be displaced from its true location. With these caveats in mind, the measured results from these two surveys are included in this discussion. They will be shown in *italics* to indicate that they may have significant distortions induced by the wide-flight-line spacing, or alternatively, the sparse sampling of the terrestrial radiation field.

In the discussion that follows, a specific nuclear test may be described to provide background information to the observed exposure rates and radioisotopes for a specific location. In such cases, the test information is taken from *United States Nuclear Tests*² unless otherwise attributed. Information regarding the locations of specific tests were obtained from the NTS Geographical Information System (GIS) database operated by Bechtel Nevada.

Table 6-1. Radioisotopes and Half-Lives.

The isotopes listed in this table were identified in aerial radiological survey reports of the NTS from the past 30 years. Some of the isotopes would not be expected to be present for more than a few years after their creation.

Isotope	Half-Life (yr)	Gamma-Ray Energies (keV)	Comments
⁵⁴ Mn	0.86		
⁶⁰ Co	5.27	1173.2, 1332.5	
⁶⁵ Zn	0.67		
¹⁰¹ Rh	3.3		
^{102m} Rh	0.57		
¹²⁵ Sb	2.77		
¹³⁴ Cs	2.06		
¹³⁷ Cs	30.1	661.6	
¹⁵² Eu	13.3	121.8, 344.3, 778.9, 964.1, 1085.9, 1112.1, 1408.0	
²⁰⁸ Tl	—	510.8, 583.2, 860.4, 2614.5	daughter of ²³² Th half-life = 14.0 *10 ⁹ yr
²¹⁴ Bi	—	609.3, 1120.3, 1764.5, 2204.1	daughter of ²³⁸ U half-life = 4.47 *10 ⁹ yr
²²⁸ Ac	—	338.4, 911.1, 968.9	daughter of ²³² Th half-life = 14.0 *10 ⁹ yr
^{234m} Pa	—	766.6, 1001.0	daughter of ²³⁸ U half-life = 4.47 *10 ⁹ yr
²³⁵ U	703,800,000	143.8, 185.7	
²³⁹ Pu	24,110		
²⁴¹ Am	432.2	59.5	daughter of ²⁴¹ Pu half-life = 14.7 yr

Area 1. A summary of the locations containing man-made activity, as shown in Figure 17, is presented in Table 6-2. The T1 site (ROI 32) was the location of four tower (atmospheric) tests. The Easy test was conducted on May 7, 1952, with a published yield of 12 kilotons (kt). The Simon test was conducted on April 25, 1953, with a published yield of 43 kt. The Apple-2

DISCUSSION OF RESULTS

test occurred on May 5, 1955, with a yield of 29 kt, and the Galileo test was conducted on September 2, 1957, with a yield of 11 kt.

The 1970 survey identified only one relatively high-activity region centered at the T1 location. A narrow band of activity extended from about 1 kilometer southeast of T1, up through T1, and then broadened significantly as it extended north–northwesterly from T1 into Area 4 and then into Area 2. No other localized regions of activity were observed.

The 1978 survey¹⁰ reported high-man-made activity over the T1 site and also detected four smaller “satellite” regions clustered around that site. Two of the four small satellite locations (ROIs 34 and 35) were labeled as waste dump sites in the 1978 report. The other two locations (ROI 33 and north of ROI 32) did not have any designations and contained much lower activity spread over slightly larger areas. The isotopes identified from the 1978 survey were a combination of the isotopes seen in the aerial gamma-ray spectra and the isotopes seen in spectra taken from soil samples.

The 1992 survey was conducted at a higher altitude with wide-flight-line spacings, and only the T1 site activity was detected. The reported exposure rate from the 1992 survey was significantly lower than from the other surveys since the aircraft most likely was not flown directly over the T1 location. The spatial resolution of the survey was insufficient to observe the small “satellite” regions around the T1 site.

The 1992 survey detected the same five locations as the 1994 survey. The man-made activity contours are shown in Figure 17 with the corresponding gamma-ray energy spectra for the identified ROIs in Figure 16. The man-made activity of the T1 site was roughly one-half of the level measured in 1978. The locations southeast and north of T1 did not exhibit a large change in activity levels. The two sites labeled as waste dump sites in the 1978 survey had significantly lower-activity levels in 1994 than in 1978. The three small-area ²⁴¹Am contours shown in Figure 24 are clustered around the T1 location and are expected to be statistically insignificant.

Area 2. A summary of the locations containing man-made activity, as shown in Figure 17, is presented in Table 6-3. The central test area (T2; ROI 44) hosted four tests from towers: How (June 5 1952; 14 kt), Badger (April 18, 1953; 23 kt), Turk (March 7, 1955; 43 kt), and Whitney (September 23, 1957; 19 kt). To the southeast of T2, the Shasta test was conducted

Table 6-2. Summary of Detected Man-Made Sources in Area 1

Location	ROI	Survey Date	Exposure-Rate Range (μR/h)	Isotopes Identified
T1	32	1970	200	⁶⁰ Co, ⁶⁵ Zn
		1978	300–1000	⁶⁰ Co, ¹³⁷ Cs, ¹⁵² Eu, ²⁴¹ Am
		1992	36–72	not analyzed
		1994	270–900	¹³⁷ Cs, ¹⁵² Eu, possible ⁶⁰ Co
Southeast of T1	33	1978	10–30	not analyzed
		1994	18–24	¹³⁷ Cs
Northwest of T1 (near)	34	1978	~100	not analyzed
		1994	18–24	nothing identifiable
Northwest of T1 (far)	35	1978	30–100	not analyzed
		1994	24–30	¹³⁷ Cs, ¹⁵² Eu
North of T1		1978	10–30	not analyzed
		1994	12–18	¹³⁷ Cs, ¹⁵² Eu

at site T2A (ROI 45) from a tower with a yield of 17 kt on August 18, 1957. To the northeast of T2, the Diablo test was conducted from a tower at site T2B (ROI 46) with a yield of 17 kt

DISCUSSION OF RESULTS

on July 15, 1957.

The 1970 survey identified only one relatively high-activity region that is a merger of T2 and T2B. A band of activity extended from T1 in Area 1 through the western half of Area 4 and into the southwest corner of Area 2. In addition, a narrow band of activity was observed along the southern edge of Area 2.

The 1978 survey¹⁰ reported high-man-made activity over the T2 site, slightly lower activity levels at T2A and T2B, and two little satellites northwest (ROI 47) and southwest of T2. In the northeast corner of Area 2, there were some small spots of elevated counts that appeared to be related to the SEDAN crater.

The 1992 survey recorded three rather broad, low-activity regions over three of these locations. The wide-flight-line spacing resulted in the aircraft not being directly over any of the sites. Therefore, the peak activities are low, and the center of the activity is displaced.

The 1994 survey detected six locations of man-made activity (Figure 17) with the corresponding gamma-ray energy spectra for the identified ROIs in Figure 16. The six locations include the five locations identified in the 1978 survey plus one new spot in the northeast portion of the Area 2 Camp. The small-area ²⁴¹Am contours shown in Figure 24 are clustered around the T2 location and are expected to be statistically insignificant.

Area 3. A summary of the man-made and ²⁴¹Am activity locations in Figures 17 and 24 is presented in Table 6-4. The southern portion of the three large test areas (T3B, ROI 27) is the location of just one test: Fizeau was detonated from a tower on September 14, 1957, with a yield of 11 kt.

The central test area (T3A, ROI 28) hosted two tests conducted from towers: Harry (May 19, 1953; 32 kt) and Hornet (March 12, 1955; 4 kt). Also in this same immediate area were two other test locations: S3H hosted Coulomb-A (July 1, 1957; 0 kt), a safety experiment conducted at ground level, and T3S hosted Rio Arriba (October 18, 1958; 0.09 kt) on a tower.

Table 6-3. Summary of Detected Man-Made Sources in Area 2

Location	ROI	Survey Date	Exposure-Rate Range (μR/h)	Isotopes Identified
T2	44	1970	200	⁶⁰ Co, ¹³⁷ Cs
		1978	300–1000	⁶⁰ Co, ¹³⁷ Cs, ¹⁵² Eu, ²⁴¹ Am
		1992	18–24	not analyzed
		1994	270–900	¹³⁷ Cs, ¹⁵² Eu
T2A (Shasta)	45	1978	30–100	⁶⁰ Co, ¹³⁷ Cs, ¹⁵² Eu, ²⁴¹ Am
		1992	18–24	not analyzed
		1994	30–39	¹³⁷ Cs
T2B (Diablo)	46	1970	51–100	not analyzed
		1978	30–100	⁶⁰ Co, ¹³⁷ Cs, ¹⁵² Eu, ²⁴¹ Am
		1992	18–24	not analyzed
		1994	30–39	¹³⁷ Cs
Southwest of T2		1978	10–30	not analyzed
		1992	12–18	not analyzed
		1994	12–18	¹³⁷ Cs
Northwest of T2	47	1978	100–300	not analyzed
		1994	12–18	¹³⁷ Cs, ¹⁵² Eu
Area 2 Camp	48	1994	24–30	^{234m} Pa

DISCUSSION OF RESULTS

The northern test area (T3, ROI 29) hosted four tower tests: George (June 1, 1952; 15 kt), Annie (March 17, 1953; 16 kt), Moth (February 22, 1955; 2 kt), and Franklin (June 2, 1957; 0.14 kt).

The spot just east of T3 (ROI 30) overlaid the Pike test location (U-3cy). Pike was an underground test (U-3cy) conducted on March 13, 1964, with a yield of less than 20 kt. An accidental release of radioactivity was detected off-site following this test.

The spot west of T3 (ROI 31) was closest to the location of the Otero test of September 12, 1958. That test was conducted in an unstemmed (open) shaft (U-3q) and had a yield of 0.038 kt. A strong ^{241}Am photopeak and a modest ^{137}Cs photopeak were present in the spectrum from this location.

Several other aboveground tests were conducted near the three large test areas, and those tests may have been contributors to the expanded man-made distribution around these sites. Also, there were many underground tests near these sites, and it is possible some of them contributed to the overall contamination. The data collected from aerial surveys did not indicate when the radioisotopes were deposited, and therefore, determining which test released the material must be based either on historical reports of releases from a test, geographic isolation of the tests, or some other information that could distinguish the tests.

The 1970 survey detected three spots within a larger region of slightly lower contamination. The resolution of the system was insufficient to detect the small sites, and the 800-meter (one-half-mile) flight-line spacing was large enough that the central test area was almost missed. The exposure rate at each site was underestimated since the flight lines did not pass directly over the hottest portions of the sites.

Table 6-4. Summary of Detected Man-Made Sources in Area 3

Location	ROI	Survey Date	Exposure-Rate Range ($\mu\text{R/h}$)	Isotopes Identified
T3B (Fizeau)	27	1970	200	^{60}Co , ^{65}Zn , ^{134}Cs , ^{137}Cs
		1978	300–1000	^{60}Co , ^{137}Cs , ^{152}Eu , ^{241}Am
		1992	18–24	<i>not analyzed</i>
		1994	120–270	^{137}Cs , ^{152}Eu
T3A, T3S, S3H	28	1970	~50	<i>not analyzed</i>
		1978	300–1000	^{60}Co , ^{137}Cs , ^{152}Eu , ^{241}Am
		1994	120–270	^{137}Cs , ^{152}Eu
T3	29	1970	100+	<i>not analyzed</i>
		1978	~300	^{60}Co , ^{137}Cs , ^{152}Eu , ^{241}Am
		1992	24–36	<i>not analyzed</i>
		1994	120–270	^{137}Cs , ^{152}Eu , possible ^{60}Co
Northeast of T3		1978	~100	<i>not analyzed</i>
U-3cy (Pike)	30	1978	30–100	^{60}Co , ^{137}Cs
		1994	18–24	^{137}Cs
U-3q (Otero)	31	1978	10–30	^{60}Co , ^{137}Cs
		1994	12–18	^{137}Cs , ^{241}Am
East of U-3cy	103	1978	100–300	^{137}Cs , ^{241}Am
		1994	12–18	^{241}Am
T3U (Chavez)	104	1994	18–24	^{137}Cs , ^{241}Am

DISCUSSION OF RESULTS

The 1978 survey¹⁰ detected seven distinct contaminated locations. The three main test areas all contained cobalt-60 (⁶⁰Co), cesium-137 (¹³⁷Cs), Europium-152 (¹⁵²Eu), and ²⁴¹Am. Three of the other locations contained a combination of ⁶⁰Co, ¹³⁷Cs, and ²⁴¹Am. This was a helicopter survey with a relatively high sensitivity and small spatial resolution.

The wide-flight-line spacing of the 1992 survey distorted these contaminated regions into two large areas, one approximately at the T3B location with an exposure rate of 18–24 μ R/h. The other two large sites were merged into one area with an exposure rate of 24–36 μ R/h.

The 1994 survey located five regions of man-made activity and at least two additional regions of ²⁴¹Am contamination in Area 3. The region northeast of T3, which was detected in 1978, was not detected as a distinct contaminated region, although it is within the extended man-made distribution surrounding the three major sites.

Small regions of activity appear in the ²⁴¹Am plot near each of the three main sites in Area 3. Of these small regions, the site west of T3A (and south of U-3q) is real. This ²⁴¹Am contamination overlies the T3U site (ROI 104) where the Chavez safety experiment was conducted from a tower on October 27, 1958, with a yield of 0.0006 kt. U-3cy and U-3q appear in the ²⁴¹Am plot, and the new area east of U-3cy (ROI 103) has been confirmed as ²⁴¹Am contamination through other surveys conducted at the NTS. The rest of these small regions are probably statistical fluctuations.

Area 4. A summary of the locations containing man-made activity, as shown in Figure 17, is presented in Table 6-5. The main test location (T4, ROI 36) hosted four tests conducted from towers: Fox (May 25, 1952; 11 kt), Nancy (March 24, 1953; 24 kt), Apple-1 (March 29, 1955; 14 kt), and Kepler (July 24, 1957; 10 kt). The Ray (April 11, 1953; tower; 0.2 kt) test location (T4A) is just barely detectable. It is the small, 2.5–4.5-mR/h contour region northeast of T4 and south of the “4” in the “AREA 4” designation on the map (Figure 17). There is no immediately apparent explanation for the bulbous distortions of the T4 contours southeast (ROI 37) and northeast from T4. The other extensions—further to the northeast, to the southwest (ROI 38), and to the west—appear to be the result of fallout from the tests at T4. Spectra from these extended regions exhibit ¹³⁷Cs and sometimes weak ⁶⁰Co photopeaks.

The 1970 survey detected the high level of contamination at the T4 site. This site is on the eastern edge of the wide band of contamination observed running from Area 1 through Area 4 and into Area 2. The spectrum showed photopeaks from ⁶⁰Co and ¹³⁷Cs.

The 1978 survey¹⁰ reported high-man-made activity at the T4 site and located several small satellite spots, a large bulge to the southeast, and two plumes extending northeast and southwest from T4. The activity of this site was about the same as the activity at the T1 site

Table 6-5. Summary of Detected Man-Made Sources in Area 4

Location	ROI	Survey Date	Exposure-Rate Range (μ R/h)	Isotopes Identified
T4	36	1970	200	⁶⁰ Co, ¹³⁷ Cs
		1978	300–1000	⁶⁰ Co, ¹³⁷ Cs, ¹⁵² Eu, ²⁴¹ Am
		1992	24–36	not analyzed
		1994	120–270	¹³⁷ Cs, ¹⁵² Eu
Southeast of T4	37	1978	10–30	not analyzed
		1994	18–24	¹³⁷ Cs
Southwest of T4	38	1978	~30	not analyzed
		1994	12–18	⁶⁰ Co, ¹³⁷ Cs
West of T4		1994	6–24	¹³⁷ Cs
Northwest of T4		1978	~30	not analyzed
T4A (Ray)		1978	~10	not analyzed
		1994	12–18	¹³⁷ Cs

DISCUSSION OF RESULTS

(in Area 1). The soil samples collected for analysis at the T4 site possessed high concentrations of ^{137}Cs and ^{241}Am and small, but measurable, concentrations of ^{60}Co and ^{152}Eu . There was no analyses of the isotopes present at the other contaminated regions in Area 4.

The 1992 survey also identified the T4 site but with a much lower intensity. The survey's spatial resolution did not allow it to see the smaller, low intensity items.

The 1994 survey located the same features as the 1978 survey with the exception of the small satellite spots northwest of T4. The 1994 survey provides better definition of the contamination west of T4. The small regions that appear in the ^{241}Am plot (Figure 24) are in or near the high-count-rate region of T4 and, therefore, are probably not actually ^{241}Am contamination but rather statistical fluctuations.

Area 5 and the NAFR. A summary of the locations containing man-made activity and ^{241}Am , as shown in Figures 15 and 22, is presented in Table 6-6. Small Boy was detonated on July 14, 1962, with a low yield from the top of a tower. The ground deposition was measured⁵ two days after detonation, and the highest activity level was over 20,000 $\mu\text{R/h}$ at the closest distance to the GZ that the survey encompassed (about 20 km). Another flight indicated that the exposure rates had decayed by a factor of 2–3 by the third day after detonation. However, no measurements were made close to the GZ. The Small Boy plume spectra (ROIs 16 and 17) show strong ^{241}Am and ^{137}Cs photopeaks in the 1994 data.

Table 6-6. Summary of Detected Man-Made Sources in Area 5

Location	ROI	Survey Date	Exposure-Rate Range ($\mu\text{R/h}$)	Isotopes Identified
B5A	15	1970	51–100 (off site)	^{60}Co , ^{65}Zn , ^{125}Sb , ^{134}Cs , ^{137}Cs
		1982	no value given	^{152}Eu
		1992	36–72	not analyzed
		1992A*	not reported	^{137}Cs , ^{152}Eu , ^{241}Am
		1994	120–270	^{137}Cs , ^{152}Eu
T5 (Small Boy)	16, 17	1970		not resolved from B5A
		1982	no value given	^{137}Cs , ^{241}Am
		1992		not resolved from B5A
		1992A*	not reported	^{137}Cs , ^{241}Am
		1994	50–75	^{137}Cs , ^{241}Am
RWMS (TRU Pad)	18	1982	no value given	^{241}Am , excess ^{208}Tl
		1994	39–50	^{241}Am
RWMS (northeast)	19	1994		nothing definite
RWMS (northwest)	20	1982	no value given	^{60}Co , ^{137}Cs , ^{152}Eu
		1994		nothing definite
Cotter Concentrate	21	1992	not seen	not analyzed
		1994	120–270	excess ^{214}Bi , ^{208}Tl
Sugar Bunker		1982	not reported	^{241}Am
Kay Blockhouse		1970	21–30	none reported
		1982	not reported	^{152}Eu
T5I (Hamilton)	101	1994	~25	^{241}Am
GMX	102	1982	not reported	^{241}Am
		1994	12–18	^{241}Am

* This is the detailed helicopter survey of the B5A and Small Boy sites.

The large test area (B5A; ROI 15) hosted six experiments: Encore (May 8, 1953; airdrop; 27 kt), Grable (May 25, 1953; airburst; 15 kt), Met (April 15, 1955; tower; 22 kt), Priscilla (June 24, 1957; balloon; 37 kt), Wrangell (October 22, 1958; balloon; 0.115 kt), and Sanford (October 26, 1958; balloon; 4.9 kt). In close proximity to this area, there was no sign of any effects from the Able (April 1, 1952; airdrop; 1 kt) test.

Another tower test, named Hamilton (October 15, 1958; 0.0012 kt; ROI 101), is located very close to B5A and only appears as a distinct entity in the ^{241}Am plot (Figure 22). Another nearby multi-test area (A5) shows no activity although it was the site of five airdrop tests: Able (January 27, 1951; 1 kt), Baker (January 28, 1951; 8 kt), Easy (February 1, 1951; 1 kt), Baker-2 (February 2, 1951; 8 kt), and Fox (February 6, 1951; 22 kt).

The 1970 survey covered most of the eastern and northern portions of Area 5. While it did detect B5A and the deposition from the Small Boy test, it located the most intense activity well off-site instead of at the NTS boundary. The 1970 survey also detected the Kay Blockhouse location, but since the increase in activity was not significant, no spectral investigation was conducted.

In 1982, a survey¹³ was conducted to map the Small Boy deposition as well as much of the surrounding, relatively flat terrain. Besides the B5A and Small Boy sites, anomalous activity levels were recorded at five other locations in the northern end of Area 5. The results of the survey were not reported as exposure-rate levels but rather as MMGC rate levels.

The 1992 survey identified the B5A and Small Boy depositions, but the fixed-wing aircraft did not pass directly over the center of activity (causing the recorded intensity to be low), and the wide-flight-line spacing used in the survey caused a slight displacement of the center of activity. Even so, a detectable level of activity of the deposition was found as far as 8 kilometers east of the NTS boundary. The survey was unable to detect any of the other three locations as a result of the wide-flight-line spacing and the small physical size of the locations.

The Small Boy region was surveyed again¹⁶ in 1992 using helicopters at 30 meters AGL. The intent of the survey was to investigate any correlation between the ^{241}Am concentrations (an indication of plutonium contamination from nuclear tests but not easy to detect from typical aerial survey altitudes) and the ^{137}Cs concentrations (a fission-product fallout from nuclear tests and a much easier isotope to measure from a distance). The survey carefully mapped the americium and cesium depositions over a region extending to more than 12 kilometers east of the GZ. However, no correlation was found between the locations where these two isotopes were deposited.

The 1994 survey produced a relatively detailed map of the Small Boy deposition extending 7 kilometers east of the NTS boundary. Two locations detected in 1982 (Kay Blockhouse and Sugar Bunker) were not detected in the 1994 survey.

The Area 5 Radioactive Waste Management Site (RWMS) site contains several different regions of activity. In the southeast corner, the TRU Pad (ROI 18) can be seen in both the terrestrial exposure-rate plot (Figure 4) and the man-made plot (Figure 15). In Figure 4, the northern part of the RWMS is merged into one large bulls-eye contour. In the man-made plot, the northern part of the RWMS appears as two distinct regions (ROIs 19 and 20).

The location in the northeastern corner (ROI 21) was a temporary storage location for the Cotter Concentrate material (which was removed from the NTS in 1997). Much of the Cotter Concentrate's very rich supply of uranium was extracted during the Manhattan Project. The gamma-ray spectrum from this location exhibits increased ^{214}Bi activity (one of the daughters in the ^{238}U decay chain). The GMX site (ROI 102) was observed in both the 1982 and 1994 surveys although in 1994 it is only visible in the ^{241}Am plot (Figure 22).

Area 6. A summary of the locations containing man-made activity, as shown in Figure 13, is presented in Table 6-7. The 1970 survey detected the old decon pond and identified ^{60}Co as the only prominent isotope present. The survey included Yucca Lake, but no man-made activity was detected at the decon pond location.

The 1978 survey¹⁰ identified two regions of man-made radioactivity in this area. The Decontamination Facility Evaporation Pond on the edge of Yucca Lake and the Leach Pond (old decontamination facility) near the control point (CP) facilities just west of Mercury Highway are clearly visible in the data. The report for this survey stated that the Leach Pond

Table 6-7. Summary of Detected Man-Made Sources in Area 6

Location	ROI	Survey Date	Exposure-Rate Range ($\mu\text{R/h}$)	Isotopes Identified
Decon Pond	14	1978	30–100	not analyzed
		1994	18–24	^{60}Co , possible ^{137}Cs
Leach Pond (old decon pond)		1970	~50	^{60}Co
		1978	~10	not analyzed

had been cleaned up between 1978 and 1981. The report did not present any analyzed spectra for these two locations.

The southeast corner of Area 6 was included as part of the 1982 survey¹³ of Frenchman Flat. This small portion of Area 6 did not include either decontamination facility location. No anomalous regions were detected in the survey.

The 1992 survey did not detect any anomalous activity sites, principally due to the low-activity levels and the wide-flight-line spacing.

The 1994 survey detected the man-made isotopes at the decontamination pond in Yucca Lake (ROI 14). Small ^{60}Co photopeaks are present in the spectrum and a ^{137}Cs photopeak may also be present.

Area 7. A summary of the locations containing man-made and ^{241}Am activity, as shown in Figures 17 and 24, is presented in Table 6-8. There are two distinct areas in the data plots related to atmospheric testing. The southernmost (ROI 40) of the two areas was probably created from tests conducted at three principal locations within the overall ROI. The highest activity region contains the B7B and T7-4 sites. Site B7B hosted 13 tests where the nuclear device was carried in a balloon: Stokes (August 7, 1957; 19 kt), Doppler (August 23, 1957; 11 kt), Franklin Prime (August 30, 1957; 4.7 kt), Laplace (September 8, 1957; 1 kt), Newton (September 16, 1957; 12 kt), Eddy (September 19, 1958; 0.083 kt), Mora (September 29, 1958; 2 kt), Hidalgo (October 5, 1958; safety experiment; 0.077 kt), Lea (October 13, 1958; 1.4 kt), Dona Ana (October 16, 1958; 0.037 kt), Socorro (October 22, 1958; 6 kt), De Baca (October 26, 1958; 2.2 kt), and Santa Fe (October 30, 1958; 1.3 kt). Just two tests (both airdrop tests) were conducted at T7-4 (also known as A7). Wasp occurred on February 18, 1955, with a yield of 1 kt and Wasp Prime occurred on March 29, 1955, with a yield of 3 kt.

Table 6-8. Summary of Detected Man-Made Sources in Area 7

Location	ROI	Survey Date	Exposure-Rate Range ($\mu\text{R/h}$)	Isotopes Identified
T7C and T7-1A	39	1970	~50	<i>not reported</i>
		1978	300–1000	^{152}Eu , ^{241}Am , possible ^{60}Co , ^{137}Cs
		1992	~18	<i>not analyzed</i>
		1994	120–270	^{152}Eu , possible ^{137}Cs
B7B, T7-4, T7-3, T7-3A, and T7-5A	40	1970	~50	<i>not reported</i>
		1978	100–300	^{137}Cs , ^{152}Eu , ^{241}Am
		1994	50–75	^{152}Eu
East of T7C		1978	30–100	^{60}Co , ^{137}Cs , ^{241}Am

DISCUSSION OF RESULTS

Southeast of these two locations was the T7-3 site (also known as A7) that appears to be responsible for the slight bulge on the southeast side of ROI 40. T7-3 hosted eight airdrop tests: Baker (October 28, 1951; 3.5 kt), Charlie (October 30, 1951; 14 kt), Dog (November 1, 1951; 21 kt), Baker (April 15, 1952; 1 kt), Charlie (April 22, 1952; 31 kt), Dog (May 1, 1952; 19 kt), Dixie (April 6, 1953; 11 kt), and Climax (June 4, 1953; 61 kt). Two other tests were conducted within this ROI, but there is no apparent indication of their locations in the data. The Able test (October 22, 1951; <0.1 kt) was conducted on a tower at T7-5A, and the Ruth test (March 31, 1953; 0.2 kt) was conducted on a tower at T7-3A.

The northern test area (ROI 39) hosted four tower tests at two locations within the highest activity contours: Bee (March 22, 1955; 8 kt) and Zucchini (May 15, 1955; 28 kt) at site T7-1A and Boltzmann (May 28, 1957; 12 kt) and Quay (October 10, 1958; 0.079 kt) at site T7C.

The 1970 survey covered the western half of Area 7 and detected a rather large region of contamination with an exposure-rate range of 31–50 $\mu\text{R}/\text{h}$. Within this region were two small spots of activity in the 51–100- $\mu\text{R}/\text{h}$ range. These two small spots are the result of two flight lines passing just east and west of the two ROIs. Since the aircraft did not fly directly over the ROIs, the measured activity was significantly lower and displaced from its true location.

The 1978 survey¹⁰ also covered the western half of Area 7 but produced a much better-defined plot of the contamination. Three sites were identified. According to the soil sample analysis, the northern site (T7C) was contaminated with ¹⁵²Eu, ²⁴¹Am, and possibly ⁶⁰Co and ¹³⁷Cs. The southern site (B7B and T7-4) had ¹³⁷Cs, ¹⁵²Eu, and ²⁴¹Am while the small-area east of T7C was contaminated with ⁶⁰Co, ¹³⁷Cs, and ²⁴¹Am.

The resolution of the 1992 survey was poor enough that only a single area (with a low-exposure rate) was observed.

The 1994 survey detected the two large sites (Figure 17) seen in the 1978 survey but did not detect the small site east of T7C. ROI 39 was contaminated with ¹⁵²Eu and possibly ¹³⁷Cs while ROI 40 only exhibited gamma rays from ¹⁵²Eu. The contours in the ²⁴¹Am plot (Figure 24) probably do not represent real ²⁴¹Am contamination; even the larger-area contour that is centered over ROI 39 exhibits no convincing evidence of an ²⁴¹Am photopeak.

Area 8. A summary of the locations containing man-made and ²⁴¹Am activity, as shown in Figures 17 and 24, is presented in Table 6-9. Smoky was conducted from a tower (T2C) on August 31, 1957, with a yield of 44 kt. Ceres and Titania were safety experiments conducted on towers on October 26 and 30, 1958, with 0.0007-kt and 0.0002-kt yields, respectively. Baneberry had a 10-kt yield, and this test was conducted underground (U-8d) on December 18, 1970. There was an accidental release of radioactivity from Baneberry that was detected off-site.

Table 6-9. Summary of Detected Man-Made Sources in Area 8

Location	ROI	Survey Date	Exposure-Rate Range ($\mu\text{R}/\text{h}$)	Isotopes Identified
U-8d (Baneberry)	50, 51	1978	300–1000	⁶⁰ Co, ¹³⁷ Cs, ²⁴¹ Am
		1992	3–9	<i>not analyzed</i>
		1994	120–270	⁶⁰ Co, ¹³⁷ Cs
T2C (Smoky)	52	1978	~300	⁶⁰ Co, ¹³⁷ Cs, ¹⁵² Eu
		1992	9–27	<i>not analyzed</i>
		1994	120–270	¹³⁷ Cs, ¹⁵² Eu
T8C (Titania)	106	1994	30–39	¹³⁷ Cs, ²⁴¹ Am
T8B (Ceres)	107	1994	30–39	¹³⁷ Cs, ²⁴¹ Am

The 1970 survey did not include Area 8. Approximately the southern half of Area 8 was surveyed¹⁰ in 1978. The Baneberry plume was mapped as far north as the survey boundary, and the Smoky test location was also identified.

DISCUSSION OF RESULTS

The 1992 survey recorded these two locations, but the spatial resolution was not very good. The survey did indicate that the Baneberry plume continued through the northern part of Area 8 and ended halfway through Area 15.

The 1994 survey identified the same two locations of man-made activity in Area 8. The Baneberry plume was mapped in full and found to consist of ^{60}Co and ^{137}Cs . The Smoky region contained ^{137}Cs and ^{152}Eu . Titania (ROI 106) is observable only in the ^{241}Am plot (Figure 24). Ceres (ROI 107) is observable in both the man-made and ^{241}Am plots but was initially overlooked in the man-made data. Both safety experiment sites exhibit photopeaks for ^{137}Cs and ^{241}Am in their spectra. The ^{137}Cs likely originated from Sedan (in Area 10) as the fallout pattern from Sedan extends well into Area 8. The rest of the ^{241}Am contours present in Figure 24 are not expected to represent real contamination.

Area 9. A summary of the locations containing man-made and ^{241}Am activity, as shown in Figures 17 and 24, is presented in Table 6-10. There are three distinct areas related to atmospheric testing. The largest area (B9A) hosted eight tests, all conducted from balloon platforms: Lassen (June 5, 1957; 0.0005 kt), Wilson (June 18, 1957; 10 kt), Hood (July 5, 1957; 74 kt), Owens (July 25, 1957; 9.7 kt), Wheeler (September 6, 1957; 0.197 kt), Charleston (September 28, 1957; 12 kt), Morgan (October 7, 1957; 8 kt), and Rushmore (October 22, 1958; 0.188 kt). In addition, the location for Sugar (a surface-level test conducted on November 19, 1951, with a yield of 1.2 kt) is southeast of the GZ and well inside this area's contours, but it is not visible in the man-made data.

The second largest contour area contains two separate test areas: T9B was the site for the tower-based test named Tesla (March 1, 1955; 7 kt) and S9G was the site for the Ganymede safety experiment conducted at ground-level on October 30, 1958; 0 yield). In addition, the Mazama test (October 29, 1958; tower; 0 yield) was conducted from a tower on the eastern edge of this area's contours, but no separate, identifiable region of activity is visible in the man-made data.

The third contour area also contains two separate test areas: T9C was the site for the tower-based test named Post (April 9, 1955; 2 kt), and S9E was the site for a ground-level safety experiment named Vesta (October 17, 1958; 0.024 kt). In addition, the ground-level safety

Table 6-10. Summary of Detected Man-Made Sources in Area 9

Location	ROI	Survey Date	Exposure-Rate Range ($\mu\text{R/h}$)	Isotopes Identified
B9A	41	1970	200	^{60}Co , ^{65}Zn , ^{137}Cs , possible ^{125}Sb
		1978	300–1000	^{60}Co , ^{137}Cs , ^{152}Eu , ^{241}Am
		1992	9–27	not analyzed
		1994	270–900	^{137}Cs , ^{152}Eu , possible ^{60}Co
T9B and S9G	42	1970	51–100	not reported
		1978	100–300	^{60}Co , ^{137}Cs , ^{152}Eu , ^{241}Am
		1992	3–9	not analyzed
		1994	~120	^{137}Cs , ^{152}Eu
T9C and S9E	43	1970	31–50	not analyzed
		1978	10–30	^{60}Co , ^{137}Cs , ^{152}Eu
		1992	1–3	not analyzed
		1994	18–24	^{137}Cs , ^{152}Eu , ^{241}Am
East of B9A	105	1994	6–12	^{241}Am , possible ^{137}Cs
Southeast of B9A		1978	~30	^{137}Cs , ^{152}Eu , ^{241}Am

experiment named Juno (October 24, 1958; 0.0017 kt) was conducted on the western edge of this area's contours, but it is not visible in the 1994 man-made data. The 1970 survey

DISCUSSION OF RESULTS

covered the western half of Area 9 and detected just one extended region of man-made activity. The 1978 survey¹⁰ also surveyed only the western half of Area 9 but was able to separate the extended man-made activity region into four distinct bulls-eyes. The survey identified ⁶⁰Co, ¹³⁷Cs, and ¹⁵²Eu at each site and ²⁴¹Am at ROIs 41 and 42. (There was no mention of whether ²⁴¹Am was detected at ROI 43.)

With its wide-flight-line spacing, the 1992 survey did not characterize this region very well. The quoted exposure rates for these locations are significantly lower than the exposure rates specified in other surveys. The general shape of the contamination is correctly modeled by the data, but the amplitudes are not correct. No analyses of specific isotopes was conducted.

The 1994 survey identified three of the sites found in the 1978 survey. The fourth location (ROI 105) identified in the 1994 data is situated east of B9A. It appears as a location of weak, man-made activity (Figure 17) and weak ²⁴¹Am activity (Figure 24). The only definite area of ²⁴¹Am contamination in Area 9 extends northeast and southwest from the S9E (Vesta) site.

Area 10. A summary of the locations containing man-made and ²⁴¹Am activity, as shown in Figures 17 and 24, is presented in Table 6-11. Sedan (ROI 49) was a Plowshare test conducted on July 6, 1962, with a yield of 104 kt. This excavation experiment created a crater with a depth of 100 meters and a diameter of 400 meters. The test resulted in the release of radioactivity that was detected off-site.

The 1970 survey detected one large region with an exposure-rate maximum of 450 μ R/h. The spectrum of this region contained ⁶⁰Co, ⁶⁵Zn, and ¹³⁷Cs. The survey did not cover the northern or western edges of the Sedan crater or any regions beyond Sedan.

The 1978 survey¹⁰ of Yucca Flat covered the western portion of Area 10. In addition to the Sedan crater area, the survey recorded three other locations south of Sedan plus the plume extending north-northeast into Area 15 and a region of elevated activity extending from Sedan to another location in Area 8.

The flight lines in the 1992 survey did not pass directly over the Sedan crater, so the exposure rate that was recorded was very low. The wide-flight-line spacing also prevented the survey from recognizing any of the small regions elsewhere in Area 10; however, the survey was able to track the main plume from Sedan northward through Area 15 and onto the Nellis Air Force Range.

The 1994 survey recorded essentially the same features as the 1978 survey but at lower intensities and with more detail. The ²⁴¹Am contours (Figure 24) in the Sedan area are likely to be statistical fluctuations since the count rate is very high in the spectra from this region.

Area 11. A summary of the locations of man-made and ²⁴¹Am activity, as shown in Figures 15 and 22, is presented in Table 6-12. The southeast corner of Area 11 was included as part of the Frenchman Flat survey¹³ in spring of 1982. A small region of increased ¹³⁷Cs activity was detected off the southeast corner of Massachusetts Mountain. This was the location (U-11b) of an underground nuclear test named Pin Stripe (ROI 22), detonated on April 25, 1966, with a yield less than 20 kt.

Table 6-11. Summary of Detected Man-Made Sources in Area 10

Location	ROI	Survey Date	Exposure-Rate Range (μ R/h)	Isotopes Identified
U-10H (Sedan)	49	1970	>100	⁶⁰ Co, ⁶⁵ Zn, ¹³⁷ Cs
		1978	300–1000	⁶⁰ Co, ¹⁰¹ Rh, ^{102m} Rh, ¹³⁷ Cs, ²⁴¹ Am
		1992	27–80	not analyzed
		1994	120–270	⁶⁰ Co, ¹³⁷ Cs

Table 6-12. Summary of Detected Man-Made Sources in Area 11

Location	ROI	Survey Date	Exposure-Rate Range ($\mu\text{R/h}$)	Isotopes Identified
U-11b (Pin Stripe)	22	1982	not reported	^{137}Cs
		1994	18–24	^{137}Cs
Project 56 No. 4	23	1982	80–140	^{137}Cs , ^{241}Am
		1994	39–50	^{241}Am
Project 56 No. 3	24	1982	45–80	^{241}Am
		1992_g	26–270*	^{235}U , ^{239}Pu , ^{241}Am
		1994	18–24	^{241}Am
Project 56 No. 2	25	1982	25–45	^{241}Am
		1992_g	25–118*	^{235}U , ^{239}Pu , ^{241}Am
		1994	18–24	^{241}Am
Project 56 No. 1	26	1982	14–18	^{235}U
		1992_g	27–33*	^{235}U , ^{241}Am
Waste Dump		1982	14–18	^{241}Am

* Each ground-based measurement made in 1992 viewed a much smaller area than the aerial measurements at each site. Very small, high-activity regions will be averaged with regions of little or no activity when viewed from an aerial system whereas a ground-based system that views only the contaminated region will report a much higher-exposure rate.

The four safety experiments in Plutonium Valley (in the northern end of Area 11) were the object of a helicopter survey¹² in January 1982. These tests were named Project 56, No. 1–4, and occurred during November 1955 through January 1956. Only No. 4 exhibited any nuclear yield. Besides the four safety-experiment locations, identifiable amounts of ^{241}Am were detected (a) at a waste dump about 1000 meters west of No. 4 site, (b) along a short deposition trail extending southwesterly from No. 4 site, (c) at a small area about 200 meters west of No. 3 site, and (d) in a low-level deposition plume extending northerly through Plutonium Valley from No. 3 and No. 4 sites.

Only a small piece of the southeast corner of Area 11 was flown during the 1970 survey. It did not detect any anomalous regions. The relatively low activity and the small size of the contamination regions coupled with the wide-flight-line spacing made the locations in this area nearly invisible to the 1992 survey.

In May and June 1992, a series of ground-based measurements¹⁷ were conducted at the Project 56 No. 1, 2, and 3 sites using a collimated Ge detector suspended about 7 meters above the ground. The only isotopes of interest to the study were ^{241}Am , plutonium-239 (^{239}Pu), and ^{235}U . All three sites possessed significant quantities of ^{241}Am whereas ^{239}Pu was only detected at the GZ for Sites No. 2 and 3. Site No. 1 had a significant ^{235}U concentration while Sites Nos. 2 and 3 possessed ^{235}U at levels slightly above the detectable limit of the system.

The 1994 survey detected Pin Stripe in the man-made analysis and the Project 56 No. 2, 3, and 4 sites (ROIs 23, 24, and 25) in the gross count, man-made, and ^{241}Am analyses. The principal contributor at these three Project 56 sites was ^{241}Am . The ^{235}U contamination reported at the No. 1 site (ROI 26) from the 1982 aerial and 1992 ground-based surveys does not appear in either the man-made or ^{241}Am analyses. It is very probable that the flight-line spacing was large enough and positioned appropriately that the weak radioactivity at the No. 1 site was not recorded in any 1-second measurement. The net spectrum for ROI 26 exhibits only residual amounts of the natural radionuclides.

Area 12. A summary of the locations containing man-made and ^{241}Am activity, as shown in Figures 17 and 24, is presented in Table 6-13. The 1970 survey only measured a very small area in the northwest corner of Area 12 and did not detect any anomalies. The 1978 survey¹⁰ covered the southeast corner of Area 12 and detected an anomaly that contained ^{60}Co and ^{137}Cs isotopes.

Table 6-13. Summary of Detected Man-Made Sources in Area 12

Location	ROI	Survey Date	Exposure-Rate Range ($\mu\text{R/h}$)	Isotopes Identified
T Tunnel Portal	54	1992	18 - 24	<i>not analyzed</i>
		1994	39 - 50	^{137}Cs
E Tunnel Portal	55	1992	12 - 18	<i>not analyzed</i>
		1994	30 - 39	^{137}Cs
G Tunnel Portal	56	1994	24 - 30	^{137}Cs
B Tunnel Portal	57	1992	12 - 18	<i>not analyzed</i>
		1994	24 - 30	^{137}Cs , ^{241}Am
Northwest quadrant		1984	19 - 26	^{137}Cs
U-12-09 vent line		1984	22 - 30	^{137}Cs , "other fission products"
Southeast quadrant		1978	10 - 30	^{60}Co , ^{137}Cs
		1992	12 - 18	<i>not analyzed</i>

The 1984 survey¹⁵ only covered a small region in the northwest and western part of Area 12. Several spots of elevated ^{137}Cs activity were observed. One location was identified as a vent line from the test at U-12-09, and the spectrum of this location clearly exhibits ^{137}Cs .

The 1992 survey identified several regions of slightly elevated activity (1–3 $\mu\text{R/h}$ of man-made activity). Another region corresponds to the portal at "T" tunnel. The third region is a rather extensive area in the southeast quadrant and is connected to the radiation fields beginning in Areas 8 and 2. The high-altitude (and large-detection footprint) of the survey definitely smeared these locations.

The 1994 survey did not detect any of the weak ^{137}Cs spots identified by the 1984 survey. The survey did detect man-made contamination at the portals to four of the tunnels. The "B" tunnel portal also exhibits the only ^{241}Am contamination in Area 12.

Area 14. The 1970 survey only covered the northern portion of this area. The 1992 and the 1994 surveys covered the whole area. None of the surveys detected any radioactive anomalies.

Area 15 and the NAFR. A summary of the locations containing man-made activity, as shown in Figure 17, is presented in Table 6-14. The 1970 survey covered a small region in the eastern part of Area 15 and a large region extending north and east from Area 15. The survey did not detect any anomalous radiation readings. The 1978 survey¹⁰ covered only a small region in the southwestern portion of Area 15 and detected lower-radiation levels from the Sedan test in Area 10, but nothing originating in Area 15.

The 1984 survey¹⁵ covered the western half of Area 15 and detected locations having increased ^{60}Co and ^{137}Cs activity. These areas of increased activity appear to be related to the depositions from the Sedan (Area 10) and Baneberry (Area 8) tests.

Table 6-14. Summary of Detected Man-Made Sources in Area 15

Location	ROI	Survey Date	Exposure-Rate Range ($\mu\text{R/h}$)	Isotopes Identified
U-15e (Tiny Tot)	53	1994	12–18	^{137}Cs

DISCUSSION OF RESULTS

The 1992 survey recorded low levels of activity extending from the Sedan crater through the middle of Area 15 and about 13 kilometers onto the NAFR north of Area 15 (slightly west of the area surveyed in 1970). It also recorded elevated activity levels in the western portion of Area 15 that appear to have originated at the Baneberry GZ in Area 8. No spectral information was analyzed.

The region north of Area 15 was surveyed again¹⁶ in 1992 using a helicopter flown at an altitude of 30 meters AGL and a ground speed of 60 knots. The intent of this survey was to determine how much of the Sedan plume could be detected outside the boundaries of the NTS. The survey mapped the area as far as 11 kilometers (7 miles) north of the NTS boundary. Low levels of ¹³⁷Cs were detected as far as the northern boundary of the survey area. A search for ²⁴¹Am was negative. No attempt was made to identify other isotopes in this region.

The 1994 survey detected only one anomaly that originated from a source in Area 15. The MMGC plot (Figure 17) indicates one source location (ROI 53) that is distinct from the Sedan plumes. This location was the tunnel entrance to the Tiny Tot test, U-15e, which was detonated on June 17, 1965, with a yield of less than 20 kt. The gamma-ray spectrum of this location shows ¹³⁷Cs as the only contaminant. The plumes extending from the Sedan and Baneberry tests are visible in both the exposure-rate and MMGC plots. Isolated contour islands of activity appear in the MMGC plot (Figure 5) more than 10 kilometers north of the NTS boundary.

Area 16. A summary of the locations containing man-made activity, as shown in Figure 13, is presented in Table 6-15. The 1970 survey only covered a small portion in the southeastern quadrant of this area. The 1970 survey and the 1992 survey did not record any radioactive anomalies.

The 1983 helicopter survey¹⁴ used a special set of analysis techniques to extend the lower level of detectability. This resulted in the identification of several regions of elevated ¹³⁷Cs concentration that would have been missed by the previous processing algorithms. These large areas are located along the eastern edge of Area 16 and are contained within regions having lower average exposure rates than most of Area 16.

The 1983 survey identified one location that exhibited unmistakable ¹³⁷Cs contamination. This location does not appear in the gross count (exposure-rate) plot. It was identified as a vent line from the tests in tunnel U-16a.

The 1983 survey report shows contour levels representing increased ⁶⁰Co activity in many of the same regions as the elevated ¹³⁷Cs activity. The contour plots were generated using an algorithm that summed the spectral counts from 1100 to 1400 keV. The contoured regions possess net positive counts in this energy window, but the gamma-ray spectra from these regions do not exhibit the nearly symmetric photopeaks at 1173 and 1332 keV that should be present if ⁶⁰Co really actually exists at the sites

The 1994 survey also detected the vent-line source of ¹³⁷Cs contamination. It was too weak to appear in the exposure-rate plot, but it was present in the MMGC plot. The spectrum for this location shows a weak but well-defined ¹³⁷Cs photopeak.

Area 17. This area was not flown during the 1970 survey. The 1978 survey¹⁰ covered only a very small portion in the extreme eastern edge of this area and detected just natural background radiation.

Table 6-15. Summary of Detected Man-Made Sources in Area 16

Location	ROI	Survey Date	Exposure-Rate Range (μR/h)	Isotopes Identified
U-16a vent line	13	1983	21–25	¹³⁷ Cs
		1994	18–24	¹³⁷ Cs

DISCUSSION OF RESULTS

The 1984 survey,¹⁵ did not detect any regions of anomalous activity. However, it did map the ¹³⁷Cs activity levels and noted a variation of more than a factor of four in the concentrations on the eastern side versus the western side of Area 17. A spectrum from the highest ¹³⁷Cs activity on the eastern side also showed evidence of ⁶⁰Co contamination. Again, there were no specific locations of either ¹³⁷Cs or ⁶⁰Co contamination; in general, the contamination slowly decreases with distance from the eastern edge of the area.

The 1992 survey did not detect any anomalous activity regions. The 1994 survey also did not detect any anomalies. It did detect the large-area, low-activity-level plumes that extend into Area 17 from the aboveground test sites in Areas 2 and 4.

Area 18. A summary of the locations containing man-made and ²⁴¹Am activity, as shown in Figures 9 and 20, is presented in Table 6-16. The Danny Boy test occurred on March 5, 1962, and was buried in a shallow hole to produce a crater. It had a published yield of 0.43 kt. The Johnnie Boy test occurred on July 11, 1962, and was detonated slightly below ground level to produce a crater. It had a published yield of 0.5 kt. The Little Feller I test occurred on July 17, 1962, and was detonated slightly above ground level with a published yield of less than 20 kt. The Little Feller II test occurred on July 7, 1962, and was detonated slightly above ground level with a published yield of less than 20 kt. Radioactivity was detected off-site from all of the tests except Little Feller II.

The 1970 survey detected only the Danny Boy and Johnnie Boy tests with maximum exposure rates of 75 μ R/h. The 1992 survey did not detect any of these small-area regions. The wide-flight-line spacing used in both of these surveys caused these test locations to be missed.

The 1980 survey,¹¹ detected all four locations and recorded exposure rates somewhat higher than in either the 1970 or 1994 surveys. Since the 1980 survey had a closer flight-line spacing than the other surveys, a major contribution to the exposure-rate differences may be that the helicopter in 1980 flew directly over these four sites while the aircraft in the other surveys were sometimes flown over the hottest locations. The 1980 survey only searched for ¹³⁷Cs and did not perform any other isotopic analyses. Besides the four test sites, low levels of ¹³⁷Cs were found over large regions of the eastern third of the area.

The 1994 survey detected the four test locations in the exposure-rate data (Figure 4) as well as the MMGC data (Figure 9). The Danny Boy site exhibits a typical bulls-eye contour pattern. The other three sites possess definite plumes extending northerly. The spectra from Danny Boy and Johnnie Boy possess identifiable ¹³⁷Cs photopeaks while only the Johnnie Boy location does not exhibit any ²⁴¹Am. There is some distortion of the ¹⁵²Eu photopeaks near the energies of the ⁶⁰Co photopeaks in both the Danny Boy and the Johnnie Boy spectra. This distortion may be the remnants of the ⁶⁰Co detected in the 1970 survey.

Table 6-16. Summary of Detected Man-Made Sources in Area 18

Location	ROI	Survey Date	Exposure-Rate Range (μ R/h)	Isotopes Identified
U-18A (Danny Boy)	6	1970	75	⁶⁰ Co, ¹³⁷ Cs
		1980	90–200	¹³⁷ Cs
		1994	75–120	¹³⁷ Cs, ¹⁵² Eu, ²⁴¹ Am, possible ⁶⁰ Co
S18 (Johnnie Boy)	7	1970	75	⁶⁰ Co, ¹³⁷ Cs
		1980	~90	¹³⁷ Cs
		1994	39–50	¹³⁷ Cs, ¹⁵² Eu, possible ⁶⁰ Co
S18 (Little Feller I)	8	1980	30–45	¹³⁷ Cs
		1994	30–39	²⁴¹ Am
S18 (Little Feller II)	9	1980	~45	¹³⁷ Cs
		1994	24–30	²⁴¹ Am

Area 19. The 1970 survey and the 1992 survey did not detect any anomalies in this area. The 1984 survey¹⁵ also did not detect major anomalies. The 1984 survey did measure several, very spotty, and slightly elevated concentrations of ¹³⁷Cs in some of the valleys in the southeastern quadrant of Area 19.

The 1994 survey did not find any locations of definite man-made activity. There are a few, small-area, low-activity, scattered spots of man-made activity throughout the area, although these may only be statistical fluctuations. There is a weak ¹³⁷Cs photopeak in the spectra of this region, but a firm isotopic identification is difficult because the number of 1-second measurements available to form a spectrum is very small.

Area 20 and the NAFR. A summary of the locations containing man-made and ²⁴¹Am activity, as shown in Figures 7 and 19, is presented in Table 6-17. There are two main regions of contamination in Area 20, the Schooner region and the region around Palanquin and Cabriole. All three tests were part of the Plowshare program. The Palanquin test occurred on April 14, 1965. It had a yield of 4.3 kt. The Cabriole test occurred on January 26, 1968, with a yield of 2.3 kt.

The Schooner test occurred on December 8, 1968, with a yield of 30 kt. During December 1968, the radioactive deposition north of the test location was mapped⁷ with a fixed-wing aircraft. The first mapping flight, on December 15, ranged 15–55 kilometers from the GZ, and recorded activity levels 2–150 times background (the measured background was about 12 μ R/h). The second mapping flight, on December 21, recorded levels 5–75 times background over the range of 1–15 kilometers from the GZ. The third mapping flight, on December 28, was the most extensive and used 1.6-kilometer flight-line spacings over the range of 1–50 kilometers from the GZ. Radioactivity levels on this final survey were 2–100 times background.

The 1970 survey recorded a relatively large area from the Schooner test with an activity level greater than 100 μ R/h. The text in the report describes an exposure rate above 200 μ R/h, presumably at the GZ. No spectral data were reported. The Palanquin and Cabriole GZs are relatively close together and were not well resolved spatially during the 1970 survey. The survey recorded terrestrial and cosmic-ray activity levels greater than 200 μ R/h over the general area of the two GZs. The survey also identified the two strongest radioisotopes in the gamma-ray spectrum from over the GZ areas as manganese-54 (⁵⁴Mn) at 835 keV and ⁶⁰Co at 1173 and 1332 keV.

Table 6-17. Summary of Detected Man-Made Sources in Area 20

Location	ROI	Survey Date	Exposure-Rate Range (μ R/h)	Isotopes Identified
U-20U (Schooner)	1, 2	1970	200 +	<i>not analyzed</i>
		1980	200–900	⁶⁰ Co, ¹³⁷ Cs
		1992	72–360	<i>not analyzed</i>
		1992A	not reported	¹⁵² Eu, ²⁴¹ Am
		1994	270–900	¹⁵² Eu, possible ²⁴¹ Am
U-20K (Palanquin)	3	1970	200 +	⁵⁴ Mn, ⁶⁰ Co
		1980	~ 900	⁶⁰ Co, ¹³⁷ Cs
		1992	36–72	<i>not analyzed</i>
		1994	270–900	⁶⁰ Co, ¹³⁷ Cs, ²⁴¹ Am
U-20L (Cabriole)	4	1980	200–900	⁶⁰ Co, ¹³⁷ Cs
		1992	24–36	<i>not analyzed</i>
		1994	75–120	⁶⁰ Co, ¹³⁷ Cs, ²⁴¹ Am
East-central Area 20	5	1994	75–120	possible ^{234m} Pa

The 1980 survey,¹¹ used a helicopter at much lower altitude than the 1970 fixed-wing aircraft survey. As a result, spatial resolution was much better and maximum exposure-rate intensities were higher since there was a much higher probability that the helicopter flew directly over the GZ and averaged the high-activity spots over a smaller footprint.

The 1992 survey, with its very wide-flight-line spacing missed the centers of activity and reported much lower-exposure rates.

The region north of the Schooner test and outside the NTS boundary was surveyed again¹⁶ in the fall of 1992, but this time a helicopter was used. The ²⁴¹Am deposition was mapped for more than 3 kilometers from the NTS border. The deposition of man-made isotopes was mapped for almost 6 kilometers. The survey identified ¹⁵²Eu and ²⁴¹Am in the spectra.

The 1994 survey produced a detailed map of the Schooner plume (Figure 7). The exposure rate of the GZ area was comparable to the value from the 1980 survey. The gamma-ray spectrum over the GZ area exhibited photopeaks from ¹⁵²Eu but no ¹³⁷Cs. The spectrum from the plume area hints at the presence of ²⁴¹Am, although the photopeak is not well defined.

Palanquin has a moderate-sized plume extending in a northerly direction while Cabrioleet appears as a bulls-eye pattern with only a hint of a plume in the man-made contour plot. Both sites have clearly identifiable ⁶⁰Co, ¹³⁷Cs, and ²⁴¹Am photopeaks.

The 1994 survey also found one small spot of man-made activity in the east-central portion of Area 20. There are no known nuclear test or radioactive work areas at this location. The spectrum of this region does not exhibit any identifiable photopeaks, although an argument could be made for the presence of depleted uranium based on the possible photopeaks at 767 and 1001 keV. However, these photopeaks may be just statistical fluctuations.

The ²⁴¹Am contour plot (Figure 19) shows well-defined ²⁴¹Am plumes at the Palanquin and Cabrioleet sites. The contours at the Schooner site are only over the high-count-rate region of the site, and combined with the poorly defined photopeaks in the gamma-ray spectra, the presence of ²⁴¹Am contamination at Schooner should be considered suspect.

Area 22. The 1970, 1992, and 1994 surveys did not detect any anomalies in this area.

Area 23. No anomalous regions of activity were detected in this area where the Mercury base camp is located. This area was flown only during the 1992 and 1994 surveys.

Area 25. A summary of the locations containing man-made activity, as shown in Figure 11, is presented in Table 6-18. The NRDS region was covered during the 1970 survey. Four locations of man-made activity were detected in the region. The survey also reported a region of elevated activity in Forty-Mile Canyon, but details on the specific isotopes that were present was not given.

The area over the NRDS was surveyed⁹ in 1976 with a helicopter flown at a 60-meter altitude. Elevated radiation levels were recorded at six locations with activity levels ranging from 10 μ R/h to above 5000 μ R/h. The survey did not find any anomalous radioactivity in Forty-Mile Canyon.

The 1992 survey did not detect any regions of anomalous activity. This can be understood since most work had ceased in this area, and the remaining activities were low-level and the locations were small in size.

The 1994 survey located only two sites of man-made activity in Area 25. Test Cell A exhibited an exposure rate between 120–270 μ R/h, and its spectrum exhibited ¹³⁷Cs and ¹⁵²Eu photopeaks with possible photopeaks for ⁶⁰Co. Test Cell C had an exposure rate between 50–75 μ R/h, and the spectrum from this location showed a well-defined ¹³⁷Cs photopeak and two possible peaks at the energies for ⁶⁰Co, although such an assignment is not very strong.

Area 26. The 1970 survey did not include this area.

The 1976 survey⁹ covered only the southwest portion of Area 26 and reported elevated radiation levels over the Test Bunker. The exposure rate was reported as 10–20 μ R/h, and a spectrum of the area showed the presence of ⁶⁰Co.

Table 6-18. Summary of Detected Man-Made Sources in Area 25

Location	ROI	Survey Date	Exposure-Rate Range ($\mu\text{R/h}$)	Isotopes Identified
Test Cell C	11	1970	<i>not detected</i>	
		1976	50–100	^{60}Co , ^{137}Cs
		1994	50–75	^{137}Cs , possible ^{60}Co
Test Cell A	12	1970	>150	<i>not analyzed</i>
		1976	200–300	^{60}Co , ^{137}Cs
		1994	120–270	^{137}Cs , ^{152}Eu , possible ^{60}Co
Test Cell D		1970	31–50	<i>not analyzed</i>
		1976	50–100	^{60}Co
Location between EMAD* and Test Cell C		1970	> 250	^{60}Co
		1976	> 5000	^{60}Co
EMAD		1976	10–20	^{60}Co , ^{137}Cs
Waste Dump southeast of RMAD**		1970	> 150	^{60}Co
		1976	2000–3000	^{60}Co , ^{137}Cs
Rock Valley Irradiation Facility		1970	>100	^{137}Cs (30 kCi source)
Forty-Mile Canyon		1970	31–50	<i>not reported</i>

*EMAD = Engine Maintenance, Assembly, and Disassembly

**RMAD = Reactor Maintenance, Assembly, and Disassembly

The 1992 survey and the 1994 survey did not detect any regions of anomalous activity.

Area 27. The 1970 survey did not include this area. The 1992 survey and the 1994 survey did not detect any regions of anomalous activity.

Area 29. The 1970 survey did not include this area. The 1992 survey and the 1994 survey did not detect any regions of anomalous activity.

Area 30. A summary of the locations containing man-made and ^{241}Am activity, as shown in Figures 9 and 20, is presented in Table 6-19. The Buggy test (ROI 10) included a series of five simultaneous detonations on March 12, 1968, as part of the Plowshare program. The purpose of the test was to assess the ability to carve a channel through the ground using nuclear devices. Each of the five devices produced a published yield of 1.08 kt. The area was not included in the 1970 aerial radiological survey.

Table 6-19. Summary of Detected Man-Made Sources in Area 30

Location	ROI	Survey Date	Exposure-Rate Range ($\mu\text{R/h}$)	Isotopes Identified
U-30A,B,C,D,E (Buggy)	10	1983	180–500	^{60}Co , ^{137}Cs
		1992	24–36	<i>not analyzed</i>
		1994	120–270	^{60}Co , ^{137}Cs , ^{241}Am

In the 1983 helicopter survey,¹⁴ the Buggy site was well-defined in the exposure-rate, ^{60}Co , and ^{137}Cs plots. Several regions were detected containing excess amounts of ^{40}K , possibly caused by changes in the geologic formations. The survey also identified a small region of slightly increased ^{137}Cs and possibly ^{60}Co activity was identified 4–5 kilometers north of the Buggy site. The only isotopes analyzed from the 1983 survey analyzed were ^{60}Co and ^{137}Cs .

The 1992 survey detected a single anomaly near the Buggy site. Even though the aircraft was not flown directly over the site, some of the radiation was detected. The wide-flight-line spacing used in the survey distorted the apparent location and the intensity of this measurement.

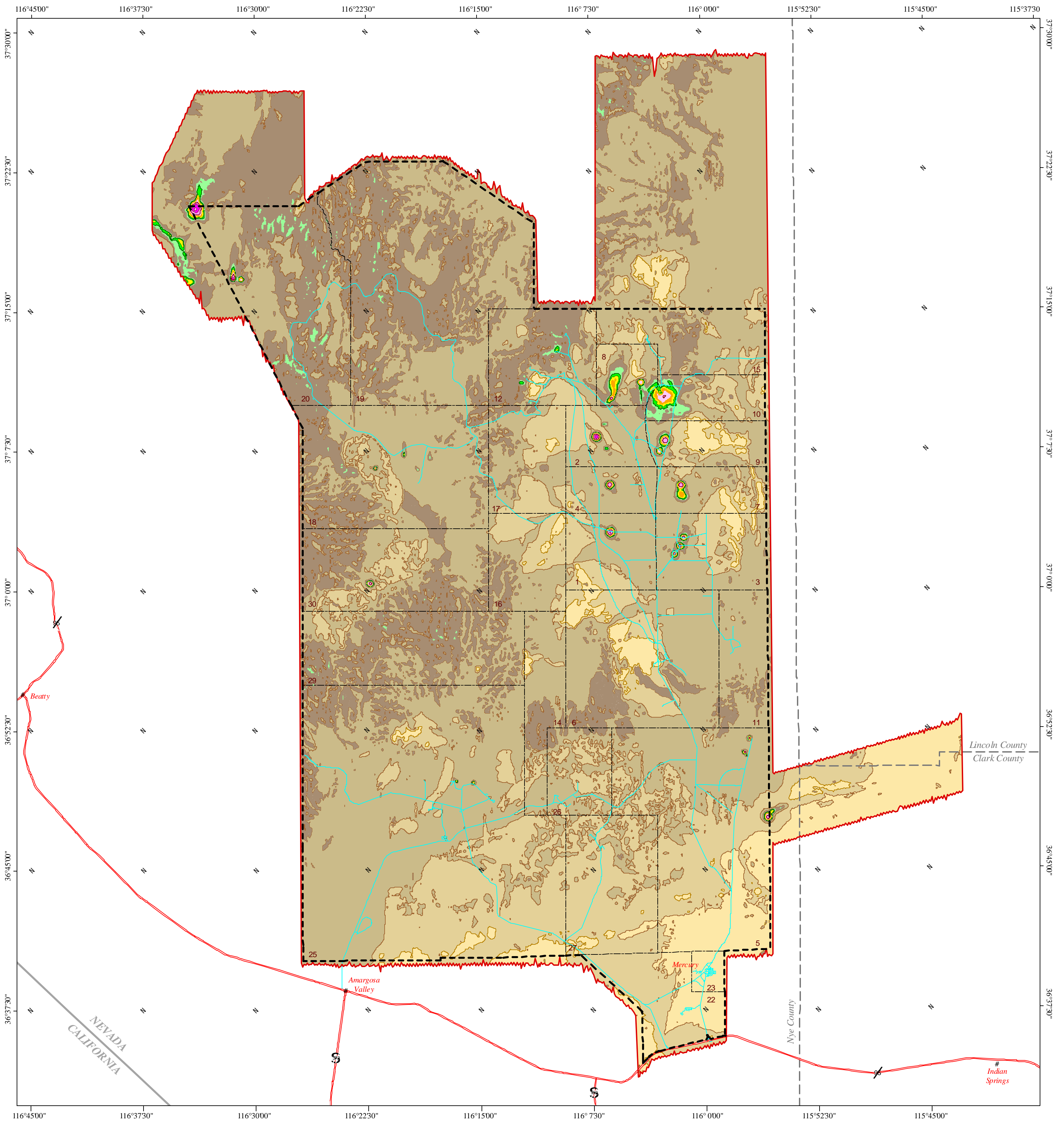
The 1994 survey detected the Buggy Site anomaly at exposure-rate levels comparable to the 1983 survey. The spectrum (Figure 8) recorded a large ^{137}Cs photopeak and small, but definite, ^{60}Co photopeaks. Figure 20 displays a well-defined region of ^{241}Am located within, but slightly west of, the man-made activity bulls-eye contours.


7.0 SUMMARY

Through an aerial radiological survey conducted during August and September 1994, the terrestrial radiation field over the NTS and three regions extending onto the NAFR were extensively mapped, remeasuring regions mapped from 1962 to 1993 by previous DOE aerial surveys.

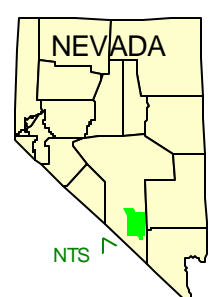
The agreement between the various aerial surveys is very good in regions where natural radiation is compared. The surveys produced nearly identical exposure rates for the naturally occurring background radiation (which is expected since the principle isotopes governing these decay chains have half-lives greater than one billion years).

Many locations containing man-made radiation appeared in the data collected for this survey. Nearly all of the locations containing man-made activity were identified with known radiation sources. Several locations, which exhibited low levels of man-made activity, were actually deviations in the abundances of the naturally occurring radionuclides. In regions of man-made radioactivity, the differences between this survey and previous surveys are qualitatively consistent with the decay of the radioactive isotopes present at each location and with human actions occurring during the intervening time period.



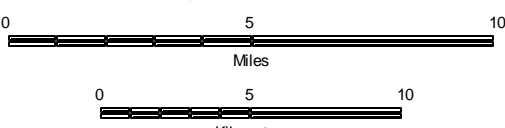



This aerial radiological survey was conducted in support of the Aerial Measuring System Program under the direction of the U.S. Department of Energy, Nevada Operations Office. For additional information regarding these data, contact the Aerial Measuring System Program Manager at the U.S. Department of Energy, Nevada Operations Office.



Map Projection: Transverse Mercator
 Coordinate System: State Plane
 Zone: Nevada Central Zone
 Datum: NAD83
 Spheroid: GRS80
 Graticules: 7.5 Minutes
 Base-Layer Data: NTS GIS Database
 Date Map Produced: June 28, 1999

Map Scale: 1:250,000

- NTS Boundary
- NTS Operational Area
- Highway
- Primary NTS Road
- Survey Boundary

Microroentgens per Hour
 Calculated for 1 Meter Above Ground Level

0 - 6
6 - 12
12 - 18
18 - 24
24 - 30
30 - 39
39 - 50
50 - 75
75 - 120
120 - 270
270 - 900

Nevada Test Site (NTS) Aerial Radiation Survey Terrestrial Exposure Rate

1994 Survey

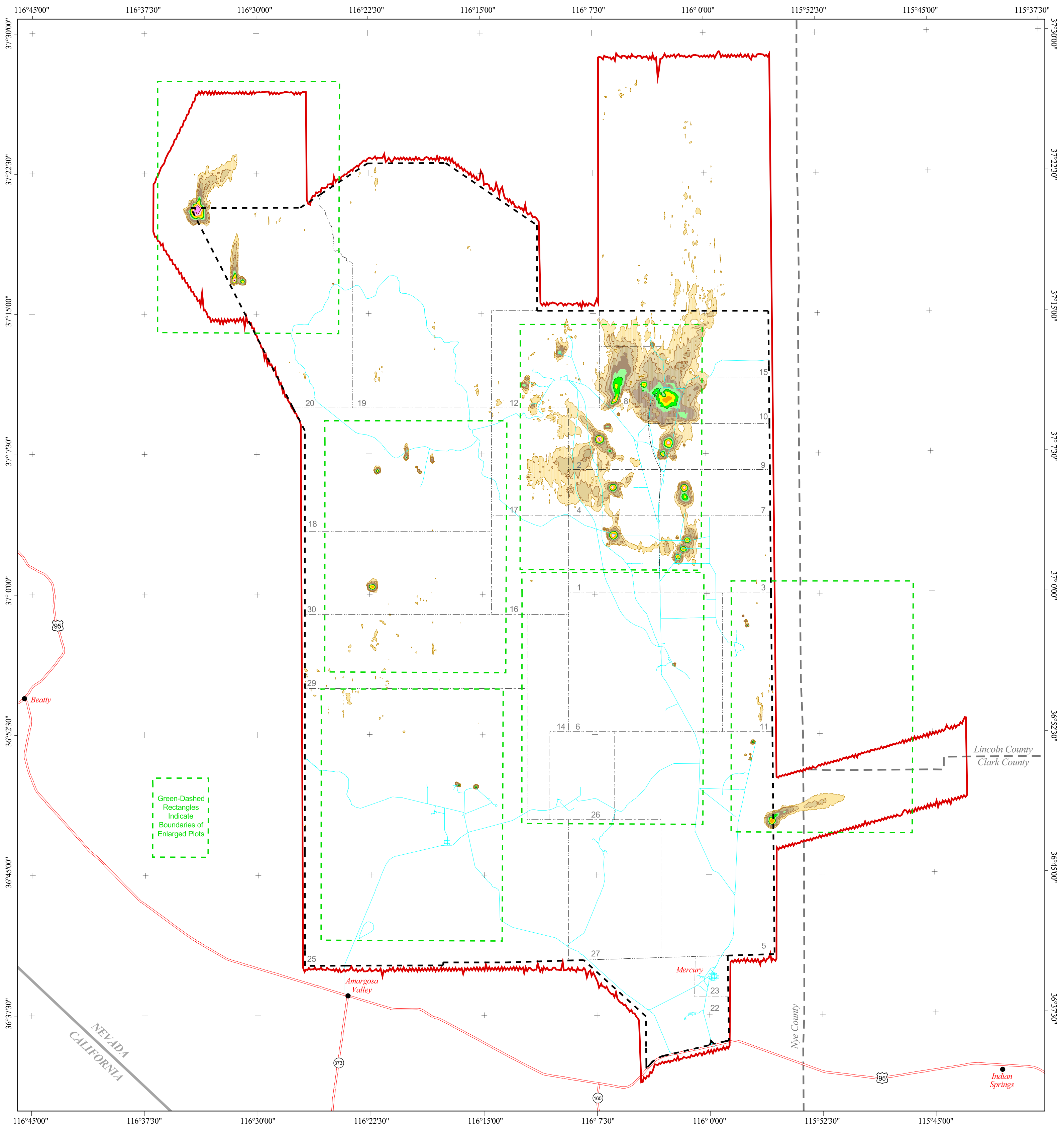
Cosmic-ray exposure contributions are not included in the data that are presented. Cosmic-ray contributions range from 4.6 to 7.4 microroentgens per hour between the elevations of 3000 and 7000 feet, respectively.

Bechtel Nevada

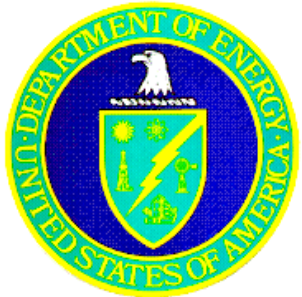
NTS GIS 99124.6

Exposure rates only apply accurately to regions of natural background activity. The rates in regions of man-made activity are primarily useful as relative indicators.

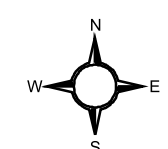
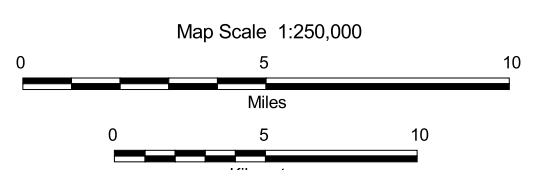
FIGURE 4. SITE-WIDE TERRESTRIAL EXPOSURE-RATE CONTOUR PLOT



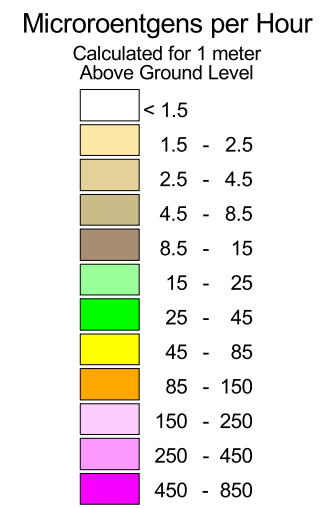
Green-Dashed Rectangles Indicate Boundaries of Enlarged Plots



Map Projection: Transverse Mercator
 Coordinate System: State Plane
 Zone: Nevada Central Zone
 Datum: NAD83
 Spheroid: GRS80
 Graticules: 7.5 Minutes
 Base-Layer Data: NTS GIS Database
 Date Map Produced: June 28, 1999



- NTS Boundary
- NTS Operational Area
- Highway
- Primary NTS Road
- Survey Boundary



Nevada Test Site (NTS) Aerial Radiation Survey Man-Made Exposure Rate

1994 Survey



The gamma-ray spectral composition in regions of man-made activity is significantly different from the composition observed in regions of natural background activity. Therefore, the exposure rates are estimates that are useful for relative comparisons but not as absolute values.

NTS GIS 99123.6

This aerial radiological survey was conducted in support of the Aerial Measuring System Program under the direction of the U.S. Department of Energy, Nevada Operations Office. For additional information regarding these data, contact the Aerial Measuring System Program Manager at the U.S. Department of Energy, Nevada Operation Office.

Transportation data were obtained from the U.S. Geological Survey Digital Line Graph files. The NTS boundaries, Operational Areas, and primary roads were obtained from the NTS GIS database. Two helicopters were used simultaneously in conducting this high-resolution, medium-altitude aerial radiological survey, and the entire NTS and various adjacent areas were covered. The survey parameters provided approximately 100 percent coverage of the site. The survey was flown in a north-south direction, at an altitude of 200 feet above ground level, and with flight lines spaced 500 feet apart. The survey and data analysis were conducted by the U.S. Department of Energy's Remote Sensing Laboratory, which is located in Las Vegas, Nevada, and operated by Bechtel Nevada.

FIGURE 5. SITE-WIDE MMGC-RATE CONTOUR PLOT

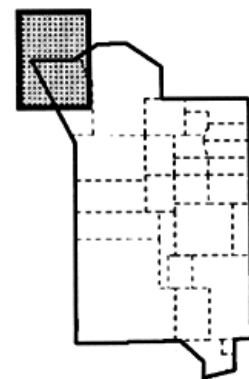
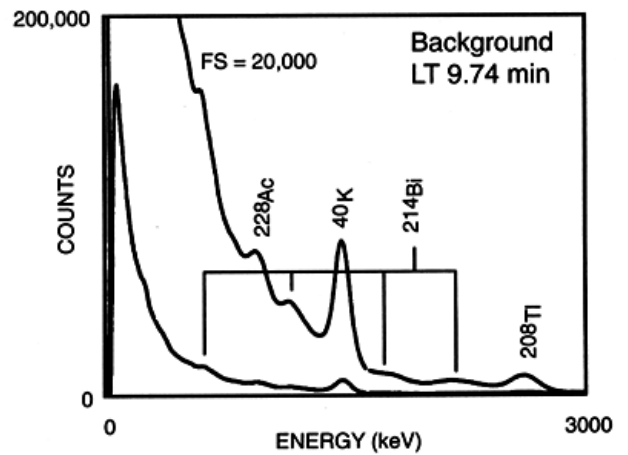
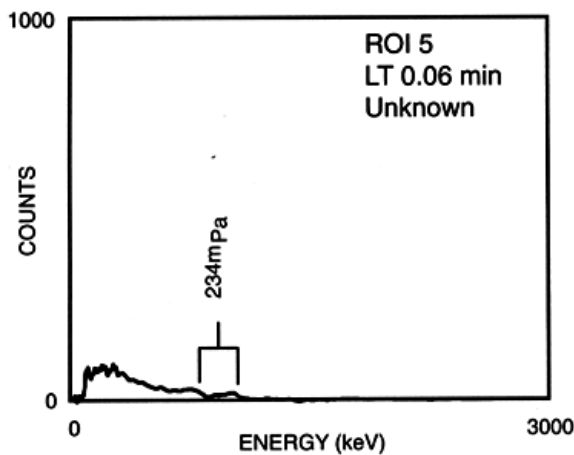
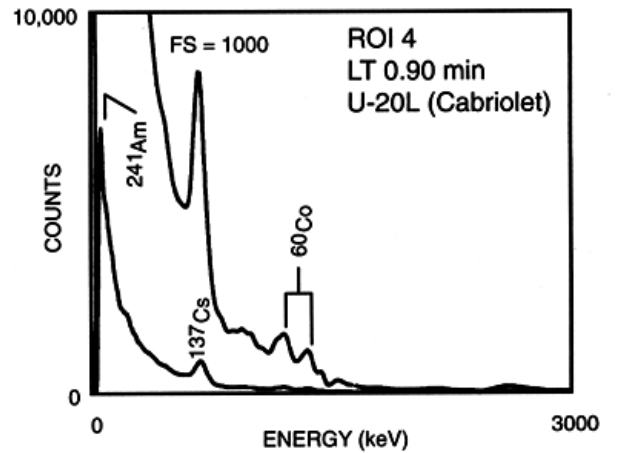
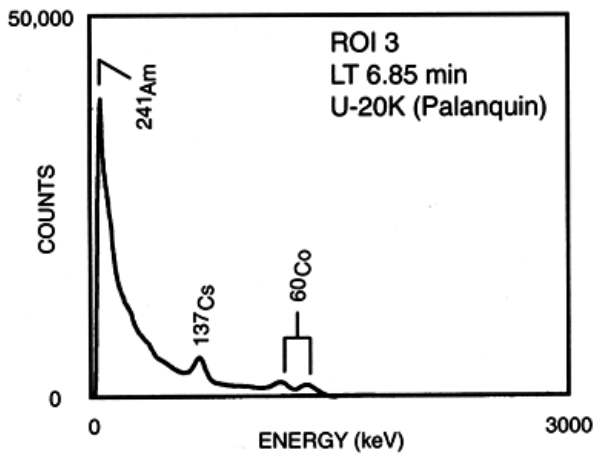
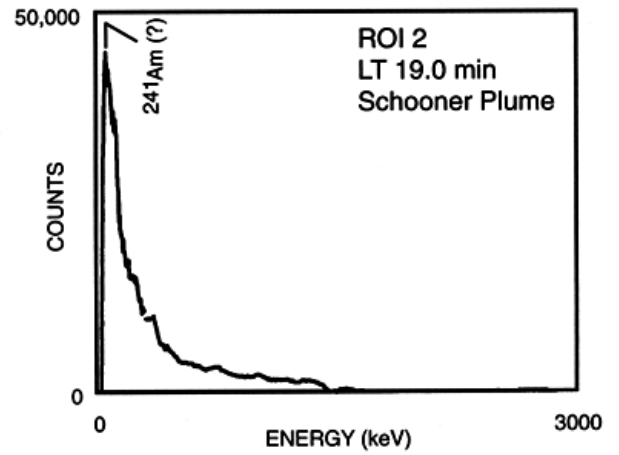
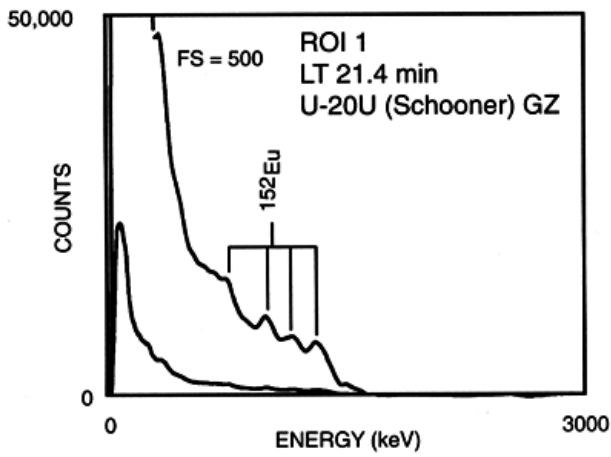
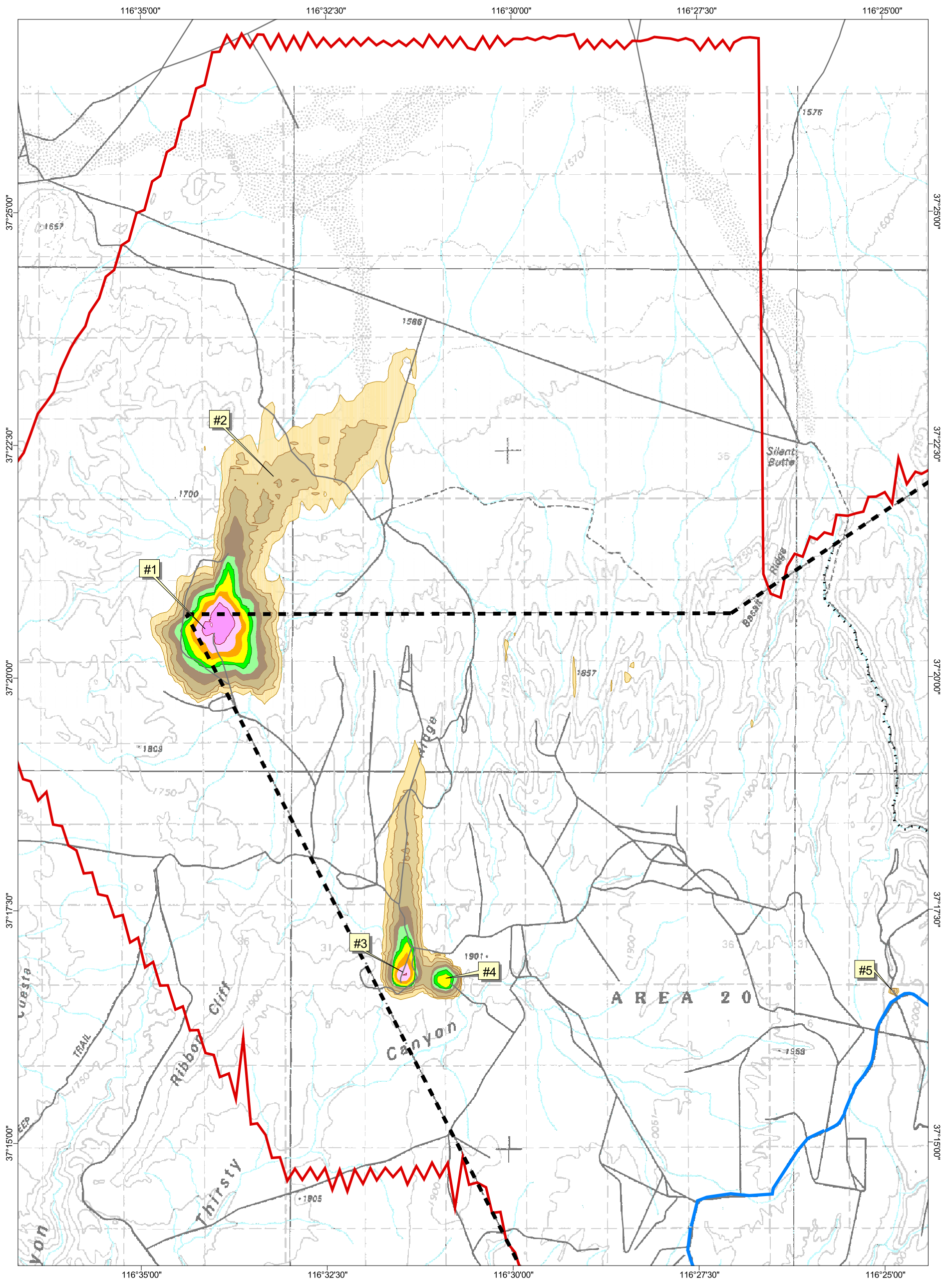


FIGURE 6. NET GAMMA SPECTRA FOR ROIs IDENTIFIED IN FIGURE 7



This aerial radiological survey was conducted in support of the Aerial Measuring System Program under the direction of the U.S. Department of Energy, Nevada Operations Office. For additional information regarding these data, contact the Aerial Measuring System Program Manager at the U.S. Department of Energy, Nevada Operation Office.

NEVADA
NTS

Map Projection: Transverse Mercator
 Coordinate System: State Plane
 Zone: Nevada Central Zone
 Datum: NAD83
 Spheroid: GRS80
 Graticules: 2.5 Minutes
 Base-Layer Data: NTS GIS Database
 Date Map Produced: June 28, 1999

Microroentgens per Hour
 Calculated for 1 Meter
 Above Ground Level

< 1.5
1.5 - 2.5
2.5 - 4.5
4.5 - 8.5
8.5 - 15
15 - 25
25 - 45
45 - 85
85 - 150
150 - 250
250 - 450
450 - 850

- NTS Boundary
- NTS Operational Area
- Highway
- Primary NTS Road
- Secondary Road and Trail
- Survey Boundary
- Region of Interest Identifier

The gamma-ray spectral composition in regions of man-made activity is significantly different from the composition observed in regions of natural background activity. Therefore, the exposure rates are estimates that are useful for relative comparisons but not as absolute values.

Nevada Test Site (NTS) Aerial Radiation Survey Man-Made Exposure Rate 1994 Survey

Map Scale 1:75,000

Bechtel Nevada
NTS GIS 99187.6

FIGURE 7. MAN-MADE ACTIVITY IN AREA 20

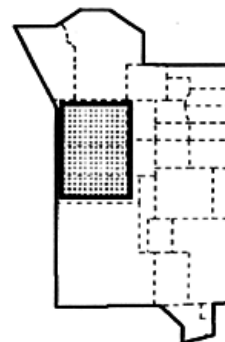
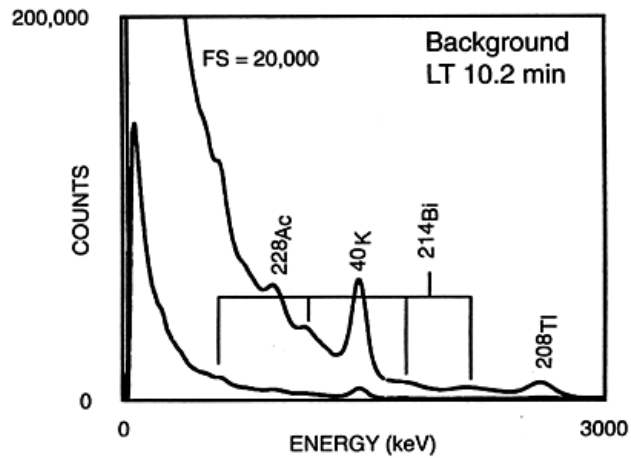
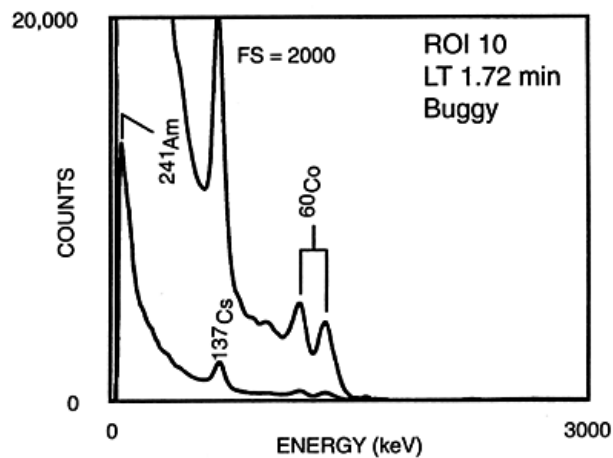
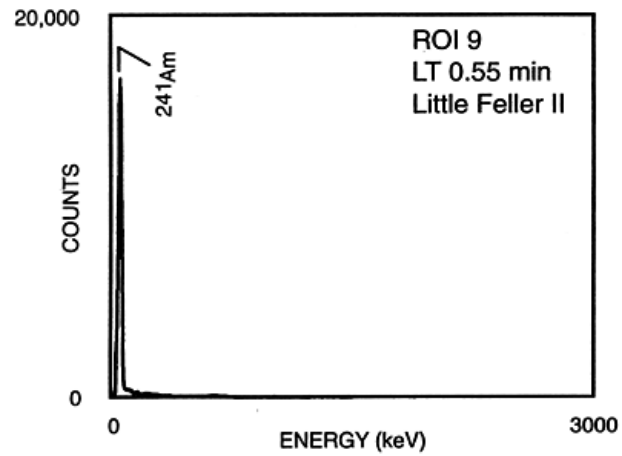
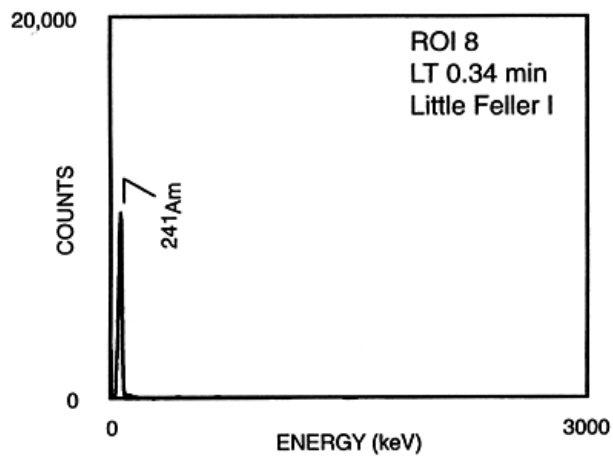
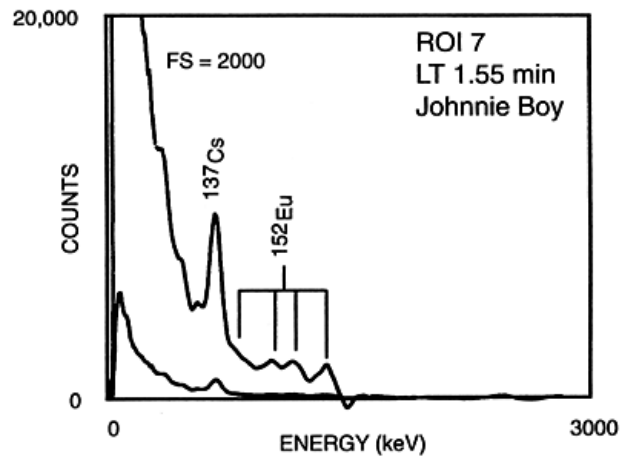
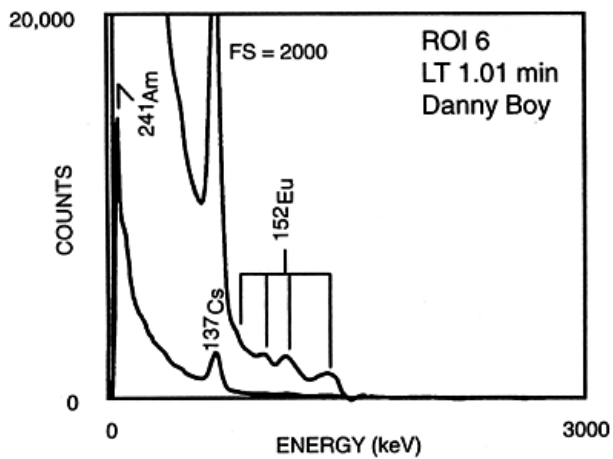
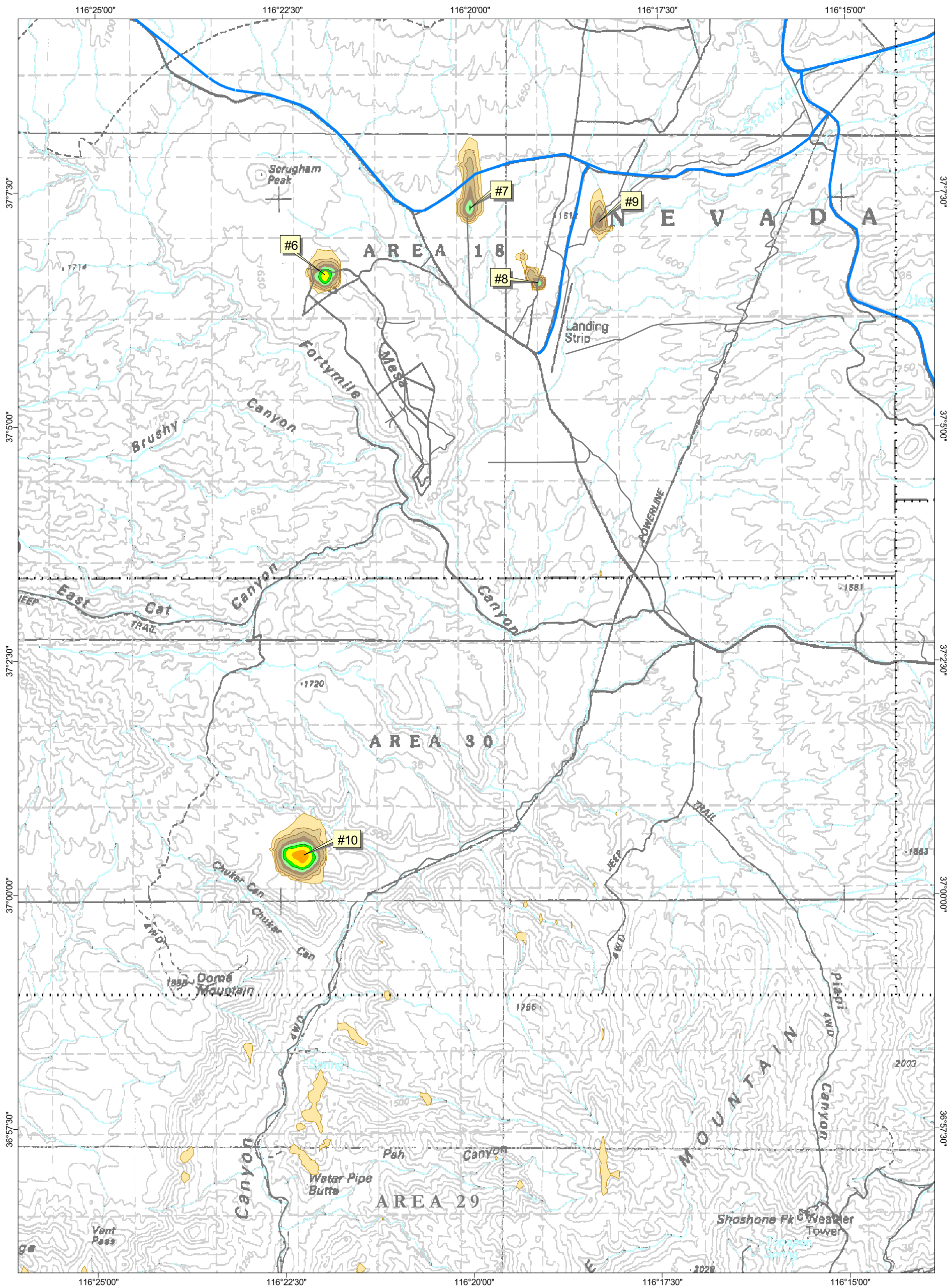


FIGURE 8. NET GAMMA SPECTRA FOR ROIs IDENTIFIED IN FIGURE 9



This aerial radiological survey was conducted in support of the Aerial Measuring System Program under the direction of the U.S. Department of Energy, Nevada Operations Office. For additional information regarding these data, contact the Aerial Measuring System Program Manager at the U.S. Department of Energy, Nevada Operation Office.

NEVADA
NTS

Map Projection: Transverse Mercator
 Coordinate System: State Plane
 Zone: Nevada Central Zone
 Datum: NAD83
 Spheroid: GRS80
 Graticules: 2.5 Minutes
 Base-Layer Data: NTS GIS Database
 Date Map Produced: June 28, 1999

Transportation data were obtained from the U.S. Geological Survey (USGS) Digital Line Graph files. The NTS boundaries, Operational Areas, and primary roads were obtained from the NTS GIS database. Basemap obtained from USGS 1:100,000 scale digital raster graphic, Pahute Mesa and Beatty quadrangles. Elevation values are shown in meters above mean sea level. Two helicopters were used simultaneously in conducting this high-resolution, medium-altitude aerial radiological survey, and the entire NTS and various adjacent areas were covered. The survey parameters provided approximately 100 percent coverage of the site. The survey was flown in a north-south direction, at an altitude of 200 feet above ground level, and with flight lines spaced 500 feet apart. The survey and data analysis were conducted by the U.S. Department of Energy's Remote Sensing Laboratory, which is located in Las Vegas, Nevada, and operated by Bechtel Nevada.

Microroentgens per Hour
 Calculated for 1 Meter Above Ground Level

< 1.5
1.5 - 2.5
2.5 - 4.5
4.5 - 8.5
8.5 - 15
15 - 25
25 - 45
45 - 85
85 - 150
150 - 250
250 - 450
450 - 850

- NTS Boundary
- NTS Operational Area
- Highway
- Primary NTS Road
- Secondary Road and Trail
- Survey Boundary
- Region of Interest Identifier

The gamma-ray spectral composition in regions of man-made activity is significantly different from the composition observed in regions of natural background activity. Therefore, the exposure rates are estimates that are useful for relative comparisons but not as absolute values.

Nevada Test Site (NTS) Aerial Radiation Survey Man-Made Exposure Rate 1994 Survey

Map Scale: 1:75,000

0 1 Miles
0 1 Kilometers

N

Bechtel Nevada
NTS GIS 99188.6

FIGURE 9. MAN-MADE ACTIVITY IN AREAS 18 AND 30

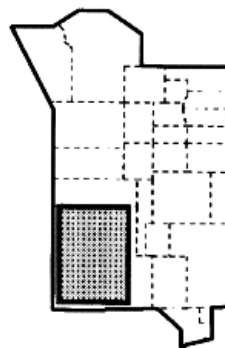
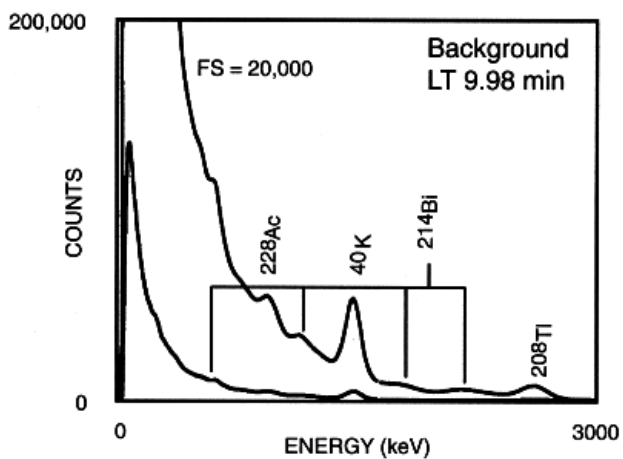
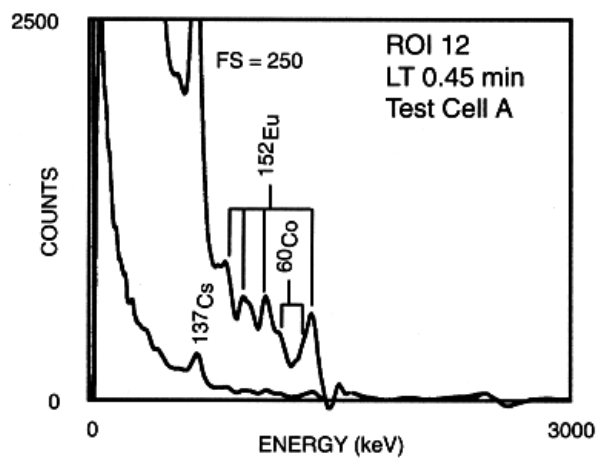
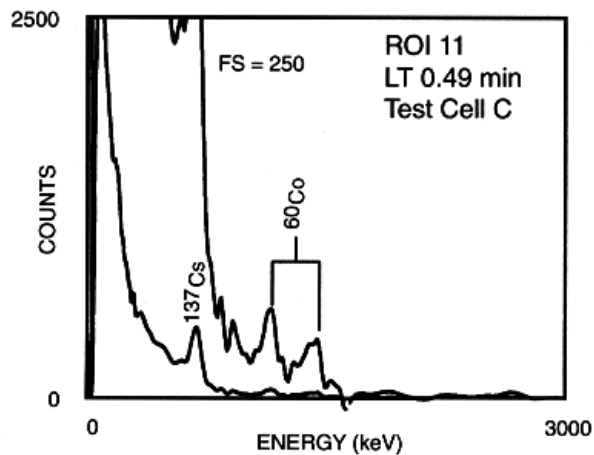
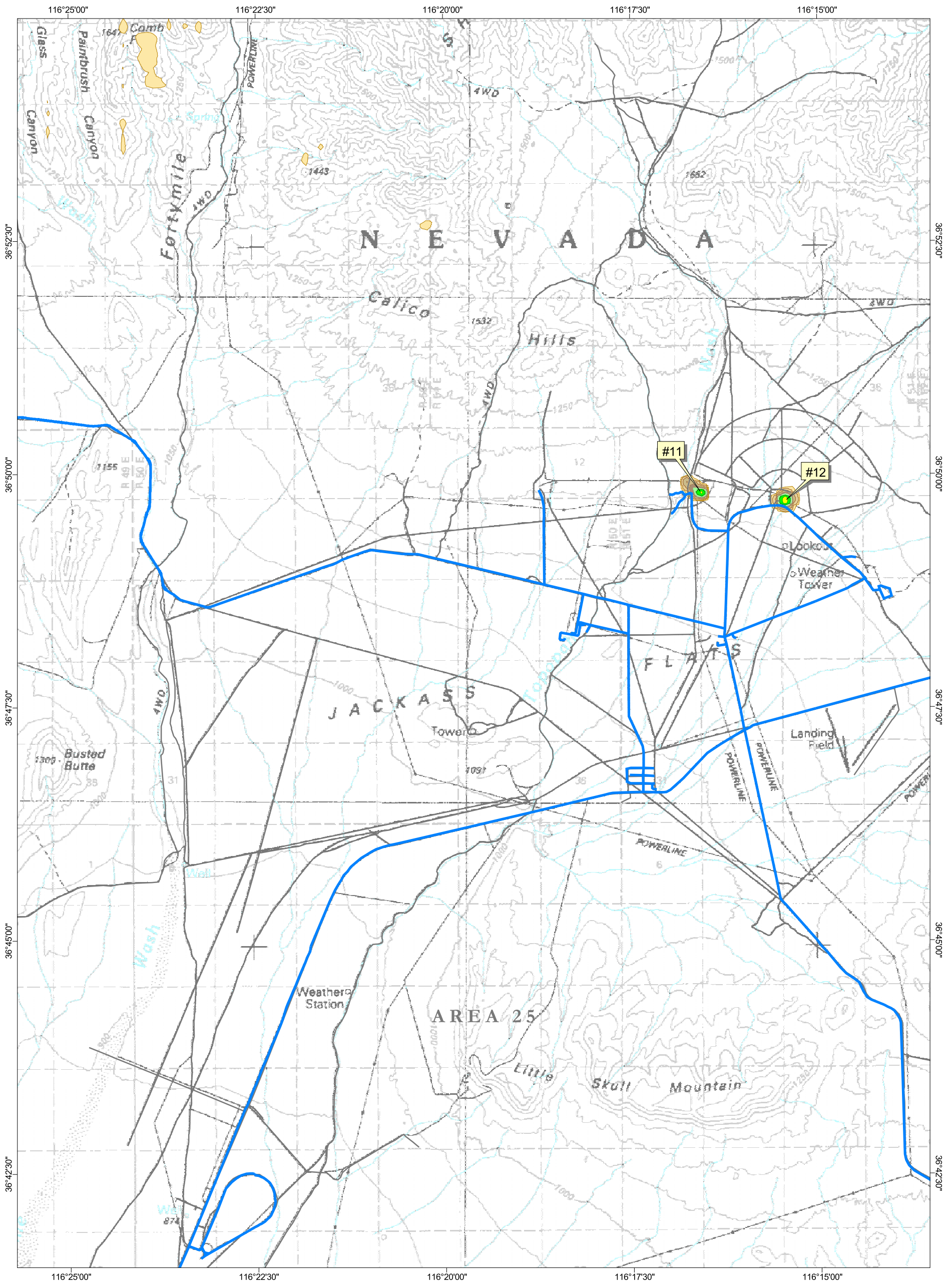


FIGURE 10. NET GAMMA SPECTRA FOR ROIs IDENTIFIED IN FIGURE 11



This aerial radiological survey was conducted in support of the Aerial Measuring System Program under the direction of the U.S. Department of Energy, Nevada Operations Office. For additional information regarding these data, contact the Aerial Measuring System Program Manager at the U.S. Department of Energy, Nevada Operations Office.

NEVADA
NTS

Map Projection: Transverse Mercator
 Coordinate System: State Plane Nevada Central Zone
 Zone: NAD83
 Datum: GRS80
 Spheroid: 2.5 Minutes
 Graticules: NTS GIS Database
 Base-Layer Data: June 28, 1999
 Date Map Produced:

Microroentgens per Hour
 Calculated for 1 Meter Above Ground Level

< 1.5
1.5 - 2.5
2.5 - 4.5
4.5 - 8.5
8.5 - 15
15 - 25
25 - 45
45 - 85
85 - 150
150 - 250
250 - 450
450 - 850

NTS Boundary
 NTS Operational Area
 Highway
 Primary NTS Road
 Secondary Road and Trail
 Survey Boundary
 Region of Interest Identifier

Nevada Test Site (NTS) Aerial Radiation Survey Man-Made Exposure Rate 1994 Survey

Map Scale 1:75,000

Bechtel Nevada
 NTS GIS 99189.6

The gamma-ray spectral composition in regions of man-made activity is significantly different from the composition observed in regions of natural background activity. Therefore, the exposure rates are estimates that are useful for relative comparisons but not as absolute values.

FIGURE 11. MAN-MADE ACTIVITY IN AREA 25

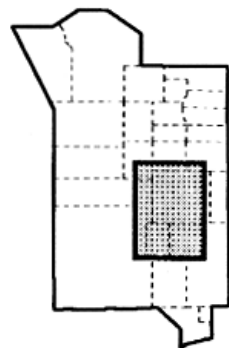
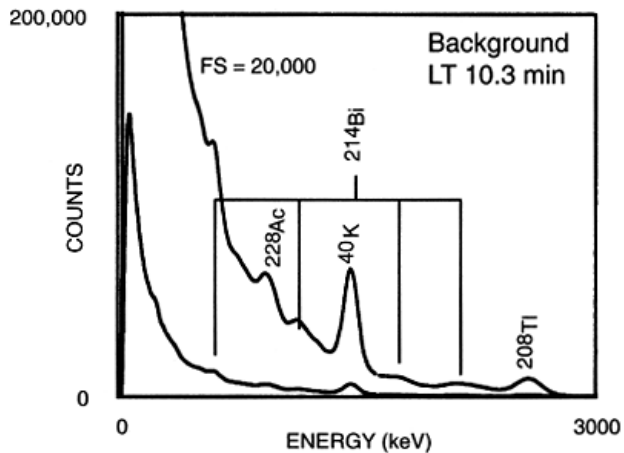
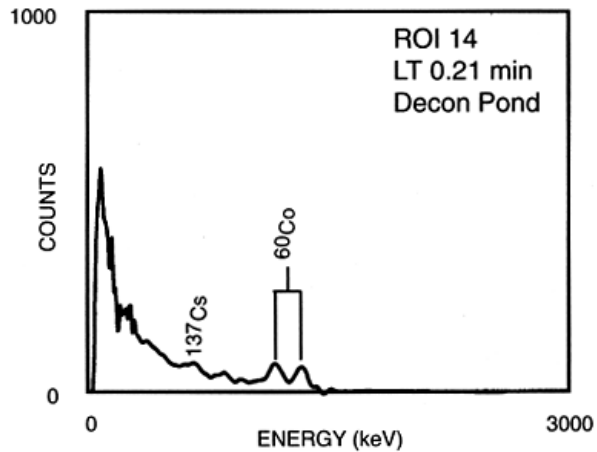
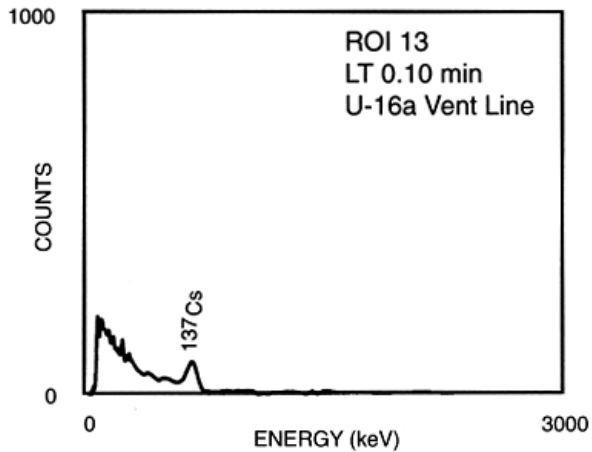
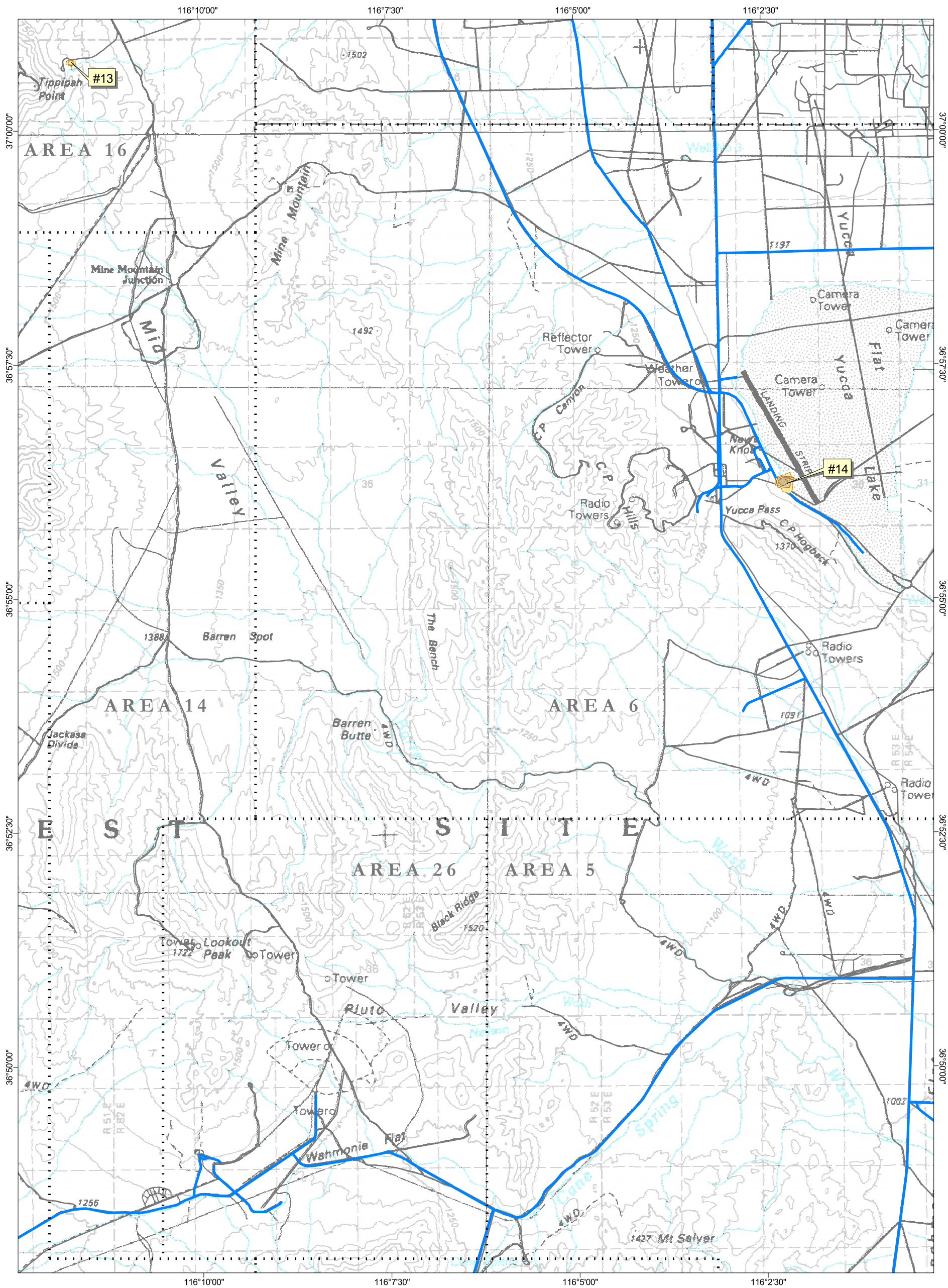


FIGURE 12. NET GAMMA SPECTRA FOR ROIs IDENTIFIED IN FIGURE 13



This aerial radiological survey was conducted in support of the Aerial Measuring System Program under the direction of the U.S. Department of Energy, Nevada Operations Office. For additional information regarding these data, contact the Aerial Measuring System Program Manager at the U.S. Department of Energy, Nevada Operations Office.

NEVADA
NTS

Map Projection: Transverse Mercator
 Coordinate System: State Plane Nevada Central Zone
 Datum: NAD83
 Spheroid: GRS80
 Graticules: 2.5 Minutes
 Base-Layer Data: NTS GIS Database
 Date Map Produced: June 28, 1999

Microroentgens per Hour
 Calculated for 1 Meter Above Ground Level

< 1.5
1.5 - 2.5
2.5 - 4.5
4.5 - 8.5
8.5 - 15
15 - 25
25 - 45
45 - 85
85 - 150
150 - 250
250 - 450
450 - 850

- NTS Boundary
- NTS Operational Area
- Highway
- Primary NTS Road
- Secondary Road and Trail
- Survey Boundary
- Region of Interest Identifier

The gamma-ray spectral composition in regions of man-made activity is significantly different from the composition observed in regions of natural background activity. Therefore, the exposure rates are estimates that are useful for relative comparisons but not as absolute values.

Nevada Test Site (NTS) Aerial Radiation Survey Man-Made Exposure Rate 1994 Survey

Map Scale 1:75,000

0 1
Miles
0 1
Kilometers

Bechtel Nevada
NTS GIS 99190.6

FIGURE 13. MAN-MADE ACTIVITY IN AREAS 6 AND 16

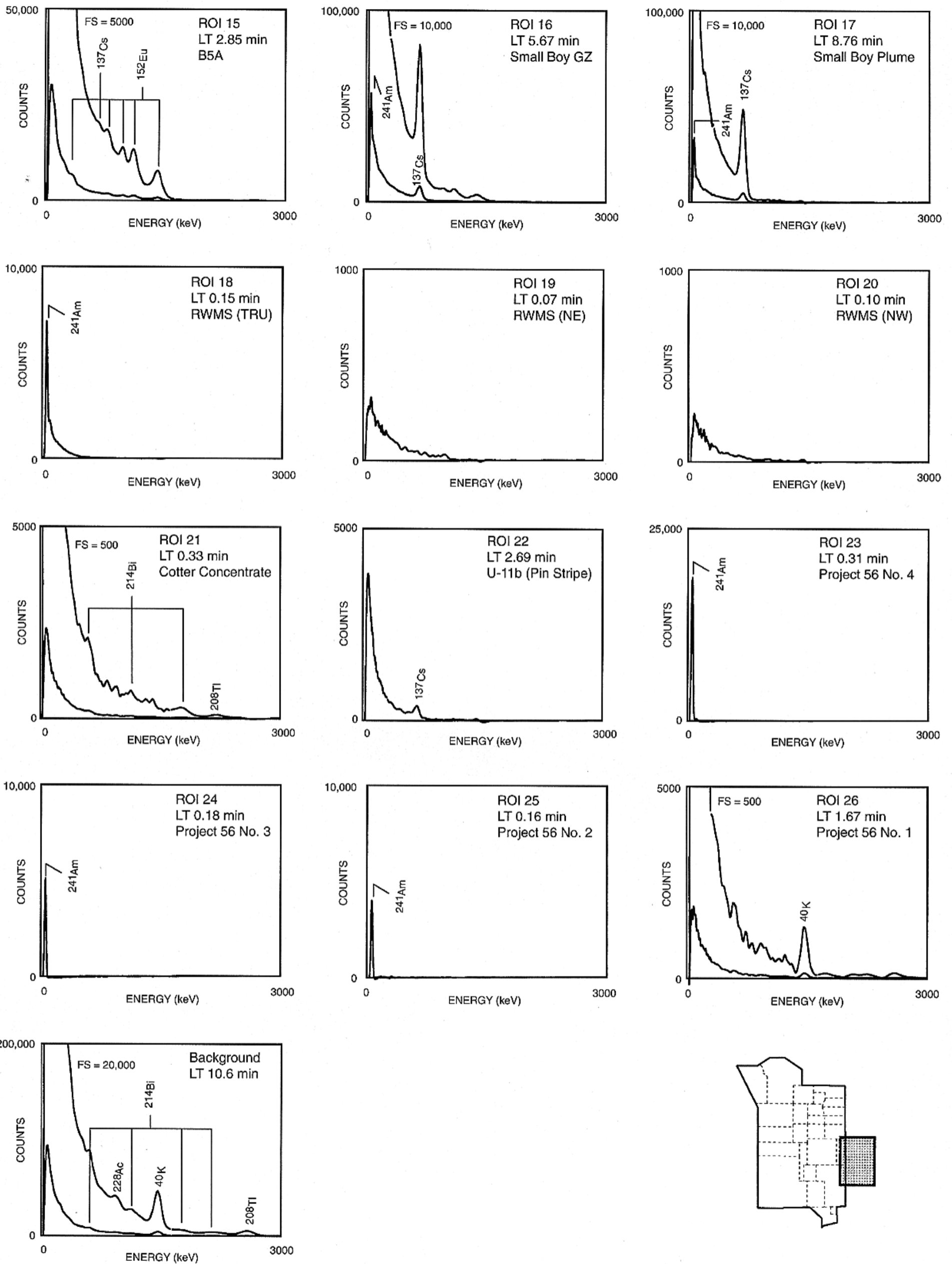
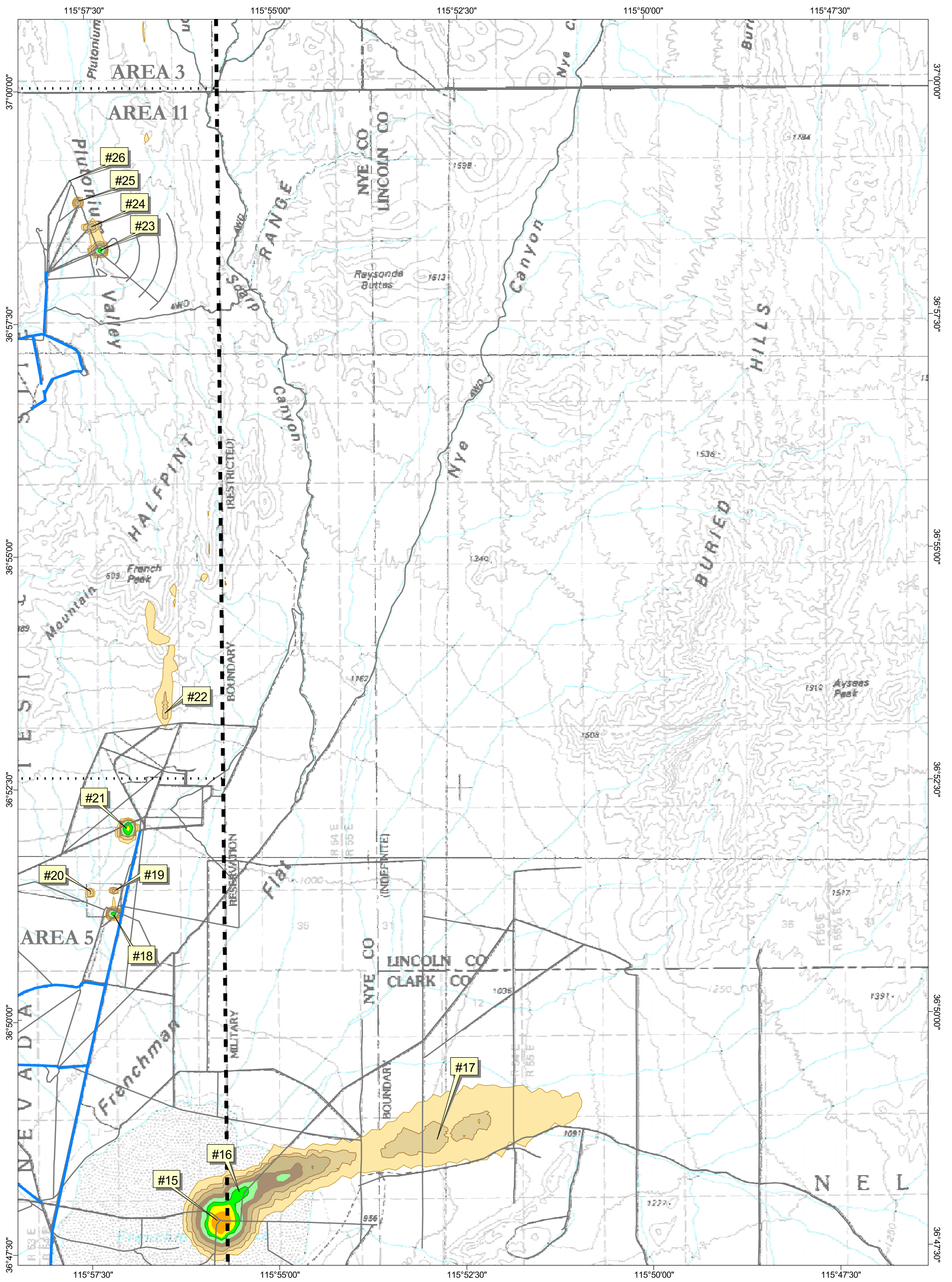


FIGURE 14. NET GAMMA SPECTRA FOR ROIs IDENTIFIED IN FIGURE 15



This aerial radiological survey was conducted in support of the Aerial Measuring System Program under the direction of the U.S. Department of Energy, Nevada Operations Office. For additional information regarding these data, contact the Aerial Measuring System Program Manager at the U.S. Department of Energy, Nevada Operations Office.

Map Projection: Transverse Mercator
 Coordinate System: State Plane Nevada Central Zone
 Datum: NAD83
 Spheroid: GRS80
 Graticules: 2.5 Minutes
 Base-Layer Data: NTS GIS Database
 Date Map Produced: June 28, 1999

Microroentgens per Hour
 Calculated for 1 Meter Above Ground Level

< 1.5
1.5 - 2.5
2.5 - 4.5
4.5 - 8.5
8.5 - 15
15 - 25
25 - 45
45 - 85
85 - 150
150 - 250
250 - 450
450 - 850

- NTS Boundary
- NTS Operational Area
- Highway
- Primary NTS Road
- Secondary Road and Trail
- Survey Boundary
- Region of Interest Identifier

The gamma-ray spectral composition in regions of man-made activity is significantly different from the composition observed in regions of natural background activity. Therefore, the exposure rates are estimates that are useful for relative comparisons but not as absolute values.

Nevada Test Site (NTS) Aerial Radiation Survey Man-Made Exposure Rate 1994 Survey

Map Scale 1:75,000

Bechtel Nevada
NTS GIS 99191.6

FIGURE 15. MAN-MADE ACTIVITY IN AREAS 5 AND 11

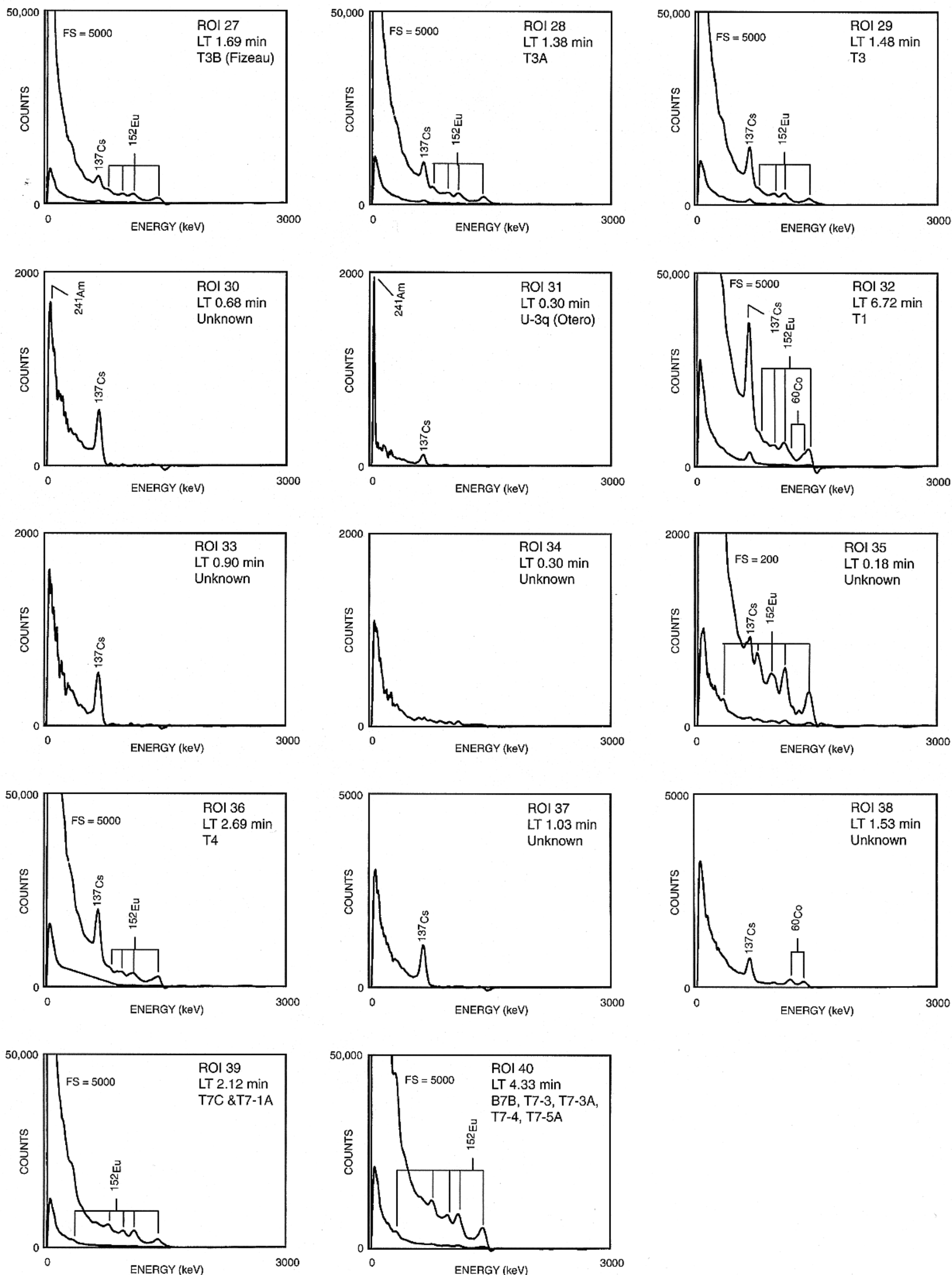


FIGURE 16a. NET GAMMA SPECTRA FOR ROIs IDENTIFIED IN FIGURE 17

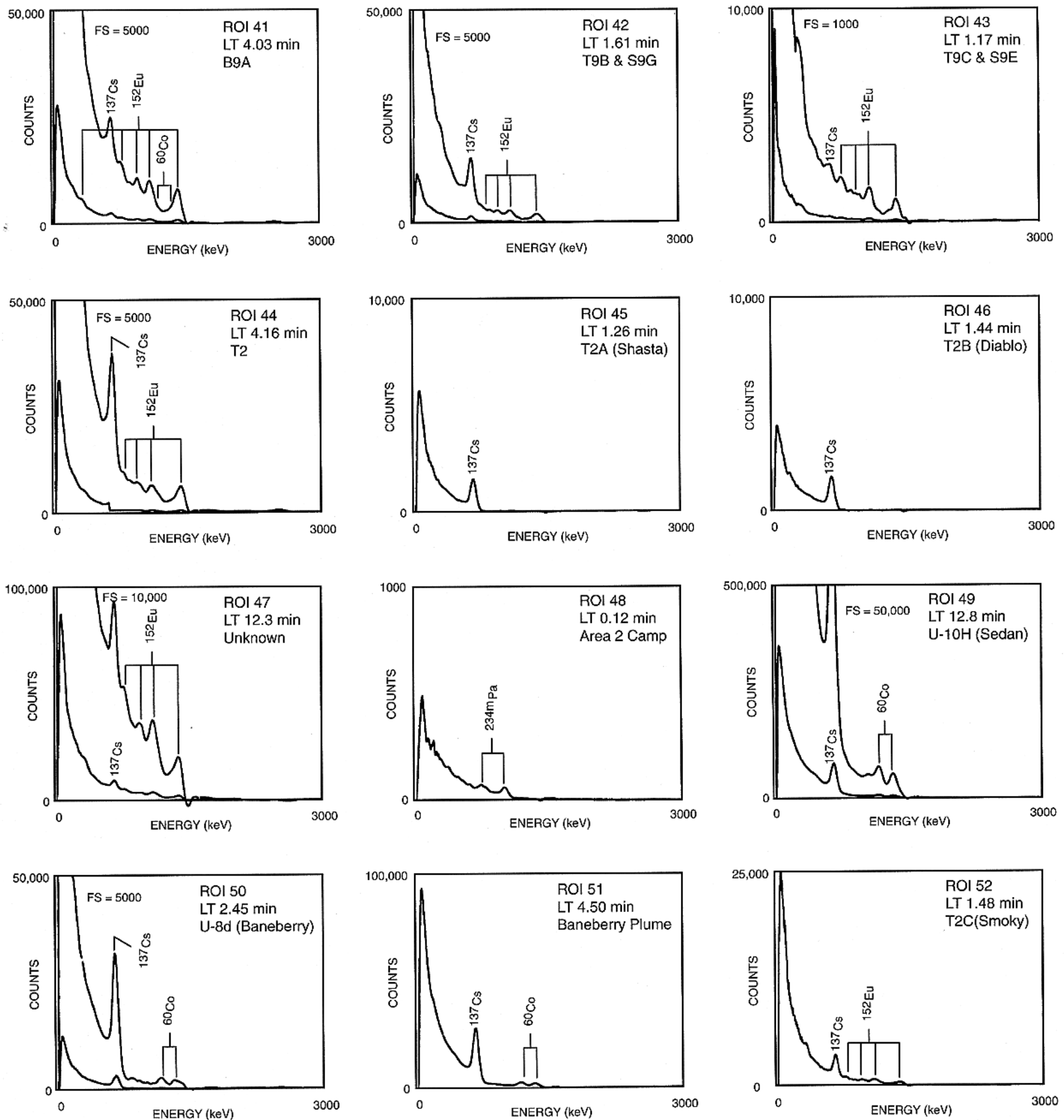


FIGURE 16b. NET GAMMA SPECTRA FOR ROIs IDENTIFIED IN FIGURE 17

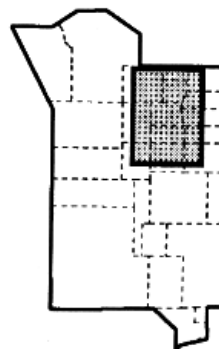
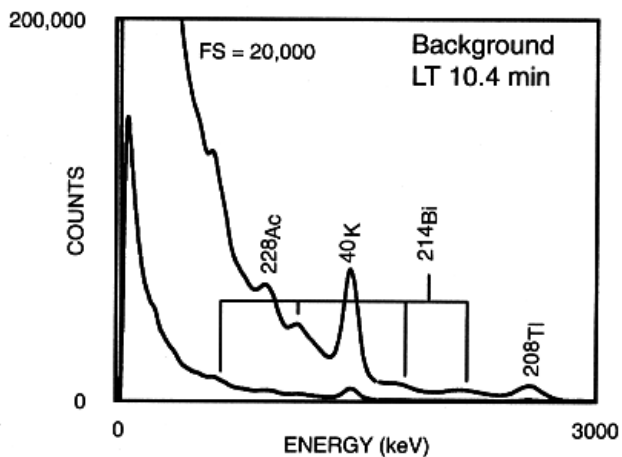
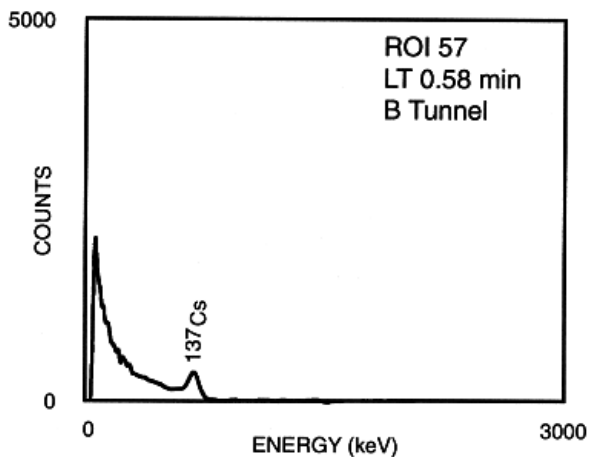
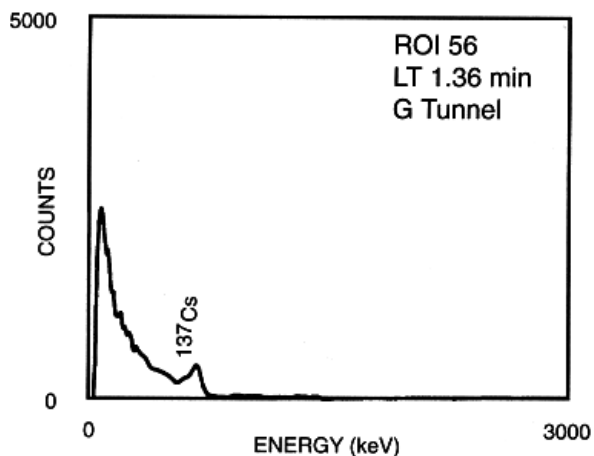
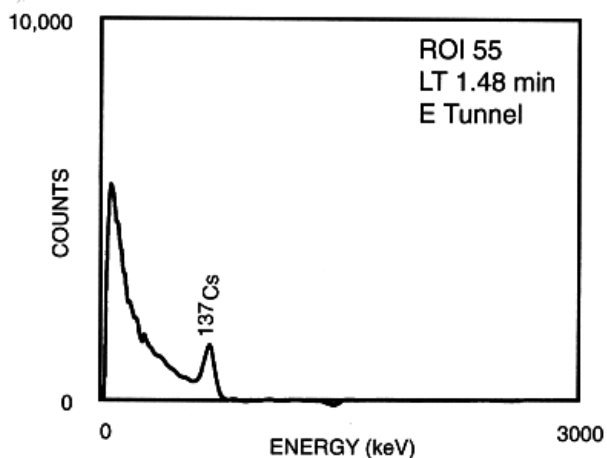
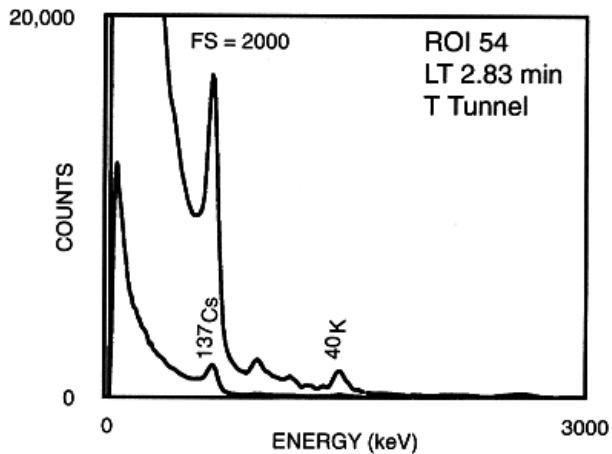
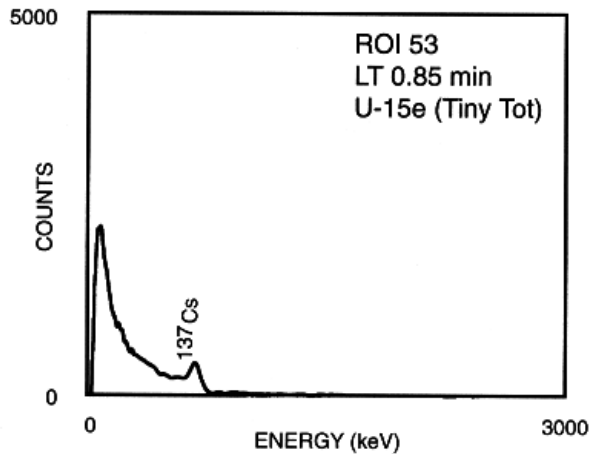
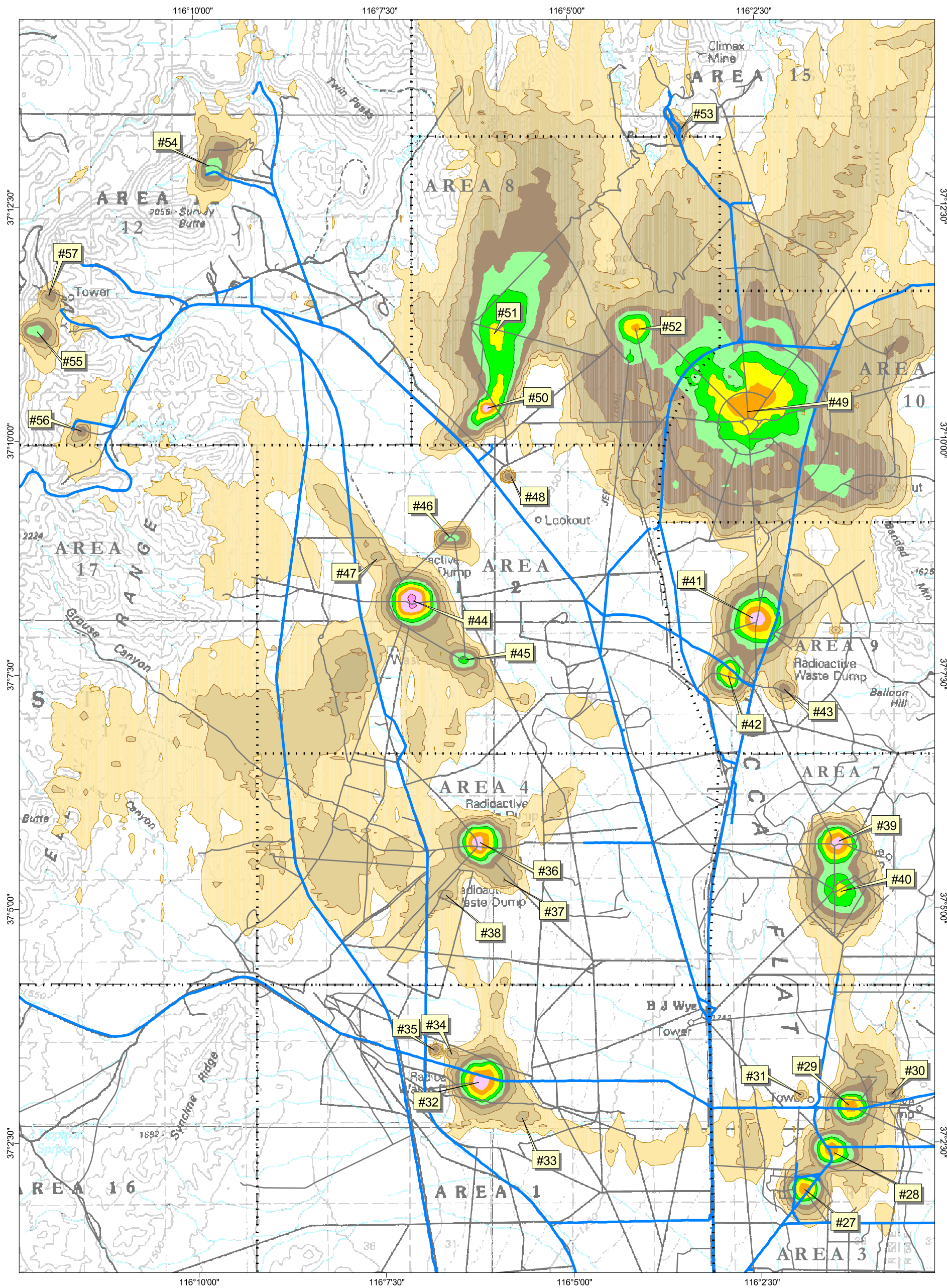


FIGURE 16c. NET GAMMA SPECTRA FOR ROIs IDENTIFIED IN FIGURE 17



Map Projection: Transverse Mercator
Coordinate System: State Plane Nevada Central Zone
Zone: Nevada Central Zone
Datum: NAD83
Spheroid: GRS80
Graticules: 2.5 Minutes
Base-Layer Data: NTS GIS Database
Date Map Produced: June 28, 1999

Microrentgens per Hour
 Calculated for 1 Meter Above Ground Level

< 1.5
1.5 - 2.5
2.5 - 4.5
4.5 - 8.5
8.5 - 15
15 - 25
25 - 45
45 - 85
85 - 150
150 - 250
250 - 450
450 - 850

- NTS Boundary
- NTS Operational Area
- Highway
- Primary NTS Road
- Secondary Road and Trail
- Survey Boundary
- Region of Interest Identifier

Nevada Test Site (NTS) Aerial Radiation Survey Man-Made Exposure Rate 1994 Survey

Map Scale: 1:75,000

Bechtel Nevada
 NTS GIS 99192.6

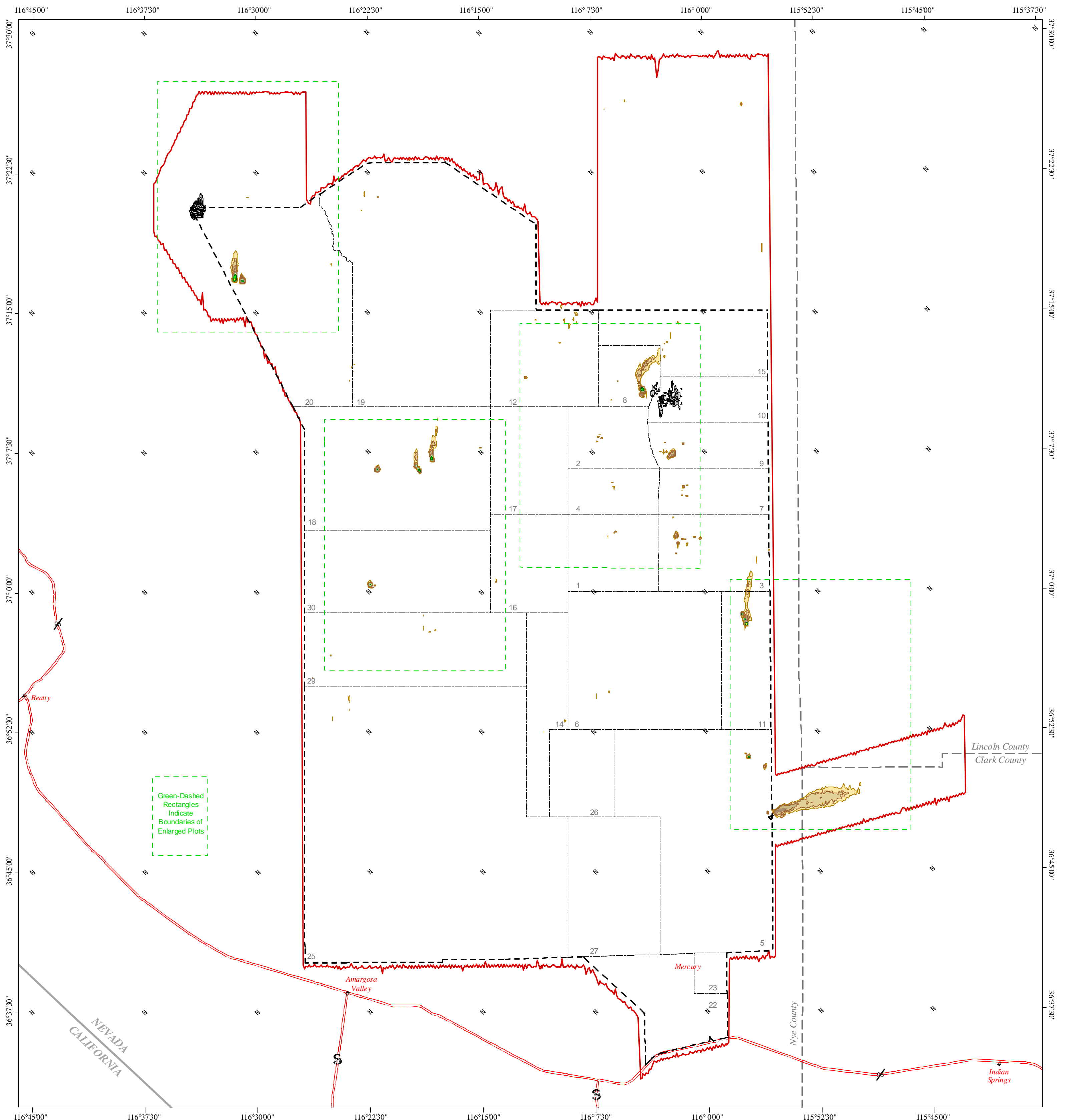
This aerial radiological survey was conducted in support of the Aerial Measuring System Program under the direction of the U.S. Department of Energy, Nevada Operations Office. For additional information regarding these data, contact the Aerial Measuring System Program Manager at the U.S. Department of Energy, Nevada Operations Office.

Transportation data were obtained from the U.S. Geological Survey (USGS) Digital Line Graph files. The NTS boundaries, Operational Areas, and primary roads were obtained from the NTS GIS database. Basemap obtained from USGS 1:100,000 scale digital raster graphic, Pahute Mesa quadrangle. Elevation values are shown in meters above mean sea level.

Two helicopters were used simultaneously in conducting this high-resolution, medium-altitude aerial radiological survey, and the entire NTS and various adjacent areas were covered. The survey parameters provided approximately 100 percent coverage of the site. The survey was flown in a north-south direction, at an altitude of 200 feet above ground level, and with flight lines spaced 500 feet apart. The survey and data analysis were conducted by the U.S. Department of Energy's Remote Sensing Laboratory, which is located in Las Vegas, Nevada, and operated by Bechtel Nevada.

The gamma-ray spectral composition in regions of man-made activity is significantly different from the composition observed in regions of natural background activity. Therefore, the exposure rates are estimates that are useful for relative comparisons but not as absolute values.

FIGURE 17. MAN-MADE ACTIVITY IN YUCCA FLAT



Green-Dashed Rectangles Indicate Boundaries of Enlarged Plots

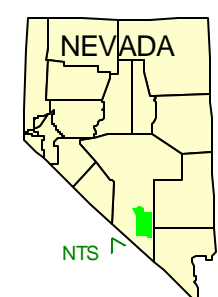
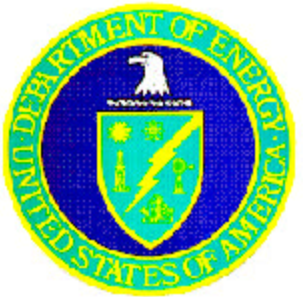
Lincoln County
Clark County

Nevada Test Site (NTS) Aerial Radiation Survey Americium Count Rate

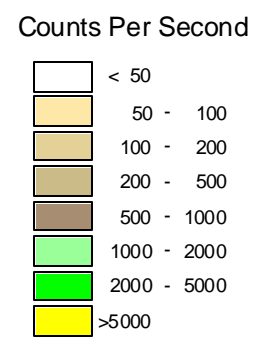
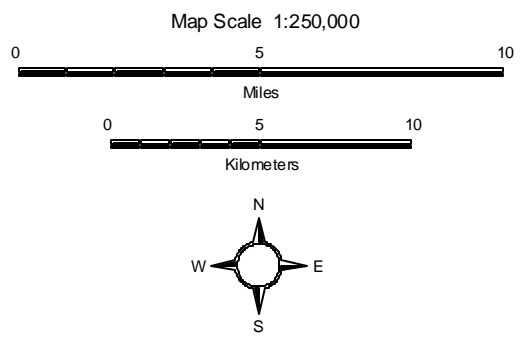
1994 Survey



NTS GIS 99193.6



Map Projection: Transverse Mercator
 Coordinate System: State Plane
 Zone: Nevada Central Zone
 Datum: NAD83
 Spheroid: GRS80
 Graticules: 7.5 Minutes
 Base-Layer Data: NTS GIS Database
 Date Map Produced: June 28, 1999



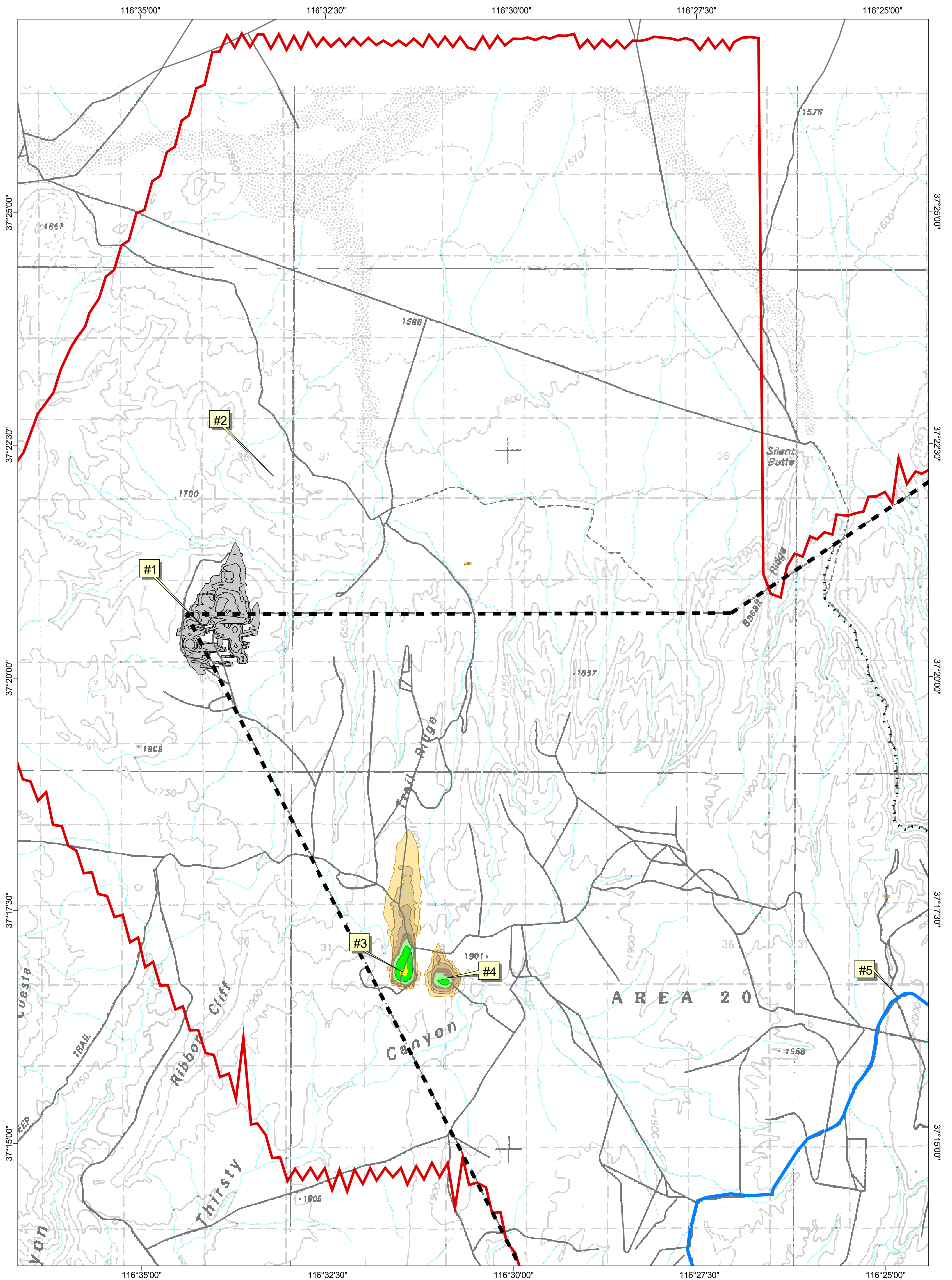
- NTS Boundary
- NTS Operational Area
- Highway
- Primary NTS Road
- Survey Boundary


This aerial radiological survey was conducted in support of the Aerial Measuring System Program under the direction of the U.S. Department of Energy, Nevada Operations Office. For additional information regarding these data, contact the Aerial Measuring System Program Manager at the U.S. Department of Energy, Nevada Operation Office.

Transportation data were obtained from the U.S. Geological Survey Digital Line Graph files. The NTS boundaries, Operational Areas, and primary roads were obtained from the NTS GIS database. Two helicopters were used simultaneously in conducting this high-resolution, medium-altitude aerial radiological survey, and the entire NTS and various adjacent areas were covered. The survey parameters provided approximately 100 percent coverage of the site. The survey was flown in a north-south direction, at an altitude of 200 feet above ground level, and with flight lines spaced 500 feet apart. The survey and data analysis were conducted by the U.S. Department of Energy's Remote Sensing Laboratory, which is located in Las Vegas, Nevada, and operated by Bechtel Nevada.


In regions of high-count rate (high-man-made activity), the Am-241 algorithm produced irregularly shaped contour levels having values that changed rapidly at the edges of the contours. These contours are suspected of being no more than statistical fluctuations in the gamma-ray spectra. Several of these contours have been shaded gray to highlight the uncertainty of their existence. Other irregularly shaped, small-area contours near aboveground test areas are probably not due to Am-241 contamination, but these small areas have not been analyzed to verify the hypothesis.

FIGURE 18. SITE-WIDE ISOTOPIC²⁴¹Am CONTOUR PLOT





This aerial radiological survey was conducted in support of the Aerial Measuring System Program under the direction of the U.S. Department of Energy, Nevada Operations Office. For additional information regarding these data, contact the Aerial Measuring System Program Manager at the U.S. Department of Energy, Nevada Operation Office.



Transportation data were obtained from the U.S. Geological Survey (USGS) Digital Line Graph files. The NTS boundaries, Operational Areas, and primary roads were obtained from the NTS GIS database. Basemap obtained from USGS 1:100,000 scale digital raster graphic, Pahute Mesa quadrangle. Elevation values are shown in meters above mean sea level.

Two helicopters were used simultaneously in conducting this high-resolution, medium-altitude aerial radiological survey, and the entire NTS and various adjacent areas were covered. The survey parameters provided approximately 100 percent coverage of the site. The survey was flown in a north-south direction, at an altitude of 200 feet above ground level, and with flight lines spaced 500 feet apart. The survey and data analysis were conducted by the U.S. Department of Energy's Remote Sensing Laboratory, which is located in Las Vegas, Nevada, and operated by Bechtel Nevada.

Map Projection: Transverse Mercator
 Coordinate System: State Plane
 Zone: Nevada Central Zone
 Datum: NAD83
 Spheroid: GRS80
 Graticules: 2.5 Minutes
 Base-Layer Data: NTS GIS Database
 Date Map Produced: June 28, 1999

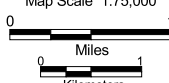

Counts Per Second

< 50
50 - 100
2.5 - 4.5
4.5 - 8.5
8.5 - 15
15 - 25
25 - 45
45 - 85

NTS Boundary
 NTS Operational Area
 Highway
 Primary NTS Road
 Secondary Road and Trail
 Survey Boundary
 Region of Interest Identifier

Nevada Test Site (NTS) Aerial Radiation Survey Americium Count Rate 1994 Survey

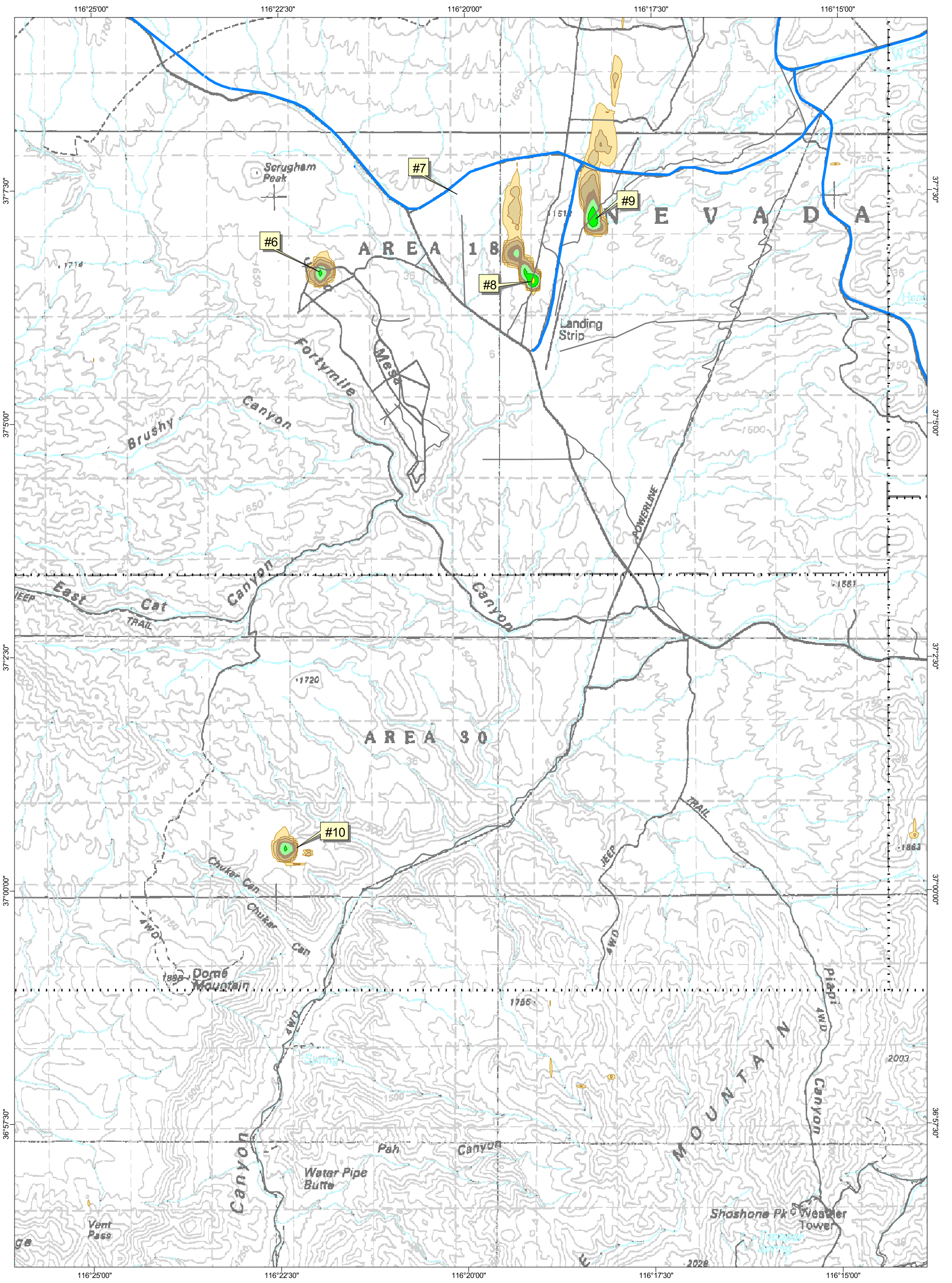
Map Scale 1:75,000

Bechtel Nevada
 NTS GIS 99194.6

In regions of high-count rate (high-man-made activity), the Am-241 algorithm produced irregularly shaped contour levels having values that changed rapidly at the edges of the contours. These contours are suspected of being no more than statistical fluctuations in the gamma-ray spectra. Several of these contours have been shaded gray to highlight the uncertainty of their existence. Other irregularly shaped, small-area contours near aboveground test areas are probably not due to Am-241 contamination, but these small areas have not been analyzed to verify the hypothesis.

FIGURE 19. ²⁴¹AM ACTIVITY IN AREA 20



Map Projection: Transverse Mercator
 Coordinate System: State Plane
 Zone: Nevada Central Zone
 Datum: NAD83
 Spheroid: GRS80
 Graticules: 2.5 Minutes
 Base-Layer Data: NTS GIS Database
 Date Map Produced: June 28, 1999

Counts Per Second

< 50
50 - 100
2.5 - 4.5
4.5 - 8.5
8.5 - 15
15 - 25
25 - 45
45 - 85

- NTS Boundary
- NTS Operational Area
- Highway
- Primary NTS Road
- Secondary Road and Trail
- Survey Boundary
- Region of Interest Identifier

Nevada Test Site (NTS) Aerial Radiation Survey Americium Count Rate 1994 Survey

Map Scale 1:75,000

Bechtel Nevada
 NTS GIS 99195.6

This aerial radiological survey was conducted in support of the Aerial Measuring System Program under the direction of the U.S. Department of Energy, Nevada Operations Office. For additional information regarding these data, contact the Aerial Measuring System Program Manager at the U.S. Department of Energy, Nevada Operation Office.

Transportation data were obtained from the U.S. Geological Survey (USGS) Digital Line Graph files. The NTS boundaries, Operational Areas, and primary roads were obtained from the NTS GIS database. Basemap obtained from USGS 1:100,000 scale digital raster graphic, Pahute Mesa and Beatty quadrangles. Elevation values are shown in meters above mean sea level.

Two helicopters were used simultaneously in conducting this high-resolution, medium-altitude aerial radiological survey, and the entire NTS and various adjacent areas were covered. The survey parameters provided approximately 100 percent coverage of the site. The survey was flown in a north-south direction, at an altitude of 200 feet above ground level, and with flight lines spaced 500 feet apart. The survey and data analysis were conducted by the U.S. Department of Energy's Remote Sensing Laboratory, which is located in Las Vegas, Nevada, and operated by Bechtel Nevada.

In regions of high-count rate (high-man-made activity) the Am-241 algorithm produced irregularly shaped contour levels having values that changed rapidly at the edges of the contours. These contours are suspected of being no more than statistical fluctuations in the gamma-ray spectra. Several of these contours have been shaded gray to highlight the uncertainty of their existence. Other irregularly shaped, small-area contours near aboveground test areas are probably not due to Am-241 contamination, but these small areas have not been analyzed to verify the hypothesis.

FIGURE 20. ²⁴¹AM ACTIVITY IN AREAS 18 AND 30

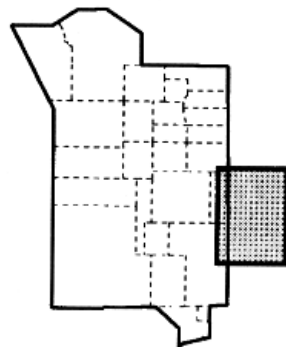
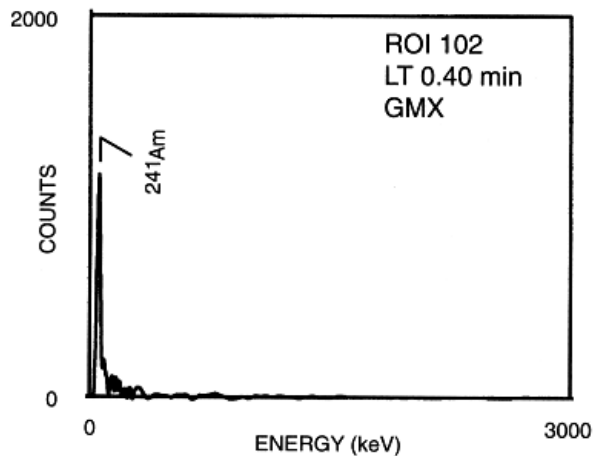
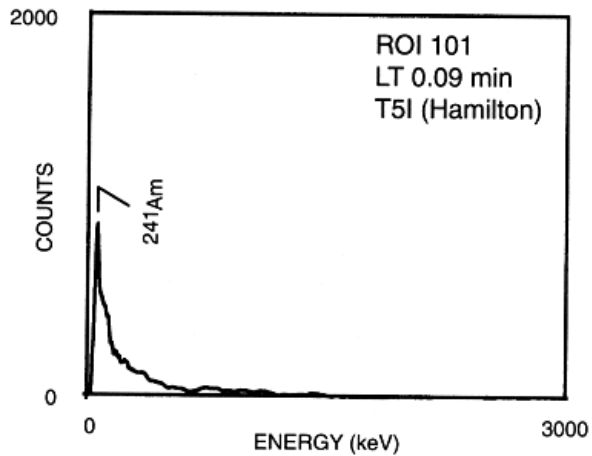
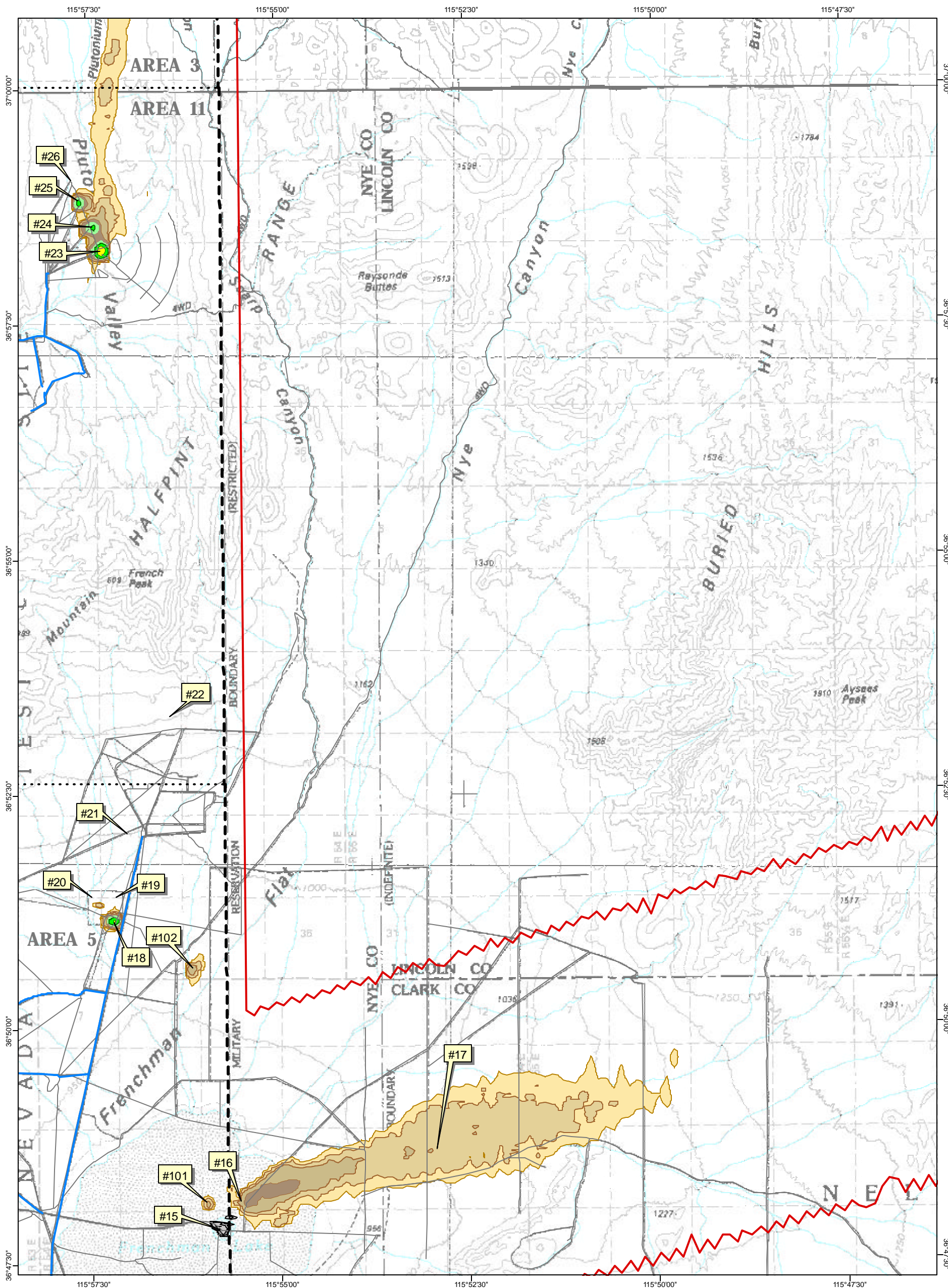


FIGURE 21. NET GAMMA SPECTRA FOR ROIs IDENTIFIED IN FIGURE 22



This aerial radiological survey was conducted in support of the Aerial Measuring System Program under the direction of the U.S. Department of Energy, Nevada Operations Office. For additional information regarding these data, contact the Aerial Measuring System Program Manager at the U.S. Department of Energy, Nevada Operations Office.

NEVADA
NTS

Map Projection: Transverse Mercator
 Coordinate System: State Plane
 Zone: Nevada Central Zone
 Datum: NAD83
 Spheroid: GRS80
 Graticules: 2.5 Minutes
 Base-Layer Data: NTS GIS Database
 Date Map Produced: June 28, 1999

Counts Per Second

< 50
50 - 100
2.5 - 4.5
4.5 - 8.5
8.5 - 15
15 - 25
25 - 45
45 - 85

NTS Boundary
 NTS Operational Area
 Highway
 Primary NTS Road
 Secondary Road and Trail
 Survey Boundary
 Region of Interest Identifier

Nevada Test Site (NTS) Aerial Radiation Survey Americium Count Rate 1994 Survey

Map Scale 1:75,000

Bechtel Nevada
NTS GIS 99196.6

In regions of high-count rate (high-man-made activity), the Am-241 algorithm produced irregularly shaped contour levels having values that changed rapidly at the edges of the contours. These contours are suspected of being no more than statistical fluctuations in the gamma-ray spectra. Several of these contours have been shaded gray to highlight the uncertainty of their existence. Other irregularly shaped, small-area contours near aboveground test areas are probably not due to Am-241 contamination, but these small areas have not been analyzed to verify the hypothesis.

FIGURE 22. ²⁴¹AM ACTIVITY IN AREAS 5 AND 11

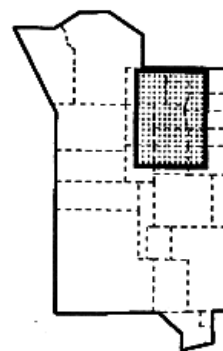
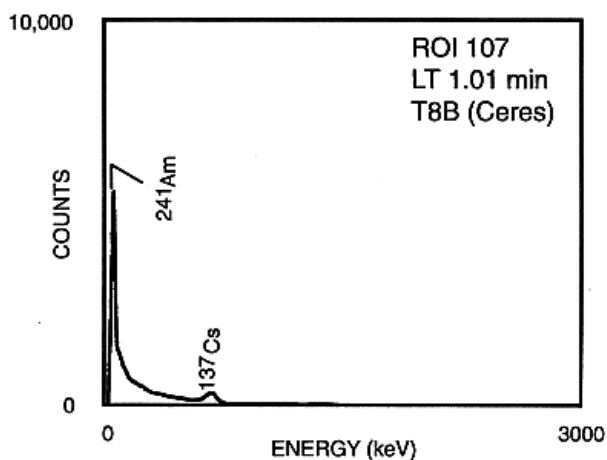
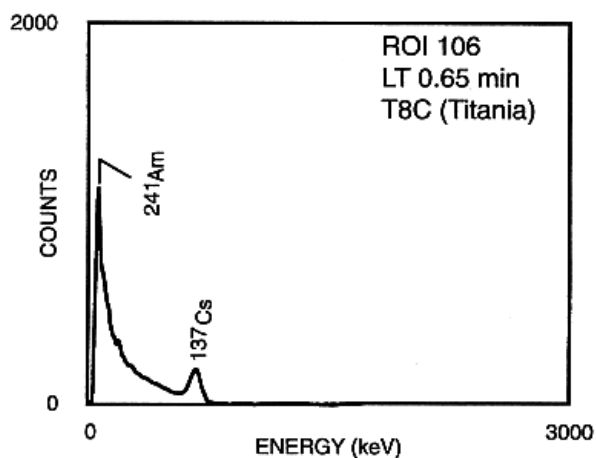
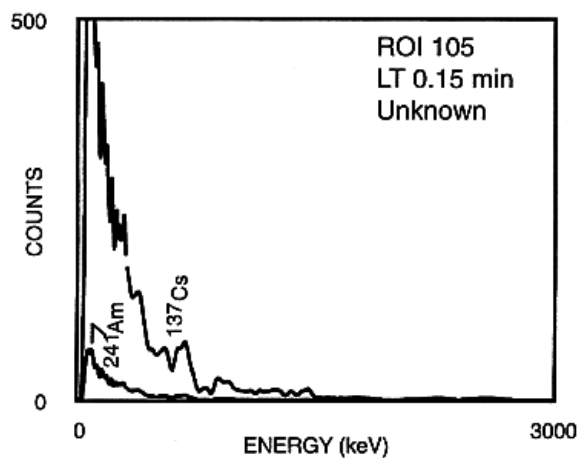
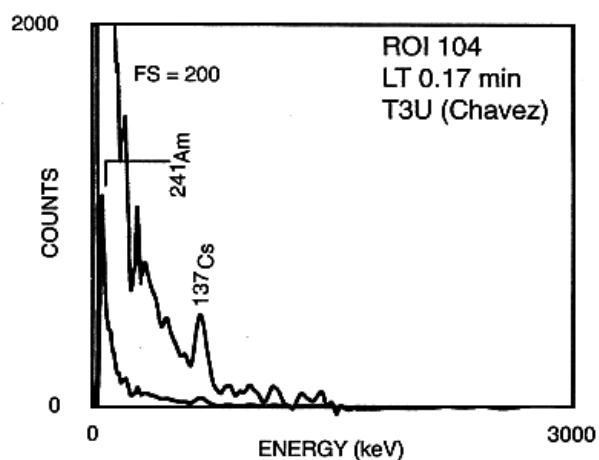
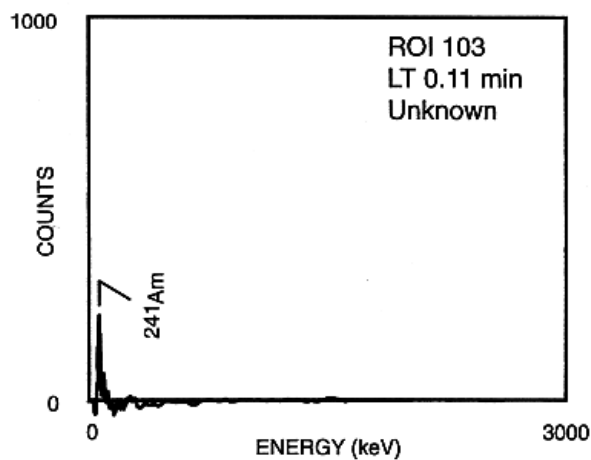
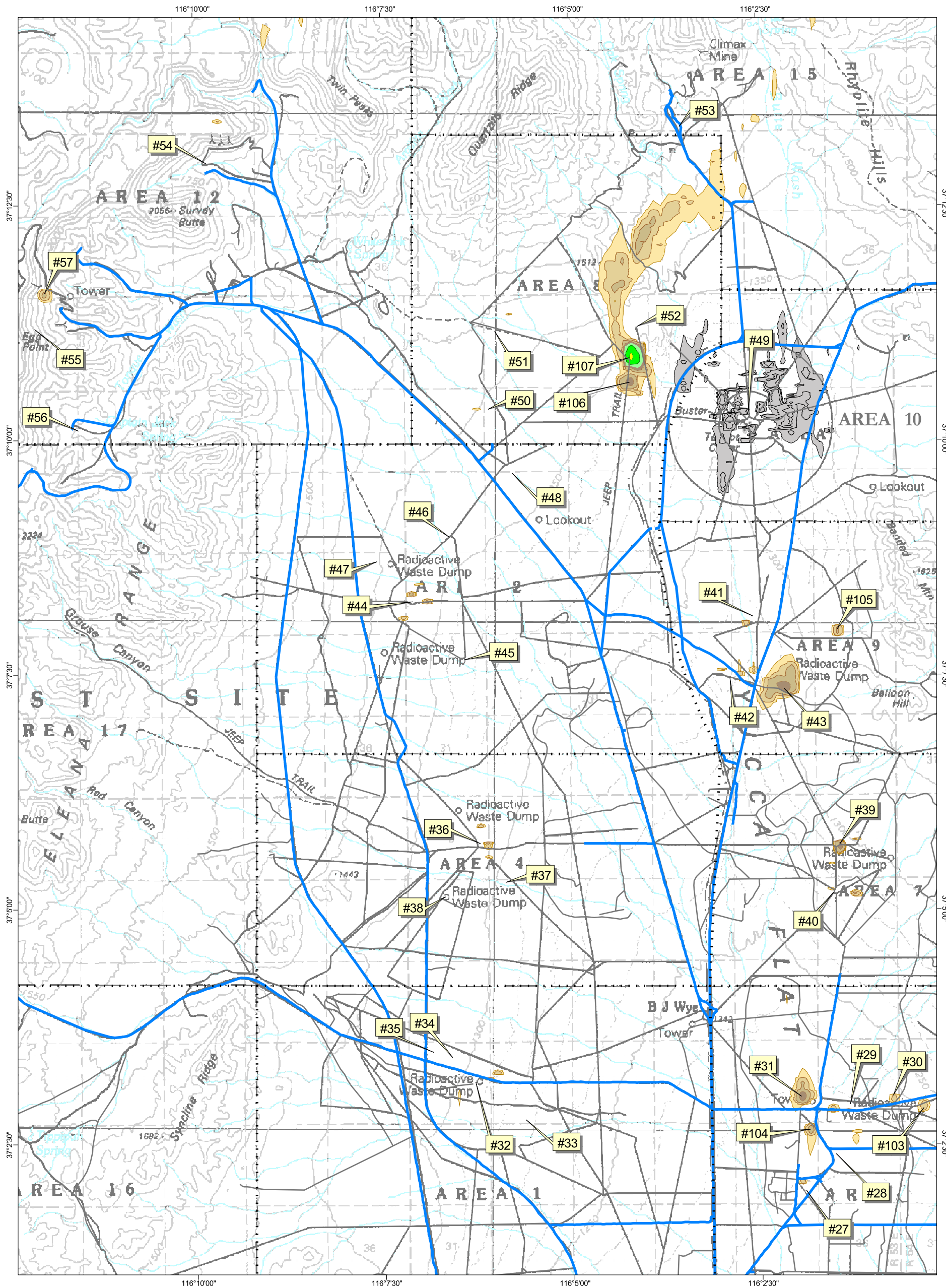


FIGURE 23. NET GAMMA SPECTRA FOR ROIs IDENTIFIED IN FIGURE 24



Map Projection: Transverse Mercator
 Coordinate System: State Plane
 Zone: Nevada Central Zone
 Datum: NAD83
 Spheroid: GRS80
 Graticules: 2.5 Minutes
 Base-Layer Data: NTS GIS Database
 Date Map Produced: June 28, 1999

Counts Per Second

- < 50
- 50 - 100
- 2.5 - 4.5
- 4.5 - 8.5
- 8.5 - 15
- 15 - 25
- 25 - 45
- 45 - 85

- NTS Boundary
- NTS Operational Area
- Highway
- Primary NTS Road
- Secondary Road and Trail
- Survey Boundary
- #1 Region of Interest Identifier

**Nevada Test Site (NTS)
 Aerial Radiation Survey
 Americium Count Rate
 1994 Survey**

Map Scale 1:75,000

Bechtel Nevada

NTS GIS 99197.6

In regions of high-count rate (high-man-made activity), the Am-241 algorithm produced irregularly shaped contour levels having values that changed rapidly at the edges of the contours. These contours are suspected of being no more than statistical fluctuations in the gamma-ray spectra. Several of these contours have been shaded gray to highlight the uncertainty of their existence. Other irregularly shaped, small-area contours near aboveground test areas are probably not due to Am-241 contamination, but these small areas have not been analyzed to verify the hypothesis.

FIGURE 24. ²⁴¹AM ACTIVITY IN YUCCA FLAT

8.0 REFERENCES

1. Hopkins, R.C. *An Aerial Radiological Survey of the Nevada Test Site and Surrounding Nellis Air Force Range*. Report No. DOE/NV/11718-022, 1997; Bechtel Nevada, Las Vegas, Nevada.
2. *United States Nuclear Tests*. Report No. DOE/NV-209 (Rev. 14), 1994; U.S. Department of Energy, Las Vegas, Nevada.
3. Burson, Z.G. *A Review of Aerial Radiological Surveys of Nevada Test Site Fallout Fields 1951 through 1970*. Report No. NVO-314, 1987; U.S. Department of Energy, Las Vegas, Nevada.
4. *Sedan Project 62.80c Aeroradioactivity Survey*. Report No. CEX-62.80c, 1965; EG&G, Santa Barbara, California.
5. *Small Boy Project 62.80b Aeroradioactivity Survey*. Report No. CEX-62.80b, 1965; EG&G, Santa Barbara, California.
6. Hand, J.E.; Weissman, V.F. *Nevada Aerial Tracking System Sedan Cobalt-60 Pellet Search*. Report No. EGG-1183-1345, 1967; EG&G, Las Vegas, Nevada.
7. Weissman, V.F.; Hand, J.E. *NATS Support Summary Schooner Event*. Report No. EGG-1183-1423, 1969; EG&G, Las Vegas, Nevada.
8. *Radiological Survey of the Nevada Test Site (Survey Period: 1970-1971)*. Report No. EGG-1183-1552, 1972; EG&G, Las Vegas, Nevada.
9. Tipton, W.J. *An Aerial Radiological Survey of Areas 25 and 26 Nevada Test Site*. Report No. EGG-1183-1745, 1979; EG&G, Las Vegas, Nevada.
10. Fritzsche, A.E. *An Aerial Radiological Survey of Areas 1, 2, 3, 4, 6, 7, 8, 9, 10, 12, 15, and 17 Yucca Flat, Nevada Test Site*. Report No. EGG-1183-1808, 1978; EG&G, Las Vegas, Nevada.
11. Feimster, E.L. *An Aerial Radiological Survey of Areas 18 and 20 Nevada Test Site*. Report No. EGG-10282-1093, 1985; EG&G/EM, Las Vegas, Nevada.
12. Clark, H.W. *An Aerial Radiological Survey of Area 11 Nevada Test Site*. Report No. EGG-10282-1004, 1983; EG&G, Las Vegas, Nevada.
13. Hopkins, R.C. *An Aerial Radiological Survey of Frenchman Flat at the Nevada Test Site*. Report No. DOE/NV/11718--012, 1997; Bechtel Nevada, Las Vegas, Nevada.
14. Bluit, C.M. *An Aerial Radiological Survey of Areas 16 and 30 Nevada Test Site*. Report No. EGG-10282-1118, 1986; EG&G/EM, Las Vegas, Nevada.
15. Jobst, J.E. *An Aerial Radiological Survey of Areas 12, 15, 17, and 19 Nevada Test Site*. Report No. EGG-10282-1113, 1986; EG&G/EM, Las Vegas, Nevada.
16. Hopkins, R.C. *Off-Site Plutonium Plume Survey Nevada Test Site*. Letter Report No. NV-93-090, 1993; EG&G/EM, Las Vegas, Nevada. (Data from this letter report is summarized in Appendix C of reference 16.)
17. Colton, D.P. *An In Situ Radiological Survey of the Area 11 Nuclear Safety Test Locations Sites A, B, and C*. Report No. NRD-93-330, 1993; EG&G/EM, Las Vegas, Nevada.
18. National Council on Radiation Protection and Measurements. *Environmental Radiation Measurements*. NCRP Report No. 50, 1976; NCRP, Washington, D.C.
19. Lindeken, C.L.; Peterson, K.R.; Jones, D.E.; McMillen, R.E. "Geographical Variations in Environmental Radiation Background in the United States," in *Proceedings of the Second International Symposium on the Natural Radiation Environment, August 7-11, 1972, Houston, Texas: Vol. 1*. Available from NTIS, Springfield, Virginia; 1972:317-332.
20. Nazaroff, W.W. "Radon Transport From Soil to Atmosphere," *Reviews of Geophysics*. 30(2):137-160; 1992.
21. National Council on Radiation Protection and Measurements. *Radon Exposure of the U.S. Population—Status of the Problem*. NCRP Commentary No. 6, 1991; NCRP, Bethesda, Maryland.
22. Eisenbud, M. *Environmental Radioactivity, Second Edition*. New York: Academic Press, 1973:192-196.

8.0 REFERENCES

23. Klement, Jr., A.W.; Miller, C.R.; Minx, R.P.; Shleien, B. *Estimates of Ionizing Radiation Doses in the United States 1960-2000*. Report No. ORP/CSD72-1, 1972; Environmental Protection Agency, Washington, D.C.
24. Lowder, W.M.; Beck, H.L. "Cosmic-Ray Ionization in the Lower Atmosphere," *J. Geophys. Res.* 71:4661-4668; 1972 [see also NCRP Report No. 35, 1966].
25. Burson, Z.G. *Population Exposure to Natural Terrestrial Gamma Radiation Around Selected Nuclear Power Plant Sites*. Report EGG-1183-1638, 1974; EG&G, Las Vegas, Nevada.
26. Mohr, R.; Franks, L. *Compilation of ¹³⁷Cs Concentrations at Selected Sites in the Continental United States*. Report No. EGG-1183-2437 (Rev), 1982; EG&G, Goleta, California.
27. Mohr, R. [Interoffice Memorandum, subject: Ion Chamber Measurements at the Bonelli Bay Calibration Range, EG&G, Goleta, California]. 1990 February 11.
28. Mohr, R. [Interoffice Memorandum, subject: Ground Measurements at the Bonelli Bay Calibration Range, EG&G, Goleta, California]. 1981 April 6.

APPENDIX A

SURVEY PARAMETERS AND RESULTS

PARAMETERS

Survey Site	Nevada Test Site, Nevada
Survey Dates	August 16 to September 28, 1994
Nominal Site Elevation	850–2250 meters (2800–7400 feet) above mean sea level
Survey Altitude	60 meters (200 feet)
Flight-line Spacing	150 meters (500 feet)
Line Direction	North–South
Aircraft Speed	39 meters per second (75 knots)
Survey Coverage	Approximately 4340 square kilometers (1680 square miles)
Base of Operation	Desert Rock Airport, Mercury, Nevada
Aircraft	Three MBB BO-105 Helicopters Tail Number N70EG August 16 to September 25, 1994 Tail Number N60EG August 17 to August 24, 1994 Tail Number N50EG August 27 to August 28, 1994
Navigation System	Differential GPS Primary Base Station Monastery (in hills west of CP-1)—Channel 5 Skull Mountain (radio repeater site)—Channel 15 Echo Peak (radio repeater site)—Channel 14 Secondary Base Station (for Area 20 portion) Pahute Mesa Road—Channel 13
Detector Arrays (each helicopter)	Eight 5- × 10- × 40-centimeter NaI One 5- × 10- × 10-centimeter NaI
Acquisition System	REDAR IV

RESULTS

Cosmic-Ray Contribution	4.5–8.5 $\mu\text{R/h}$ (elevation dependent)		
Air Attenuation Coefficient	0.005322 m^{-1} (0.001622 ft^{-1}) for helicopter N50EG 0.005820 m^{-1} (0.001774 ft^{-1}) for helicopter N60EG 0.005741 m^{-1} (0.001750 ft^{-1}) for helicopter N70EG		
Data Processing Items	Terrestrial Exposure Rate Plot MMGC Plot ^{241}Am Count Rate Plot Individual Net Gamma-Ray Spectra		
Energy Windows (keV)	Main	Background 1	Background 2
	GC	38–3026	
	MMGC	38–1394	1394–3026
	^{241}Am	50–70	38–50 70–82

APPENDIX A
SURVEY PARAMETERS AND RESULTS

CONVERSION FACTORS

1 cm	=	0.394 in	2.54 cm	=	1 in
1 m	=	3.28 ft	0.3048 m	=	1 ft
1 km	=	0.621 mi	1.609 km	=	1 mi
1 m/s	=	3.28 ft/s			
	=	2.24 mph			
	=	1.94 knots			
1 μ R/h	=	8.76 mR/yr	11.9 μ R/h	\approx	100 mrem/yr
	\approx	8.37 mrem/yr			
where the " \approx " is the approximate conversion from exposure rate to dose rate					
1 Bq	=	2.7×10^{-11} Ci	3.7×10^{10} Bq	=	1 Ci
1 Bq/kg	=	0.027 pCi/g	37 Bq/kg	=	1 pCi/g
1 kBq/m ²	=	27 nCi/m ²	0.037 kBq/m ²	=	1 nCi/m ²

Table A-1. Summary of Average Exposure Rate by Area

This table summarizes the average exposure rate in each NTS area. The exposure rates are from the almost-site-wide 1970 survey, the site-wide 1992 and 1994 surveys, and the surveys of specific NTS areas that occurred in the 1970s and 1980s. These values use the exposure-rate ranges listed in the individual reports. Each author chose the exposure-rate ranges to highlight the particular data features shown in that report.

Area	Subset	Exposure-Rate Range (μ R/h) ^a				
		1970 Survey	Survey Year	Exposure Rate (μ R/h)	1992 Survey	1994 Survey
1	West and South	4-10 ^b	1978	not reported	6-12	6-18
1	Elsewhere	11-20	1978	not reported	6-18	12-18
2	West	31-50 ^c	1978	not reported	6-18	6-12
2	Elsewhere	11-20	1978	not reported	12-18	12-18
3	East	not flown	1978	not reported	0-12	0-18
3	West	11-20	1978	not reported	12-18	12-18
4	West	21-30 ^c	1978	not reported	6-18	6-18
4	Elsewhere	11-20	1978	not reported	6-18	12-18
5	North	11-30	1982	not reported	12-18	12-18
5	Central	4-20	1982	not reported	6-12	6-12
5	South	not flown	1982	not reported	0-6	0-6
East of 5	Northwest	not flown		not flown	6-12	6-12
East of 5	Elsewhere	not flown		not flown	0-6	0-6
6	East	11-30	1978	not reported	12-18	12-18
6	Central and Northwest	not flown	1978	not reported	0-12	0-12
6	West	not flown	1978	not reported	12-18	12-24
7	East	not flown	1978	not reported	0-18	0-18
7	Central	11-20	1978	not reported	6-18	6-18
7	West	11-20	1978	not reported	12-18	12-18
8	North	not flown	1978	not reported	6-18	6-18
8	South	not flown	1978	not reported	12-18	12-18
9	East	not flown	1978	not reported	0-18	0-18
9	Central	11-20 ^b	1978	not reported	0-12	0-12

APPENDIX A
SURVEY PARAMETERS AND RESULTS

Area	Subset	Exposure-Rate Range ($\mu\text{R/h}$) ^a				
		1970 Survey	Survey Year	Exposure Rate ($\mu\text{R/h}$)	1992 Survey	1994 Survey
9	West	11–50	1978	not reported	12–18	12–18
10	East	not flown	1978	not reported	6–12	6–18
10	West	no bkgnd ^d	1978	not reported	12–18	12–24
11		not flown	1982	10–18 ^b	12–18	12–18
12	North and West	not flown	1978	not reported	12–24	18–24
12	South and East	not flown	1978	not reported	6–18	6–18
14	North	11–20		not flown	12–18	12–18
14	Central	not flown		not flown	12–18	18–24
14	South	not flown		not flown	6–12	12–18
15	East	11–30 ^b	1984	22–26	6–12	6–18
15	Central	not flown	1984	13–26	12–18	18–24
15	West	not flown	1984	16–22	6–12	6–18
North of 15	East	21–50 ^b		not flown	12–18	12–18
North of 15	Elsewhere	not flown		not flown	12–18	12–24
16	North and East	not flown	1983	14–21	6–12	6–12
16	South and West	not flown	1983	21–25	12–18	12–24
17	East	not flown	1984	13–22	6–12	6–12
17	West	not flown	1984	22–26	12–18	12–24
18	East	21–30	1980	17–25	12–18	12–18
18	Central	11–30	1980	12–21	6–12	12–18
18	West	21–30 ^b	1980	17–25	12–18	18–24
19	Central	21–30	1984	22–26	12–24	18–24
19	Elsewhere	not flown	1984	22–26	12–18	12–24
20		21–30	1980	17–30	12–24	12–24
North of 20		21–30		not flown	12–24	12–24
West of 20		11–30 ^b		not flown	12–24	12–24
22	East	4–10 ^b		not flown	0–6	0–6
22	Elsewhere	4–10 ^b		not flown	0–12	6–12
23		not flown		not flown	0–6	0–6
25	Northwest	11–20 ^b	1976	15–20 ^b	12–18	18–24
25	Southwest to Northeast band	11–20	1976	15–20 ^b	6–18	12–18
25	East	not flown		not flown	6–12	6–12
25	Southeast	4–20		not flown	0–12	0–6
26		not flown	1976	15–20 ^b	6–12	12–18
27		not flown		not flown	6–12	6–12
29		not flown		not flown	12–18	18–24
30	East	not flown	1983	21–45	12–18	12–24
30	Central	not flown	1983	18–21	6–12	6–18
30	West	not flown	1983	18–45	12–18	18–24

^a 1994 Survey values do not include the cosmic contribution. The 1992 survey values are from the published report and do not include the cosmic contribution. The 1970 survey values are from the published report and do include the cosmic contribution.

^b Values are taken from surveyed areas, but the survey did not cover the full Area/Subset that was described.

^c Values are taken from surveyed areas, but the survey did not cover the full Area/Subset described and the reported values appear to be influenced by the error in the figure in the 1970 report.

^d The 1970 survey did not report any values from this Area/Subset that could be considered background.

APPENDIX B

LIST OF THE ELEMENTS

The radioactive isotopes described in this document are designated using the current version of the nuclear physics and chemistry nomenclature. The symbol designating the element is usually an abbreviation of the element's name, but sometimes the symbol derives from the Latin name of the element. The mass number of the isotope is added as a superscript preceding the symbol. For example, the radioisotope americium-241 is designated as ²⁴¹Am and cesium-137 is ¹³⁷Cs.

The following two charts list the elements ordered either by their atomic number (the number of protons in their nucleus) or alphabetized by their symbol (to facilitate finding an element discussed in the text).

List of the Elements by Atomic Number

<u>Z</u>	<u>Sym</u>	<u>Element</u>	<u>Z</u>	<u>Sym</u>	<u>Element</u>	<u>Z</u>	<u>Sym</u>	<u>Element</u>
1	H	Hydrogen	36	Kr	Krypton	70	Yb	Ytterbium
2	He	Helium	37	Rb	Rubidium	71	Lu	Lutetium
3	Li	Lithium	38	Sr	Strontium	72	Hf	Hafnium
4	Be	Beryllium	39	Y	Yttrium	73	Ta	Tantalum
5	B	Boron				74	W	Tungsten
6	C	Carbon	40	Zr	Zirconium	75	Re	Rhenium
7	N	Nitrogen	41	Nb	Niobium	76	Os	Osmium
8	O	Oxygen	42	Mo	Molybdenum	77	Ir	Iridium
9	F	Fluorine	43	Tc	Technetium	78	Pt	Platinum
			44	Ru	Ruthenium	79	Au	Gold
10	Ne	Neon	45	Rh	Rhodium			
11	Na	Sodium	46	Pd	Palladium	80	Hg	Mercury
12	Mg	Magnesium	47	Ag	Silver	81	Tl	Thallium
13	Al	Aluminum	48	Cd	Cadmium	82	Pb	Lead
14	Si	Silicon	49	In	Indium	83	Bi	Bismuth
15	P	Phosphorus				84	Po	Polonium
16	S	Sulfur	50	Sn	Tin	85	At	Astatine
17	Cl	Chlorine	51	Sb	Antimony	86	Rn	Radon
18	Ar	Argon	52	Te	Tellurium	87	Fr	Francium
19	K	Potassium	53	I	Iodine	88	Ra	Radium
			54	Xe	Xenon	89	Ac	Actinium
20	Ca	Calcium	55	Cs	Cesium			
21	Sc	Scandium	56	Ba	Barium	90	Th	Thorium
22	Ti	Titanium	57	La	Lanthanum	91	Pa	Protactinium
23	V	Vanadium	58	Ce	Cerium	92	U	Uranium
24	Cr	Chromium	59	Pr	Praseodymium	93	Np	Neptunium
25	Mn	Manganese				94	Pu	Plutonium
26	Fe	Iron	60	Nd	Neodymium	95	Am	Americium
27	Co	Cobalt	61	Pm	Promethium	96	Cm	Curium
28	Ni	Nickel	62	Sm	Samarium	97	Bk	Berkelium
29	Cu	Copper	63	Eu	Europium	98	Cf	Californium
			64	Gd	Gadolinium	99	Es	Einsteinium
30	Zn	Zinc	65	Tb	Terbium			
31	Ga	Gallium	66	Dy	Dysprosium	100	Fm	Fermium
32	Ge	Germanium	67	Ho	Holmium	101	Md	Mendelevium
33	As	Arsenic	68	Er	Erbium	102	No	Nobelium
34	Se	Selenium	69	Tm	Thulium	103	Lr	Lawrencium
35	Br	Bromine						

APPENDIX B
LIST OF THE ELEMENTS

List of the Elements Alphabetized by Symbol

<u>Z</u>	<u>Sym</u>	<u>Element</u>	<u>Z</u>	<u>Sym</u>	<u>Element</u>	<u>Z</u>	<u>Sym</u>	<u>Element</u>
89	Ac	Actinium	1	H	Hydrogen	78	Pt	Platinum
47	Ag	Silver	2	He	Helium	94	Pu	Plutonium
13	Al	Aluminum	72	Hf	Hafnium			
95	Am	Americium	80	Hg	Mercury	88	Ra	Radium
18	Ar	Argon	67	Ho	Holmium	37	Rb	Rubidium
33	As	Arsenic				75	Re	Rhenium
85	At	Astatine	53	I	Iodine	45	Rh	Rhodium
79	Au	Gold	49	In	Indium	86	Rn	Radon
			77	Ir	Iridium	44	Ru	Ruthenium
5	B	Boron						
56	Ba	Barium	19	K	Potassium	16	S	Sulfur
4	Be	Beryllium	36	Kr	Krypton	51	Sb	Antimony
83	Bi	Bismuth	57	La	Lanthanum	21	Sc	Scandium
97	Bk	Berkelium	3	Li	Lithium	34	Se	Selenium
35	Br	Bromine	71	Lu	Lutetium	14	Si	Silicon
			103	Lr	Lawrencium	62	Sm	Samarium
6	C	Carbon				50	Sn	Tin
20	Ca	Calcium	101	Md	Mendelevium	38	Sr	Strontium
48	Cd	Cadmium	12	Mg	Magnesium			
58	Ce	Cerium	25	Mn	Manganese	73	Ta	Tantalum
98	Cf	Californium	42	Mo	Molybdenum	65	Tb	Terbium
17	Cl	Chlorine				43	Tc	Technetium
96	Cm	Curium	7	N	Nitrogen	52	Te	Tellurium
27	Co	Cobalt	11	Na	Sodium	90	Th	Thorium
24	Cr	Chromium	41	Nb	Niobium	22	Ti	Titanium
55	Cs	Cesium	60	Nd	Neodymium	81	Tl	Thallium
29	Cu	Copper	10	Ne	Neon	69	Tm	Thulium
			28	Ni	Nickel			
66	Dy	Dysprosium	102	No	Nobelium	92	U	Uranium
68	Er	Erbium	93	Np	Neptunium	23	V	Vanadium
99	Es	Einsteinium						
63	Eu	Europium	8	O	Oxygen	74	W	Tungsten
			76	Os	Osmium	54	Xe	Xenon
9	F	Fluorine	15	P	Phosphorus			
26	Fe	Iron	91	Pa	Protoactinium	39	Y	Yttrium
100	Fm	Fermium	82	Pb	Lead	70	Yb	Ytterbium
87	Fr	Francium	46	Pd	Palladium			
31	Ga	Gallium	61	Pm	Promethium	30	Zn	Zinc
64	Gd	Gadolinium	84	Po	Polonium	40	Zr	Zirconium
32	Ge	Germanium	59	Pr	Praseodymium			

DISTRIBUTION

DOE/DP

J.A. Weidner, CDR USN
R. Ghetti

(1)
(1)

DOE/NSIC

R.S. Scott

(1)

DOE/NV

T.A. Cooper
D.L. Wheeler

(1)
(1)

BECHTEL NEVADA

C.M. Bluit
P.P. Guss
T.J. Hendricks
R.K. Kulm

RSL-Nellis
RSL-Andrews
RSL-Nellis
RSL-Nellis

(1)
(1)
(1)
(1)

BECHTEL NEVADA (cont.)

K.R. Lamison, Jr.
R.J. Maurer
J.T. Mitchell, Jr.
M.F. Mohar
S.R. Riedhauser
H.J. Saxton
W.P. Tasko
R.J. Vojtech
A.J. Will

RSL-Nellis
RSL-Andrews
LVAO
RSL-Nellis
RSL-Nellis
LVAO
RSL-Nellis
RSL-Andrews
RSL-Nellis

(1)
(1)
(1)
(1)
(1)
(1)
(1)
(1)
(1)

OSTI

(2)

RESOURCE CENTERS

Public Reading Facility
RSL-Andrews
RSL-Nellis
TIRC

(1)
(1)
(50)
(1)